Light pollution and navigation in two nocturnal arthropod taxa

By

Rochelle Jade Meah

School of Biological Sciences

UNIVERSITY OF BRISTOL

A dissertation submitted to the University of Bristol in accordance with the requirements for award of the degree of DOCTOR of PHILOSOPHY in the Faculty of Life Sciences

October 2022

Word count: 36 756

Abstract

Artificial light at night is a major anthropogenic pollutant. The area of artificially lit land is increasing at approximately 2% per year globally, and almost 90% of Europe is now affected by increased night sky luminance. The intensity, spectral composition, and timing of light pollution all affect different aspects of the physiology and behaviour of individual organisms. Ultimately, these changes can alter community structures and the ecology of different ecosystems.

Among nocturnal arthropods, research on the impacts of light pollution has largely focused on community-level effects or broader behavioural ecology. The effects of artificial light masking visual cues used in task-specific behaviours have received relatively little attention and there are indications that light pollution might obscure a major nocturnal cue, the skylight polarization pattern, but this has never been studied in any detail. Similarly, how light pollution might affect the timing of these behaviours is also under-studied. This PhD investigates how artificial light at night masks the skylight polarization pattern and how the loss of this cue, and the spectral composition and intensity of the artificial light, behaviourally impacts both nocturnal central-place foraging spiders of the genus *Drassodes*, and a long-distance migratory moth, *Helicoverpa armigera*. The major differences in the polarization pattern between dark and light-polluted skies across four moon phases and across a light pollution radiance gradient were established using imaging polarimetry. The ecological impact of the masking effect of light pollution to polarization-guided navigation was assessed using analysis of the tethered paths of animals exposed to polarized stimuli. Finally, the ecological impact of light pollution on the initiation and timing of nocturnal journeys was examined by observing patterns of activity under streetlights of different intensities and spectral compositions.

The skylight polarization pattern is significantly affected by light pollution which not only affects the strength of the polarization pattern, but its spatial and temporal extent. These impacts can occur even at low levels of light pollution and are exacerbated by changes in moon luminance across the phases of the lunar cycle. This has the potential to disorientate both *H. armigera* and *Drassodes* in the wild, as well as inhibit or alter time-sensitive navigational behaviour essential for survival with broader implications for dispersal, individual fitness, community composition and agroecosystems. Tuning the intensity and spectral composition of light pollution may alleviate the magnitude of these impacts through reductions in radiance and shifting the spectral character of the light away from short wavelengths.

Dedication and acknowledgements

This thesis is dedicated to my parents, Colin Meah and Susan Meah, who have always encouraged my enthusiasm for nature and supported my academic ambitions.

I would like to thank my advisors Nicholas Roberts and Lauren Sumner-Rooney for their unbridled support, encouragement, and enthusiasm throughout my project. Their belief in me and my ability has fostered a level of self-confidence that I did not have prior to moving to Bristol. I would also like to thank members of the Ecology of Vision group; Alex Tibbs, Ally Irwin, David Wilby, Emelie Brodrick, Ilse Daly, Martin How, Mike Bok, Octavia Brayley, and Sam Smithers, for their help and support and for creating a fun and friendly workplace. Special thanks to my insanely patient and hard-working research assistants, Seb Llyod, Christian Drerup, and Siân Vincent Venables, without which this project couldn't have been completed. Extra special thanks to Vun Wen Jie for being a joy to work with and building the trackball set-up to a standard far beyond my capabilities. Thanks to Chris Neal at the Wolfson Bio-imaging facility for being more enthusiastic about moth eye sectioning than I ever could be.

Thank you to my collaborators in the Genetics of Migration group at Exeter University; Karl Wotton, Toby Doyle, Will Hawkes, Kelsey Davies, Rich Massy, and Scarlett Weston. You guys made fieldwork dreamy rather than a fever dream, even if my experiment gets accidently unplugged to watch 'Withnail & I' every now and then!

I am very lucky to have met so many amazing PhD students at Bristol, who have supported and helped me throughout my project and are now lifelong friends. They made coming into work a joy and helped me weather the stormier days. I hope I fulfilled a similar role for them: Isla Davidson, Sverre Tunstad, Roky Wilson, Benito Wainwright, Sarah Dodd, Iestyn Penry-Williams, Toby Champneys, Duncan Edgley, Jack Greenhalgh, Luke Romaine, Sam England, Anne Le, and Katie Lihou. Similarly, I'd like to thank my housemates over the years; Alex Tibbs, Sadie Peacock, Rachel Budden, Adrian Davis, and Lukie White for making the COVID lockdowns bearable but mostly for making life outside of my PhD so much fun.

Finally, mahalo to my ride or die, Luke Oldridge, who's unconditional care, advice, and patience restocked my energy and self-belief when I needed it the most.

Author's declaration

I declare that the work in this dissertation was carried out in accordance with the requirements of the University's Regulations and Code of Practice for Research Degree Programmes and that it has not been submitted for any other academic award. Except where indicated by specific reference in the text, the work is the candidate's own work. Work done in collaboration with, or with the assistance of, others, is indicated as such. Any views expressed in the dissertation are those of the author.

SIGNED: ..... DATE:.....

Table of Contents

List of Tables

List of Figures

1

Introduction

The global spread of light pollution is a major threat to the nocturnal world[1,2] and is increasing in geographical area and intensity[3]. Light pollution can affect the fundamental biology of nocturnal animals with significant consequences to population and community ecology. There are numerous mechanisms driving such effects, but the interacting ways that artificial light at night affects the visual ecology of nocturnal animals is the central theme of this thesis.

Many nocturnal arthropods use visual cues to guide remarkable feats of navigation with high precision, from long-distance migrations to convoluted local journeys. Of these, the skylight polarization pattern is a common visual cue used by many diurnal and nocturnal arthropods. Light pollution threatens nocturnal navigation by masking celestial visual cues used for orientation and compass information[4,5] and disrupting the initiation of nocturnal journeys with the onset of night[6], but the consequences for polarization-sensitive arthropods is unknown. This thesis explores the potential impacts of light pollution on polarization-guided navigation and patterns of navigational activity in two arthropod species: a long-distance migratory moth, *Helicoverpa armigera*, and a central place foraging spider, *Drassodes* sp.. To begin, the anthropogenic threat of light pollution is characterised, followed by its impact on nocturnal navigation and the onset of nocturnal journeys, and ending with brief introductions to the two study species selected to investigate the central questions of this project.

1.1 Ecological light pollution

Light pollution is a pervasive anthropogenic pollutant that affects human health, climate change, biodiversity and conservation, astronomical study, financial economies, and social and cultural welfare. As such, light pollution and anthropogenic light at night (ALAN) are broad terms that encompass many facets of the study and assessment of light pollution. This thesis focuses on the ecological impacts of light pollution on nocturnal arthropods and the following review and discussion of the literature is considered within this context only.

1.1.1 Properties of ecological light pollution

Ecological light pollution is an unintended side-effect of artificial light at night that alters the night's natural light environment to the detriment of nocturnal and diurnal animals. Light pollution can be categorised as either direct or indirect, depending on its physical characteristics, but the source of both is anthropogenic light at night (Fig.1.1)[1]. Direct light pollution refers to illumination caused by light emitted from its source and includes the area of intentional illumination as well as any unintentionally affected areas (known as light trespass). Indirect light pollution refers to stray light reflected upward from its source and often scattered back to the ground through interactions with atmospheric components such as water droplets within clouds[7]. Both forms of light pollution contribute to urban skyglow, the characteristic diffuse illuminance of the night sky above brightly lit areas, which is often visible even at large distances from the sources of the light[7].

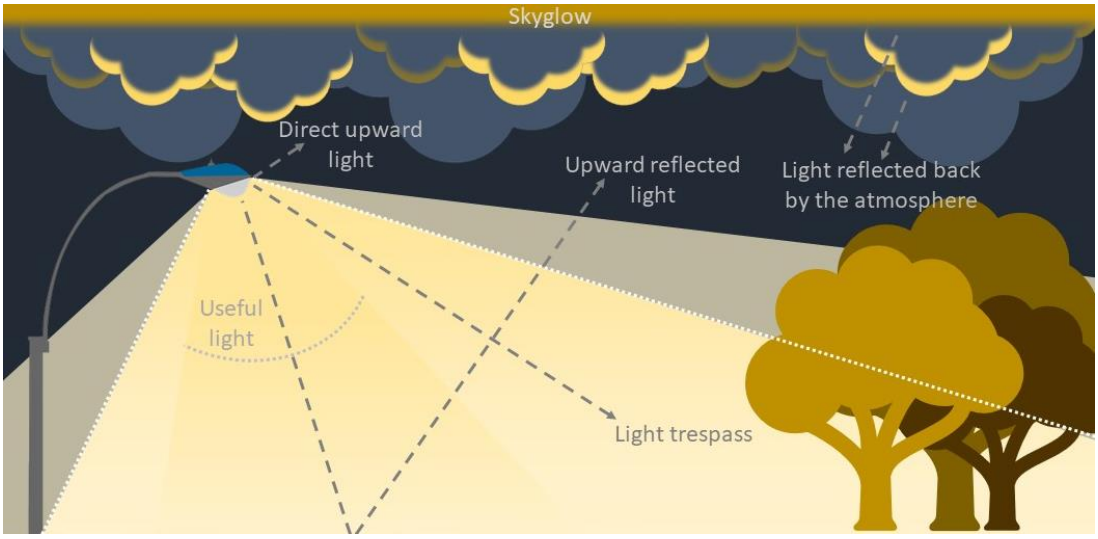

Figure 1.1. The different components of light pollution, including direct (yellow shaded areas below the white dashed line) and indirect light pollution (yellow shaded areas above the white dashed line). Both forms contribute to urban skyglow.

1.1.2 Global spread of ecological light pollution

Urban expansion and innovations in lighting technology have increased the spatial extent and radiance of light pollution by around 2% per year in the past decade[1]. The global spread of light pollution is monitored both at ground-level using cameras, light meters, and spectrophotometers, and from space using remote sensing data such as that obtained from the Visible Infrared Imaging Radiation Suite Day-Night Band (VIIRS DNB) on the Suomi National Polar-Orbiting Partnership satellite[1]. The following three sections contain research using both methods for a comprehensive summary of the extent and characteristics of this anthropogenic pollutant.

1.1.2.1 Spatial extent

The global extent of direct light pollution on the Earth's land surface was estimated at 23% in 2016[8], with indirect pollution reaching 47% between 2012 and 2019[9] (Fig.1.2). The European and North American land masses were most notably affected with 88% of Europe and 47% of the USA experiencing light-polluted skies[8]. Similarly, an estimated 22% of the world's marine and coastal environments (excluding Antarctica) was affected by light pollution in 2010[10].

The expansion of light pollution is extending into International Union for the Conservation of Nature (IUCN) designated key biodiversity areas (KBAs) and the global protected area system, increasing the number of organisms at risk and compromising the effectiveness of protected areas[11,12,13]. On land, half of the world's KBAs were affected by light pollution, with less than a third having pristine night skies in 2016[11]. This followed a large increase in the proportion of the world's protected areas exposed to light pollution between 1992 and 2010, particularly in Europe, Asia, and the Americas, which saw increases in lit area of 32-42%[12]. However, it is important to note that the definitions of light-polluted areas conflict between studies and may not be comparable. In marine protected areas, 35% were estimated to be experiencing light pollution at night in 2012, with 57% of these areas experiencing light pollution across the entire protected zone[13].

Given that the spatial extent of light pollution has been expanding by around 2% per year[1], these estimates are expected to have increased by 6-24% since their publication. The current area of the world's surface affected by light pollution may be as high as 53% on land and 46% in marine and coastal areas.

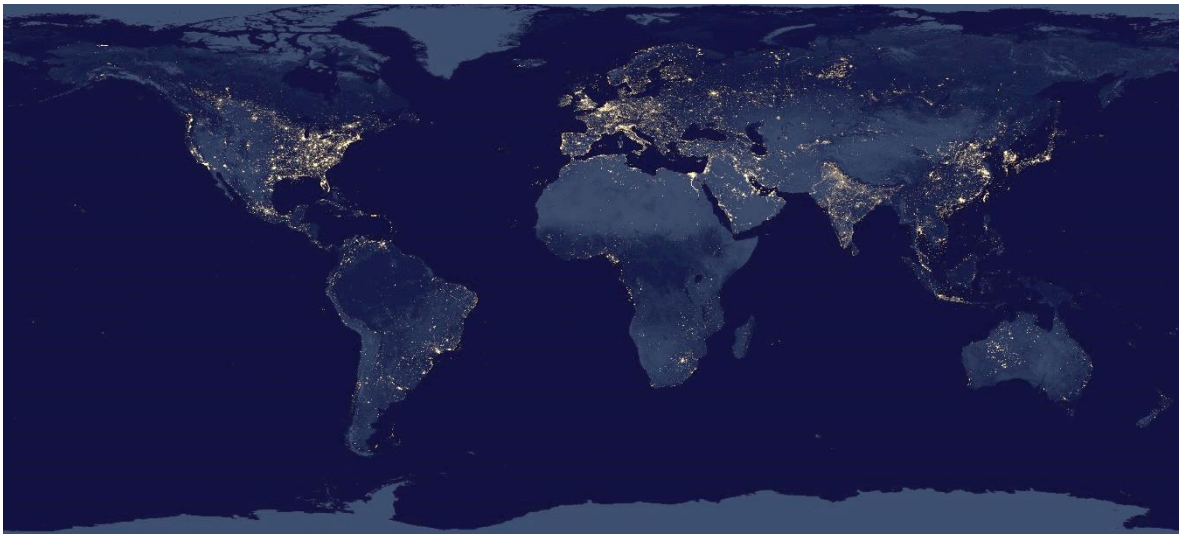

Figure 1.2. NASA Earth Observatory composite image of the Earth at night in April and May 2012, created using data from the VIIRS DNB sensor on the Suomi National Polar-Orbiting Partnership satellite.

1.1.2.2 Radiance

Current estimates predict that light pollution radiance in the lit areas of the world is increasing by 2.2% per year[1] as a result of increased LED lighting, changes in land use type, increases in population density, and economic indices[1,14-17]. The relative contribution of streetlights to night sky radiance is geographically variable (between 13-56%)[18,19,20] but has been shown to increase threefold following the widespread replacement of conventional lamps with LEDs[14,15,16,17,21,22]. Whilst this may be a direct result of increased luminance per streetlight, it is also attributed to the increased scattering of blue-rich light in the atmosphere, increasing skyglow[17,23]. Other factors correlated with increased light pollution radiance include economics and associated changes in population structure requiring increased illumination, such as increasing per capita and national gross domestic product (GDP), population density, and land-use change[1,24,25].

Spatial and temporal variation in light pollution radiance can be important when assessing the impacts of light pollution on nocturnal animals. Nocturnal activity and many nocturnal behaviours of arthropods are synchronised with, or dependent on, the reduction in ambient light intensity at night. Nightly zenith radiance of indirect light pollution decreases with time, being highest at the start of the evening and decreasing by 5-16% per hour[14,26,27]. Thus, the magnitude of the impacts of light pollution radiance may change with the progression of night and nocturnal activity may occur unimpeded later in the evening. However, crepuscular, or time-sensitive behaviours may be significantly impacted if simultaneously occurring with the brightest part of the night.

1.1.2.3 Spectral composition

Many administrative areas worldwide are retrofitting conventional lighting with more energy efficient and cost-effective LED lamps to reduce public expenditure and carbon emissions[28-31]. One of the most common conventional types being replaced is the high-pressure sodium lamp (HPS). HPS lamps have a narrow spectrum range peaking in the red (~600nm) and contain very little blue light, whereas LED lamps have a broad spectrum with a peak in the blue (~450nm) (Fig.1.3). As a result, and in addition to the radiance changes mentioned above, the transition from HPS to LED lamps causes a shift in the spectral composition of light pollution from longer to shorter wavelengths (i.e., from red to blue).

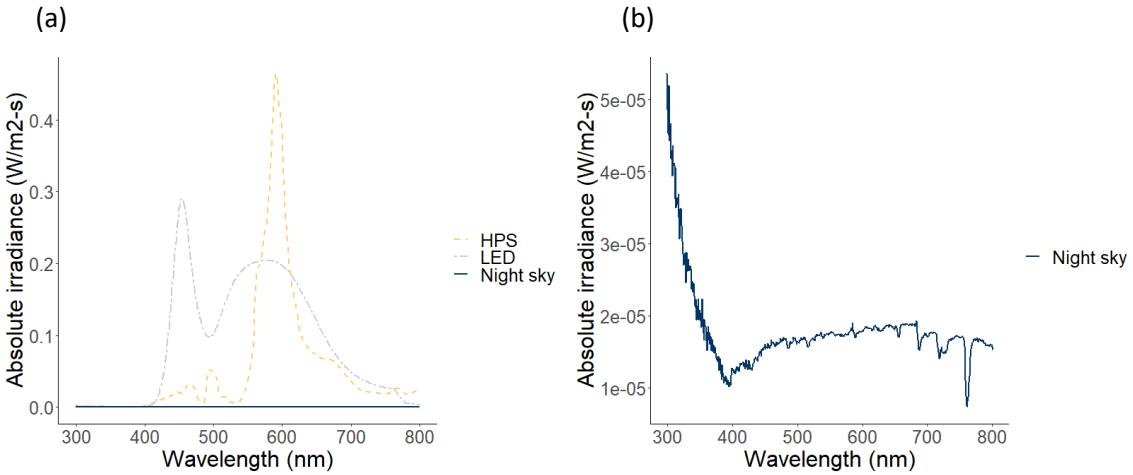

Figure 1.3. (a) Emission spectra of a white LED streetlight (dot-dash grey line), a HPS streetlight (dashed yellow line), and the natural night sky under a full moon (solid blue line). (b) Emission spectra of the natural night sky under a full moon to show the shape of the spectrum which is lost when given alongside the higher relative irradiance of the LED and HPS streetlights. The spectrum of the night sky is similar in shape to daylight, albeit slightly red-shifted, but ~500,000 times weaker in irradiance[32]. All measurements were taken in the Hautes-Pyrénées, France, on the 27th of September 2018 using a QE65000 spectrometer (Ocean Insight Inc.), calibrated to a lamp of known spectral output (DH-2000, Ocean Insight Inc.), and a wide aperture optical fibre (FT1000UMT - 0.39 NA, Ø1000 µm Core Multimode Optical Fibre, Thorlabs LTD.). The natural night spectrum is an average of 6 measurements and the spectra of both streetlights are an average of 10 measurements.

It is well known that arthropods often display a greater sensitivity to shorter wavelengths (perceived by humans as UV, blue, green) and less sensitivity to longer wavelengths (yellow, red)[33]. Broad-spectrum LED light is therefore more likely to result in higher perceived brightness of LEDs compared

to HPS, even if the measured irradiances of the two lights are equal[34-37]. Thus, nocturnal arthropods are at increased risk of disturbance from LED lights[38-41]. In general, lamps emitting low UV, blue and green wavelengths (<550 nm) are considered to be less of a risk to nocturnal arthropods[35,41] leading to the suggestion of spectrally tuning LED lights to emit longer wavelengths to minimise risk whilst maintaining energy efficiency[34].

1.1.3 The impacts of ecological light pollution on nocturnal arthropods

The global spread of light pollution has been identified as a major driver of the decline in insect diversity and biomass worldwide[42-45]. The mechanisms of this decline are varied and complex and include intraspecific to ecosystem-level effects. Generally, these can be grouped into eight key areas: 1) physiology, 2) development, 3) movement, 4) foraging, 5) activity patterns, 6) reproduction, 7) predation, and 8) communication and competition[10,42-49]. Nonetheless, many of these effects can be attributed to one principal impact of light pollution: sensory cue disruption.

Artificial light at night disrupts the use of celestial and terrestrial visual cues by obscuring the light transmitted from the source of the cue[1,6,44,45,46]. Some of these effects will be common across taxa and others may be species-specific and vary with ecology, life history, and geographic location, so it is important to distinguish interspecific effects when forecasting community-level impacts of light pollution. To address this, this thesis will focus on two visually driven behaviours in two evolutionarily and ecologically distant arthropod species. The first is the loss of the skylight polarization pattern as a navigational cue and its effect on orientation and trajectory selection. The second is the disruption of the temporal cue of changing ambient light levels between day and night and its impact on the timing of night-time activity.

1.2 Light pollution and cue disruption

1.2.1 The skylight polarization pattern

1.2.1.1 The polarization of light

A beam of light consists of many electromagnetic waves propagating through space, each with an electric field and magnetic field component that oscillate sinusoidally in orthogonal directions compared to the direction of propagation[50,51]. The polarization of light describes the direction and distribution of the oscillating electric field vectors of its constituent waves[50,51] (Fig.1.4). The angle of polarization (AoP), is the mean axis of oscillation of the constituent electric fields and is typically measured between 0 and 180°[50,51]. The degree of polarization (DoP), represents the proportion of

waves that are oscillating along this predominant axis and is measured between 0 and 1[50,51]. A third property of polarization is the ellipticity which describes the phase relationship between the constituent waves. The ellipticity can range between 0 – linear polarization when all the waves are in phase and 1 – circular polarization where the is an overall phase difference in the beam[50,51]. However, circular and elliptical polarization are rare in nature and so are not considered in this thesis. As such, all following descriptions of the polarization of light refers to linear polarization only.

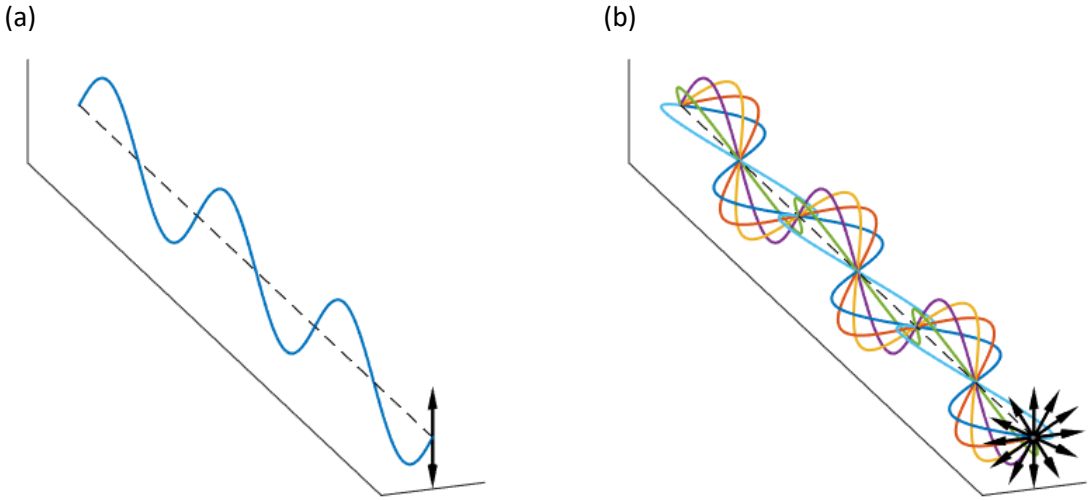

Figure 1.4. The polarization characteristics of a beam of light propagating forward in space (dashed line). (a) A beam of linearly polarized light with a DoP of 1 and an AoP of 0°shown as a single electric field vector field oscillating in the vertical direction (blue line) to aid visualisation, in nature the light beam would consist of many hundreds of light waves oscillating in the same plane. (b) A beam of unpolarized light with a DoP of 0 and no predominant AoP shown as multiple electric field vectors oscillating with a uniform angular distribution (coloured lines). Figure taken from [50].

1.2.1.2 The skylight polarization pattern

The skylight polarization pattern is a visual cue that many diurnal and nocturnal arthropods use for navigation[51]. It is created by the Rayleigh scattering of sunlight (solar polarization pattern) or moonlight (lunar polarization pattern) in the Earth's atmosphere by particles (typically nitrogen and oxygen) smaller than a wavelength of light[50,51]. The combined axes of the electric fields of the scattered light create a gradient in the DoP and AoP relative to the position of the sun or moon, forming a characteristic 'band' of polarized light in the sky (Fig.1.5). This band covers the entire celestial hemisphere and so, represents one of the most conspicuous polarization cues in the terrestrial environment[52].

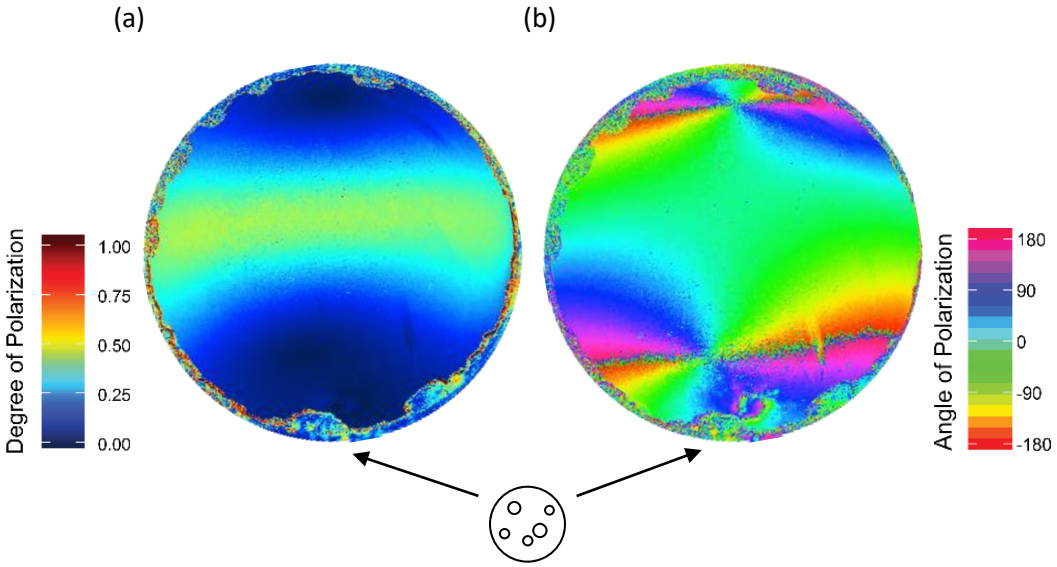

Figure 1.5. Photographic polarimetry images of the (a) DoP and (b) AoP of the skylight polarization pattern at night during a full moon in the southwest of England, UK, on the 28th of June 2018. The approximate position of the full moon is indicated by the two arrows.

Using the solar polarization pattern as an example, nearly all of the light scattered at 90° from the angle of incident sunlight (i.e., perpendicular to the sun) has the same AoP producing a wide band of polarized light of high DoP (Fig.1.6)[51]. The AoP then changes predictably with increasing distance from zenith in either direction, creating a gradient in DoP that reaches near 0 around the sun (solar) and directly opposite the sun (antisolar) (Fig.1.6c)[51,53]. This relationship between the AoP and DoP of the polarization pattern and the angle of incident light is maintained relative to the position of the sun or moon and changes over time with the movement of both celestial bodies (Fig.1.6). These spatial, temporal, and physical characteristics are detectable by polarization-sensitive arthropods even if the celestial body itself is occluded[54-57]. Thus, AoP and DoP of the skylight polarization pattern, as well as being a wide-field visual landmark, combine to provide true celestial compass information from only a small patch of visible sky[58,59].

(a) (b)

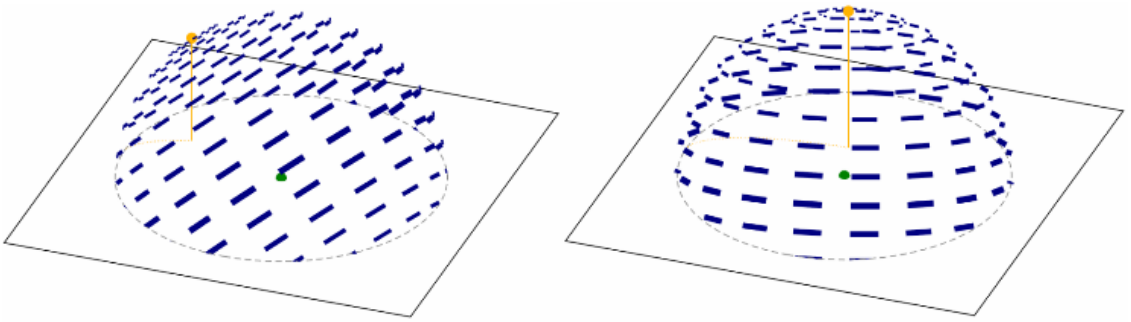

(c)

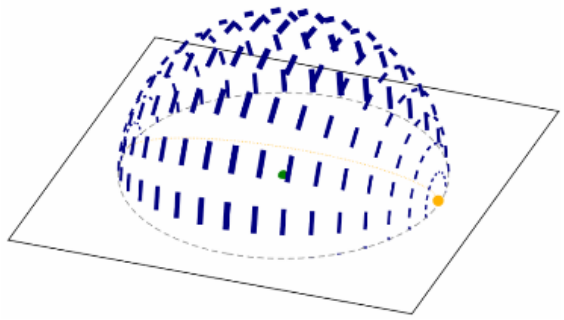

Figure 1.6. The polarization pattern of the sky as viewed by an observer (green point) on the ground with the solar/lunar zenith (yellow point and solid yellow line) relative to the observer at (a) ~45°, (b) ~90°, (c) and ~0° positions. The AoP of the pattern is indicated by the orientation of the dashed lines and the DoP of the pattern is indicated by the width of the dashed. The movement of the sun/moon relative to its starting position is shown by the dashed yellow line. Illustration by Martin How.

1.2.1.3 Fundamental biological sensing of skylight polarization in arthropods

The biological detection of the polarization of light is commonly divided into two types: polarization sensitivity and polarization vision[51,52]. An animal with polarization sensitivity could show a differential sensitivity to the polarization of light but may not be able to determine differences between polarization and chromatic and brightness information[51]. An animal with polarization vision on the other hand, can distinguish between two objects of similar size, shape and other visual properties based on the polarization of light alone, i.e. it is not influenced by the intensity or spectral composition of the light[51,52]. True polarization vision has yet to be behaviourally demonstrated in any animal but is assumed in those capable of polarization-guided navigation due to the inherent need to obtain directional information through the unambiguous detection of the skylight polarization pattern[51,52,60]. Navigation using the skylight polarization pattern is common to several major orders of arthropods, including Lepidoptera[61,62], Coleoptera[63], Araneae[64], Hymenoptera[65], Diptera[66], Decapoda[67], Orthoptera[59,68], and Stomatopoda[69]. The mechanism for detecting polarization is remarkably similar

amongst them and is typically restricted to the optical architecture of skyward-facing eyes or dorsal margins of compound eyes[58]. Generally, polarized light will only be absorbed by an eye if the AoP of light with a DoP that is within the animal's detection threshold is parallel with the mean orientation of the visual pigments[70]. In arthropods, the trans-membrane visual pigments are found in tube-like microvillar projections from the photoreceptor cells (Fig.1.7). The geometry of these microvilli naturally places a greater proportion of the visual pigments parallel with the long axis of the photoreceptors[70]. This creates a built-in dichroism, i.e., a capability to selectively absorb polarized light of different polarization angles[70].

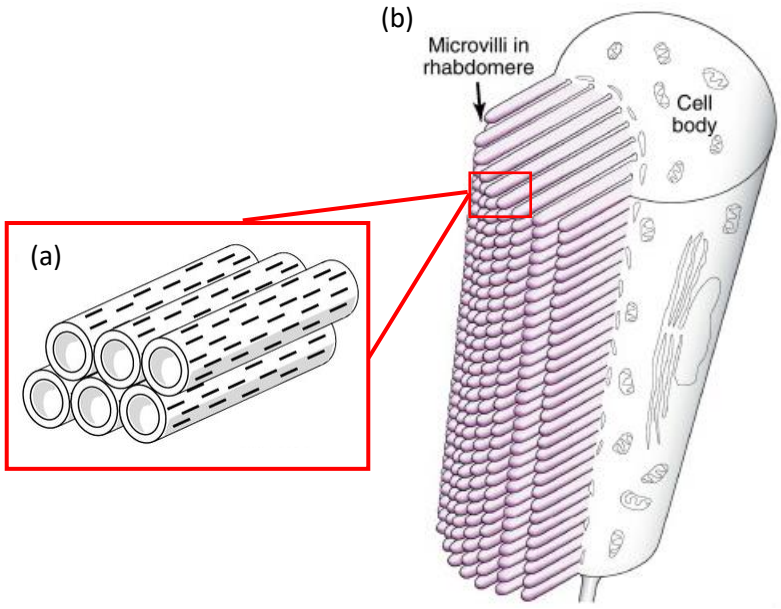

Figure 1.7. The photoreceptor anatomy responsible for detecting the polarization of light in arthropod visual systems. (a) Opsins (black lines) in the membranes of the microvilli (tubes) of the photoreceptor cells are aligned along the long axis of the microvilli. Figure taken from [60]. (b) A model of the longitudinal view of a photoreceptor cell in *Drosophila* showing the photoreceptor cell body and its microvilli projections that form the light-sensitive rhabdomere of the ommatidia of a compound eye. Figure modified from [71].

Arthropod polarization detectors range from simple perpendicular orientated eyes in the Araneae[64] to sophisticated fan-shaped arrays of microvilli aligned in multiple orientations in insects[58]. In the compound eyes of insects, the polarization-sensitive ommatidia are restricted to the top few rows of the dorsal-most part of the eye[72] (known as the dorsal rim area or DRA) (Fig.1.8a). Each patch of sky is analysed by groups of rhabdomeres (the part of the ommatidia containing the light-sensitive microvilli of the photoreceptors) with microvilli of many orientations spread in a fan-shape across the anterior-posterior DRA (Fig.1.8a). Ommatidia with microvilli of similar orientations, which are

therefore sensitive to similar angles of polarization, are grouped into a common neural signal and processed in the POL-neurons in the medulla of the optic lobe[52,73]. These POL-neurons selectively analyse and compare the signal strength (i.e. number of photons absorbed) from groups of ommatidia at axes of orientations that span the field of view of the DRA[74], in field crickets these axes are around 10°, 60°, and 120°[73] (Fig.1.8b). Therefore, each point of a 360° compass can be characterized by a particular response ratio of the POL-neurons[52], resulting in the whole-sky analysis that depends on the AoP and DoP of skylight polarization[58].

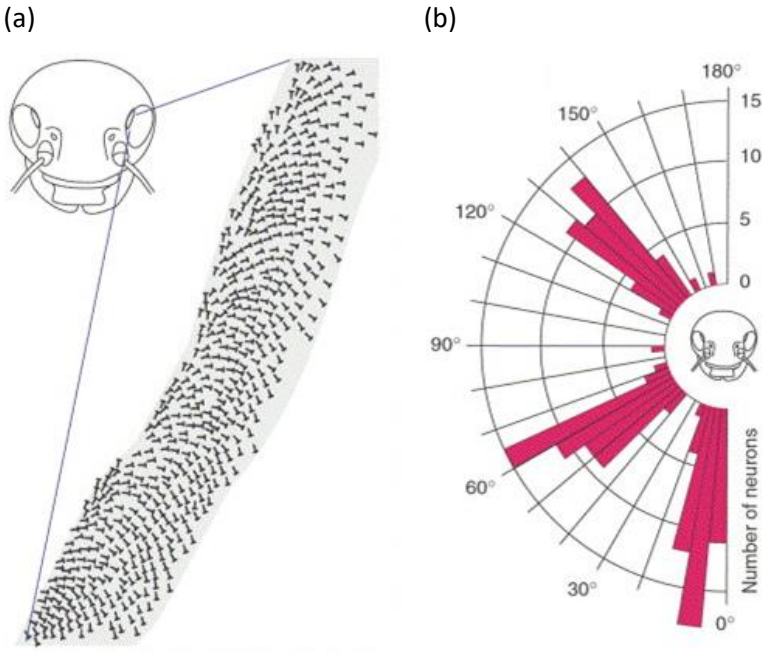

Figure 1.8. (a) The distribution and orientation of microvilli (position and direction of 'T' symbols) in the DRA of a field cricket (*Gryllus campestris*). (b) The three types of POL-neurons in the medulla of the optic lobe of a field cricket tuned to three distinct electric field vector orientations of polarized light at 10°, 60°, and 120° (shown by the histogram of angles eliciting firing in the POL-neurons) relative to the axis of the head. Figure taken from [73].

In the skyward-facing posterior median eyes (PMEs) of some gnaphosid spiders, the optical anatomy responsible for skylight polarization detection is simpler, but less is known about the neural circuitry involved in subsequent processing. The microvilli of the photoreceptors in the PMEs are aligned with the long axis of the eye and contained within a V-shaped reflecting tapetum[75] (Fig.1.9). Light with an AoP parallel to the long axis of the eye is reflected more strongly by the tapetum, enhancing the intrinsic polarization sensitivity of the eyes[75] (Fig.1.9c). The AoP and DoP of the skylight entering the two eyes results in differential absorption of that light and consequently, a differential output due to the opponent processing of the orthogonally aligned left and right eyes[75]. Which neurons and parts

of the brain are involved is currently unknown, but comparative to the neural circuitry of the three POL-neuron system of the field cricket (Fig.1.8), gnaphosid spiders are likely to have a one POL-neuron system where the signals from the two eyes converge and are processed downstream. It is speculated that a single POL-neuron system would be inferior to a three POL-neuron system for navigation, but this has not yet been tested behaviourally[52]. The lens of the PMEs in some spiders has very low focusing power and are unlikely to form sharp images[75]. A lack of focusing optics means that the photoreceptors will have a wide visual field[75] suitable for the detection of a wide-field visual cue like the skylight polarization pattern. Coupled with the polarization-enhancing properties of the V-shaped tapetum, this suggests that the PMEs of some gnaphosid spiders have been adapted for the sole function of skylight polarization detection[75].

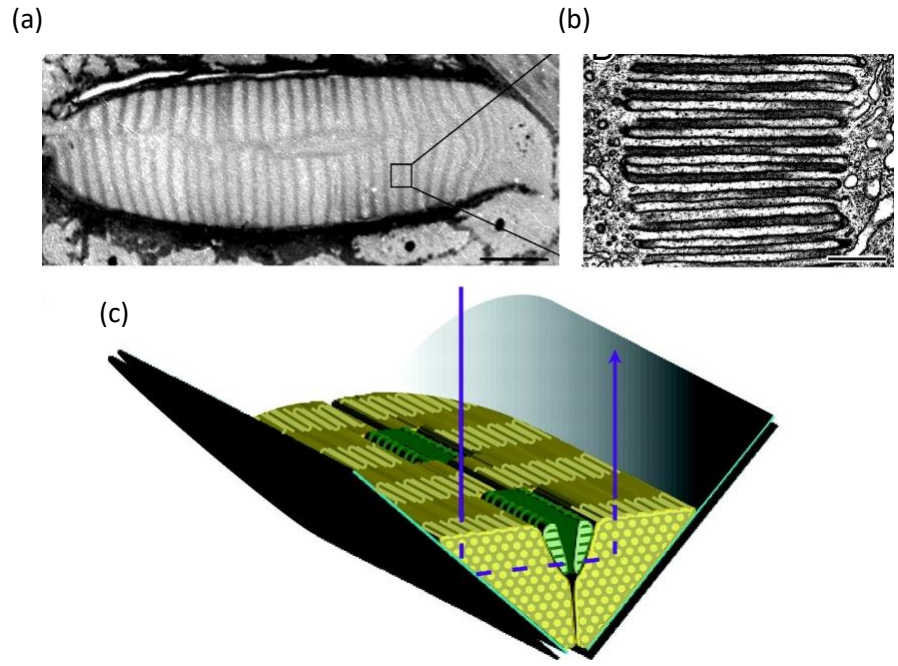

Figure 1.9. The optical anatomy of the polarization-sensitive posterior-median eye of *Drassodes cupreus*. (a) The retina of the eye showing the highly ordered spatial organisation of the photoreceptors (scale bar, 20 µm). (b) An electron micrograph of the boxed region in (a) showing the microvilli of the photoreceptors arranged parallel with the long axis of the eye (scale bar, 1 µm). (c) Schematic of the photoreceptors within the V-shaped reflecting tapetum and the path of incoming light inside the eye (arrow) following reflection by the tapetum (dashed arrow). Figure modified from [75].

1.2.1.4 Navigation using the lunar polarization pattern in arthropods

Navigation using the polarization pattern at night has been demonstrated behaviourally in Orthoptera[59], Coleoptera[63,74], Araneae[75], and the Hymenoptera[76,77]. All of these orders include species that are central place foragers, requiring accurate navigation for nest location following foraging excursions. In Coleoptera, dung beetles also use the polarization pattern for straight-line orientation when dung-rolling to maintain the most direct course away from the dung pile and prevent conspecific competition[63]. In other nocturnal insects with a DRA, polarization-guided navigation can only be assumed based on anatomical evidence or behavioural evidence from diurnal relatives.

In both nocturnal and diurnal lepidopterans, polarization-guided navigation is ambiguous despite evidence of a DRA in an abundance of species[62,78-83]. This has only been investigated behaviourally in a diurnal migrator, the monarch butterfly (*Danaus plexippus*), with conflicting results[62,84]. Reppert *et al*. (2004) showed strong directional changes in individuals inside a flight simulator following a 90° rotation of an overhead polarized cue[62]. However, Stalleicken *et al*. (2005) found limited directional changes to the same stimulus[84]. Furthermore, Stalleicken *et al*. (2005) found no evidence that the DRA plays a role in time-compensation of *D. plexippus*' sun compass when the DRA was occluded in a flight simulator experiment. However, both Stalleicken *et al*. (2006) and Heinze & Reppert (2011) recorded strong intracellular responses to changing AoPs in the ommatidia and sun-compass neurons of the *D. plexippus* DRA[61,85], respectively. It is clear there is still much to be discovered about the functional role of the DRA in the lepidopteran visual system and the importance of skylight polarization to lepidopteran navigation.

1.2.1.5 Light pollution and navigation using the lunar polarization pattern in arthropods

Generally, light from artificial sources is unpolarized (or with a DoP <0.09[86]) and, when mixed with skylight polarization pattern, reduces the proportion of polarized light reaching the ground[86]. This mixing depolarizes the skylight, diluting the DoP of the polarization pattern, and potentially compromises it as a navigational cue. Previous studies have shown that urban skyglow can decrease the mean DoP of the lunar polarization pattern of a full moon from 0.29 to 0.11[86], and the magnitude of this effect is expected to increase during moon phases of lower illuminance[87]. Whether such a reduction is significant to navigation depends on an animal's threshold for detection of polarization[58]. In diurnal arthropods, honeybees still performed accurate 'waggle dances' to direct conspecifics to areas of skylight of 0.10 DoP[88], whilst diurnal dung beetles can reorientate to a change in AoP at degrees of polarization of 0.11[89]. In nocturnal arthropods, reorientation to polarized light of 0.05-0.07 DoP has been shown in the field cricket (*Gryllus campestris* L.), with some individuals

reorientating to light as low as 0.03 DoP[59]. In the dung beetle *Escarabaeus satyrus*, reorientation occurred at an estimated average threshold of detection at 0.11 DoP[87]. All these known behavioural thresholds for polarization sensitivity are close to the observed reductions in the DoP of the polarization pattern caused by light pollution[86]. However, there is very limited studies within the scientific literature that have investigated the link between light pollution and polarization-guided navigation.

The current literature on insect navigation demonstrate declining orientation performance when certain celestial cues are removed, reduced, or misaligned[76,87,90,91,92]. A flexible navigational system is advantageous when moving through environments that experience daily and seasonal changes in meteorological conditions and celestial cycles. However, the addition of anthropogenic light pollution, a stable and persistent mask of natural visual cues, could potentially eliminate the use of cues like the polarization pattern across a large geographical area[1]. Therefore, the masking effect of light pollution on skylight polarization is expected to impact navigational performance, forcing individuals to rely on a reduced set of cues, follow an erroneous trajectory, or become disorientated depending on the magnitude of the effect[59,89-94].

It is notable that anthropogenic air pollution also reduces the DoP of the skylight polarization pattern[95,96]. Aerosols increase the scattering of light in the atmosphere, which changes the distribution of the AoP of skylight [96]. The effect of air pollution on skylight polarization may be significant, but the concentration of aerosol pollutants is highly variable at multiple spatial and temporal scales, making it difficult to assess[97,98]. Given that air pollution concentration and light pollution radiance are likely to co-occur in urban areas, the effects of both are likely to exacerbate impacts to navigating arthropods.

1.2.2 The dark sky at night

1.2.2.1 Patterns of activity and circadian rhythms

Synchronisation of circadian rhythms with the astronomical clock occurs through entrainment to diel changes in the external environment (*Zeitgebers*), the predominant *Zeitgeber* being the change in ambient light between night and day[99]. Many fundamental biological processes are tuned to this external cycle, including gene expression[100,101], metabolic processes[102], activity[103,104,105], and trophic interactions[106]. Their ubiquity across plant and animal phyla highlights the critical importance of circadian rhythms for survival.

1.2.2.2 Fundamental tuning of activity patterns to skylight in arthropods

The mechanism by which circadian rhythms are synchronised to the astronomical clock is also putatively ubiquitous across species[99]. Generally, genes and proteins interact in a molecular feedback loop, known as the transcription-translation feedback loop (TTFL), to generate complex behaviours[99]. Although some of the molecular components vary across kingdoms, the TFFL mechanism is a fundamental characteristic of biological clocks in all organisms[99]. In arthropods, gene expression and the synthesis of related proteins are entrained to ambient light, which regulates cellular activity and related behavioural or physiological activity to a near 24-hour rhythm[99]. Entrainment of this loop with ambient light occurs through the regulation of clock gene transcription by the blue-sensitive visual pigment, cryptochrome (Cry), found in clock neurons in the compound eyes and other light sensitive organs of arthropods[101,107,108,109]. Indeed, Cry and its relevant clock gene families have been linked to diverse and important biological processes such as the timing of seasonal spawning[110] and migration[111,112], time compensation[113], reproductive cycles[114], and initiating diapause[115,116,117]. However, general activity (i.e. whenever the animal is not at rest, including foraging, movement, etc.), both seasonal and diel, is the most rudimentary but arguably fundamental behaviour that is modulated by light-entrained circadian rhythms[118,119,120].

1.2.2.3 The night sky and activity in nocturnal arthropods

Almost all arthropods restrict their activity to the parts of the day that are most advantageous for their specific ecological niche. In nocturnal lepidopterans, the onset of flight[105,120,121,122], eclosion[123], courtship[124], and calling[125] are all entrained to the 24-hour light cycle. Typically, these behaviours occur when ambient light drops to 0-10 lux[105,120,122] during the early evening[120]. The onset of flight only occurs if this drop in illumination occurs at the 'correct' time as anticipated by the animal's biological clock[120], suggesting that the onset of flight is not triggered by a threshold light intensity alone and is indeed a true circadian activity rhythm. Similarly, a latency between falling light levels and the onset of flight suggests that flight only occurs following a physiological "preparatory process"[122], likely to reflect the changes in gene expression occurring in the clock neurons at dusk, providing further evidence that the onset of flight is mediated by an internal biological clock.

In the Araneae, burrow emergence[75,104,126,127,128] and possibly web-building[129] are entrained to the 24-hour light cycle. Less is known about the mechanisms and molecular components of the Araneae biological clock but, like many other organisms, entrainment to ambient light is likely to occur through a visual pathway[130]. The drop in illumination required to trigger the initiation of such behaviours is unknown in Araneae but is expected to be similar to some nocturnal lepidopterans (<10 lux) based on comparable circadian activity profiles[75,105].

1.2.2.4 Light pollution and activity in nocturnal arthropods

Artificial light pollution alters the photoperiod (day length) of the 24-hour day/night cycle[6,48,131] and increases the brightness of the night sky[1]. This can extend the perceived day length and mask the natural changes in ambient light levels that are responsible for triggering or suppressing activity[6,48]. Such disruption to the light cycle can affect both the initiation and the rhythm of activity in arthropods with direct effects on movement and dispersal[132,133,134], mating[132,135], foraging[136,137,138] and parasitism[139]. Given that lepidopteran activity is initiated when ambient light levels reduce to <10 lux, it is plausible that light pollution of similar or greater intensity will cause some maladaptive changes in behaviour in many nocturnal arthropods. In the EU and parts of the USA, streetlighting regulation limits the horizontal lux illuminance of major and minor roads to between 1 and 50 lux depending on road class, roads with vehicular traffic restricted to 7.5-50 lux and cycle and pedestrian paths restricted to 1-15 lux[140,141]. Skyglow luminance is lower, typically resulting in night-time brightness of between 0.01-1.1 lux depending on cloud cover[142], but similar lux values have been shown to alter the timing of flight behaviour in some moth species[120,122]. Therefore, both direct and indirect light pollution can increase the brightness of the night sky to levels above those required to initiate nocturnal activity and are likely to result in the loss of the natural day/night light cycle as a cue for circadian rhythm entrainment.

The magnitude of the effects of light pollution on nocturnal activity is likely to vary with brightness and spectral composition as mentioned in section 1.1. The effects will be species-specific and depend on the absolute sensitivities of different visual systems, which vary with visual pigment composition, eye morphology, and optical filtering[143]. Similarly, impacts will also differ with the spectral composition of the light, which can vary substantially depending on the lighting technology (see section 1.1.2.3), and the spectral sensitivity of the species. Indeed, among lepidopterans, light rich in short wavelengths is more likely to disrupt flight[144-147] and inhibit foraging[148] and reproduction[135]. Establishing brightness thresholds and the impact of spectral composition on nocturnal activity in a wide range of species is critically important for the effective mitigation of light pollution. If the effect of brightness and spectral composition on activity is similar across a range of species, as current evidence suggests[120,122,144,147,149,150], then simple mitigation measures such as reducing the number and intensity of lights and tuning the spectrum of the light could have widespread benefits across the nocturnal world.

1.3 Study species

In the hope of identifying common impacts of light pollution across the arthropod phylum, two arthropod taxa of considerably different ecologies and life histories, but with shared navigational strategies, were chosen for comparison. This will broaden the scope of this work, increase our understanding of the adverse effects of light pollution on the ecology of invertebrates, and provide evidence for informed and effective mitigation of light pollution. Both species are widespread across Europe and can be reliably collected in high numbers.

1.3.1 *Helicoverpa armigera* (Hübner, 1808)

Helicoverpa armigera (previously classified in *Heliothis*[151]), known as the scarce bordered straw or the cotton bollworm, is a polyphagous migratory moth in the family Noctuidae (Order: Lepidoptera). Its larval stage is a significant agricultural pest responsible for annual economic losses in high-value crops such as cotton, soybean, tobacco, and pulses worldwide[151]. It is distributed throughout the tropical and temperate regions of the world; where *H. armigera* is well established, adults undergo impressive seasonal migrations to exploit temporary changes in food availability and suitable breeding grounds.

Life history and ecology

The significance of *H. armigera* as an agricultural pest is attributed to its polyphagy, fecundity, and ability to undergo both facultative migration (adults) and diapause (pupae) in response to unfavourable conditions[151]. Sexually mature females will lay several clutches of up to 3000 eggs across a given year, depending on host plant availability and seasonal weather[151]. After hatching and development, larvae in the pre-pupal stage burrow beneath the soil and enter facultative diapause depending on latitude and season, triggered by shortening days and dropping temperatures, and over-winter as pupae until favourable conditions return in the spring[152,153]. Adults can similarly avoid seasonal weather changes and unfavourable conditions for feeding (low nectar sources) and reproduction (low host plant abundance) by facultative migration[154,155]. Generally, migration occurs *en masse* in sexually immature adults and is triggered by a suite of cues including day length, temperature, weather conditions, and nectar/host plant availability, although the exact triggering mechanisms are unknown[151,154]. Migratory flights last ~2-5 days[156-159], during which individuals can cover distances of ~400 km per night by utilising high-altitude airstreams (>150 m above ground-level)[160,161,162] for up to 11 hours of flight[158,161,162]. In Europe, this equates to impressive seasonal journeys of >1000 km between northern Europe and North Africa[151].

Adult nocturnal activity patterns

Adult *H. armigera* synchronise nocturnal flight with dusk, when ambient light levels are between 0-10 lux[105], but the facultative nature of migration in this species means that flight characteristics vary with season, geographic location, and maturity[105,123,162,163,164]. If adults eclose during a favourable season when nectar sources are plentiful, then flight activity is short in distance and duration, beginning at dusk and lasting around an hour[123]. Sexually mature adults under the same conditions initiate flight at similar times but show two flight activity peaks of 1-2 hours in the first and second halves of the night[105,123,163] and cover larger distances to find mates and oviposition sites[123]. Conversely, if adults eclose during an unfavourable season when food sources are low, many individuals will initiate migratory flight. Nonetheless, migratory flight begins immediately after dusk and lasts up to 11 hours before dropping significantly around dawn[105,161,162]. Research also suggests that the timing of migration is influenced by moonlight, possibly due to the lunar azimuth and the lunar polarization pattern being an important navigational cue[163,165,166]. However, discrepancies between relative catch rates in light and pheromone traps brings into question the reliability of data collected from bright light traps on evenings of low moon illuminance[164]. Irrespective of flight motivation and the lunar cycle, *H. armigera* synchronises the start of flight with dusk, emphasising the critical importance of this period for the entrainment of circadian rhythms in adult nocturnal activity.

Polarization vision in the DRA

A DRA has not yet been identified in *H. armigera* by histological, or physiological methods. However, specialised dorsal ommatidia that assist polarization-guided navigation are well-conserved within hexapods[72] and a DRA has been identified in several lepidopteran species of similar ecology and morphology[79-83,167]. Generally, the lepidopteran DRA comprises ~100 ommatidia distributed across 2-4 rows[85,168] at the base of the antenna[80,85,167,168] (Fig.1.10). The rhabdoms and POL-neurons of the DRA detect skylight polarization using opponent processing as described in section 1.2.1.3 and probably have high polarization sensitivity[85,167] similar to the DRA of the compound eyes of other insects[169-172]. However, behavioural thresholds of polarization sensitivity are yet to be established in the Lepidoptera. The spectral sensitivity of the lepidopteran DRA is also likely to be consistent with other insects, with peak sensitivities in the UV, blue, or green[85,167]. Indeed, short- (~400 nm), medium- (~550 nm), and longer-wavelength (>550 nm) sensitive opsins have been identified in the compound eyes of *H. armigera*[100] but their distribution across the eye is unknown.

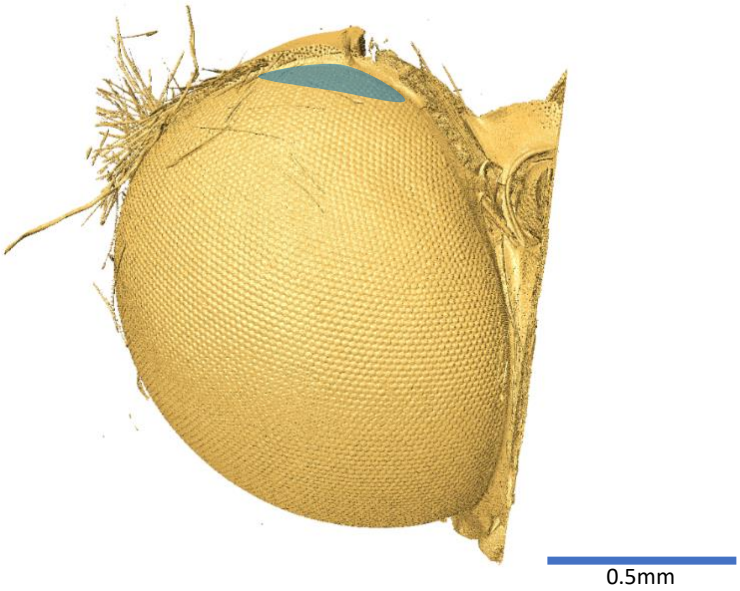

Figure 1.10. A reconstructed 3D image of the of the right eye of *Helicoverpa armigera*, with the approximate location of a potentially polarization-sensitive DRA indicated by the blue shaded area. Produced in Avizo Lite v9.4 (Thermo Fisher) using radiographic projections acquired during synchrotron X-ray microtomography at beamline I13-2 of Diamond Light Source (Harwell, UK).

1.3.2 *Drassodes* spp.

Species within the genus *Drassodes* (Order: Araneae) are members of the family of spiders known as the ground spiders (Gnaphosidae) due to their use of active hunting rather than the prey-capture web commonly associated with spiders[173,174]. They are distributed throughout the tropical and temperate regions of the world, with >20 species found in Europe and three species found in the UK[173,174]. Two of the most common and widespread species in Europe and the UK, *Drassodes cupreus* (Blackwall, 1834) and *Drassodes lapidosus* (Walckenaer, 1802), are anatomically indistinct and share similar habitat preferences[173]. As such, it is assumed that the individuals used in the experiments of the following chapters are both *Drassodes cupreus* and *Drassodes lapidosus*. As the two species are anatomically and ecologically indistinguishable, their behavioural responses are expected to be similar and the inclusion of both is not expected to affect the results of the experiments.

Life history and ecology

Drassodes spp., commonly known as the stone spiders, has a strong association with rocky habitats and rocky features within grassland and heathland such as dry-stone walls[173]. During the day, *Drassodes* spp. shelter in silken retreats between stones or grassy tussocks, emerging in the evening

to forage[173]. They are aggressive nocturnal hunters of ground-dwelling arthropods, including other spiders, that they actively chase and immobilise with silk before consuming[173,175]. As central place foragers, *Drassodes* spp. return to their retreats after feeding, with evidence that they use the skylight polarization pattern to guide the homeward trajectory[75]. The duration and distance of these foraging and homing journeys are unknown. Adults are active in the spring and summer, when females will lay up to ~50 eggs in silk cocoons that she will then guard until the spiderlings hatch and disperse (unpublished observation). *Drassodes* spp. are predominantly solitary, but mature males can sometimes be found in the retreats of late-instar juvenile females with whom they will mate upon reaching sexual maturity[173].

Nocturnal activity patterns

Drassodes spp. synchronise nocturnal foraging activity with dusk[75] with maximum peaks in activity occurring immediately after sunset and remaining high for around 4 hours, before declining to very low levels of activity before dawn[75]. Variation in activity patterns in relation to life history stage is unknown, as are the effects of unfavourable conditions and prey availability on foraging characteristics. Nonetheless, the entrainment of foraging activity to dusk emphasises the critical importance of the natural 24-hour light cycle to foraging success.

Polarization vision in the PMEs

The physiological basis of skylight polarization detection in the PMEs of *Drassodes* spp. is described in section 1.2.1.3. Generally, polarization information detected by each eye is thought to be converted to a signal and the relative signal strength from the two perpendicular PMEs (Fig 1.11) are presumably compared through opponent processing[75]. The polarization sensitivity of the PMEs is high, similar to the DRA of some insects[169-172]. However, like the lepidopterans, a behavioural threshold of polarization detection is yet to be established in any spider. The spectral sensitivity of the *Drassodes* spp. PMEs was also consistent with the DRA of insects and other spiders[85,167,**176**], with wavelengths of maximum absorbance at 350 nm and 500 nm[75]. As the PMEs lack image-forming optics, polarization information may be integrated across the visual field of the whole eye (~60°)[75]. Thus, unlike the Ledpioptera, *Drassodes* sp. almost certainly cannot detect high-resolution spatial information from the skylight polarization pattern such as gradients in DoP and AoP. It has been suggested that such an eye design is best suited for the detection of the polarization pattern at dusk and dawn, when the AoP and DoP gradients are more uniform, and that *Drassodes* spp. synchronises peak foraging activity with dusk to maximise the efficacy of polarization-guided navigation[75]. However, *Drassodes* spp. are active throughout the night and the length and duration of their journeys is unknown; individuals may begin

their outward journey around sunset and forage for several hours post-sunset before returning to their retreats.

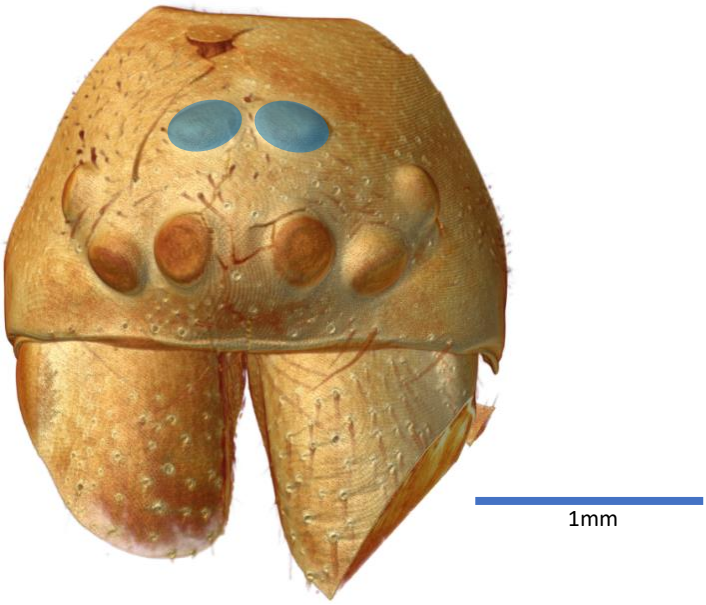

Figure 1.11. A reconstructed 3D image of the head of *Drassodes* sp., the ventral section of the chelicera containing the fangs are cropped, the location of the polarization-sensitive PMEs are shown by the blue shaded areas. Produced in Avizo Lite v9.4 (Thermo Fisher) using radiographic projections acquired during synchrotron X-ray microtomography at beamline I13-2 of Diamond Light Source (Harwell, UK).

1.4 Research questions

This PhD project aims to answer important questions on the physical and behavioural mechanisms linking light pollution to widespread insect declines, with a particular emphasis on the effect of cue disruption on polarization-guided navigation and the timing of nocturnal activity. Previous research comparing skylight DoP in an urban and non-urban location has demonstrated that light pollution diminishes the skylight polarization pattern[86], but nocturnal skylight is dynamic and the spatial and temporal changes in skylight polarization under light pollution across the lunar cycle is yet to be documented. Therefore, the first question was, **1. How does light pollution affect the characteristics of the skylight polarization pattern across the lunar cycle (chapter 2)?** Similarly, the relationship between light pollution radiance and the characteristics of the skylight polarization pattern has yet to be established, so, the second question was, **2. How does the diminishing effect of light pollution on the skylight polarization pattern change with radiance (chapter 2)?** This led to the related question,

3. Does a model of the nocturnal arthropod visual system show a similar relationship between light pollution radiance and the detection of the polarization pattern (chapter 2)?

The answer to these initial research questions informed the development of a behavioural assay to test for the effect of a diminished polarization pattern on polarization-guided navigation in *H. armigera* and *Drassodes* sp.. There is no research on the effects of light pollution on polarization-guided navigation, nor on the mechanisms that might drive such effects, and polarization-guided navigation has yet to be discovered in any nocturnal lepidopteran despite phylogenetic and morphological indications it might be present. Additionally, behavioural thresholds of polarization sensitivity are largely unknown across the arthropod phyla, so how such thresholds correspond to the spatial and temporal degradation of the skylight polarization pattern by light pollution has yet to be explored. It was therefore also important to establish **4. How does light pollution affect polarization-guided navigation in moths (chapter 3) and spiders (chapter 4)?,** and **5. What are the behavioural thresholds of polarization detection in moths and spiders and how do they correlate with light pollution radiance (chapter 4)?**

Preliminary experiments and observations of the behaviour of *H. armigera* and *Drassodes* sp. in the wild led to additional questions about the effects of light pollution on the more fundamental aspects of behaviour, most notably the nocturnal activity patterns in flight and foraging. Light is a major *Zeitgeber* for the entrainment of activity and light pollution increases the brightness of the night sky which led to the question, **6. Does light pollution affect the timing and onset of migratory flight and foraging in moths and spiders (chapter 5)?** It is well known that the visual systems of most arthropods are maximally sensitive to shorter wavelengths, which has raised concerns within the scientific community about the impact of the global transition from long-wavelength-shifted lighting technology to short-wavelength rich LEDs. There is much literature on the impacts of different lighting technologies on lepidopteran behaviour and abundance but little on the onset of migratory flight, and there is no existing research on the impacts of artificial light of any kind on ground spiders. Therefore, the final questions were, **7. How does artificial light of different spectral compositions affect the timing of flight and foraging behaviour in spiders and moths (chapter 5)?** and the related question, **8. Does the magnitude of this effect scale with radiance (chapter 5)?**

These questions will establish how different characteristics of light pollution affects the availability of important visual cues for navigation, and how this might subsequently impair effective navigation and the timing and initiation of nocturnal journeys. In working to answer them, this project will open new research avenues for determining behavioural links between light pollution and the global loss of

invertebrate biodiversity and provide evidence of specific relevance for mitigating the impacts of light pollution on the nocturnal world.

References

1. Owens ACS, Cochard P, Durrant J, Farnworth B, Perkin EK, Seymoure B. 2020. Light pollution is a driver of insect declines. *Biological Conservation*, **241**: 108259. (DOI: 10.1016/j.biocon.2019.108259)
2. Gaston KJ, Ackermann S, Bennie J, Cox DTC, Phillips BB, de Miguel AS, Sanders D. 2021. Pervasiveness of biological impacts of artificial light at night. *Integrative and Comparative Biology*, **61**(3): 1098-1110. (DOI: 10.1093/icb/icab145)
3. Kyba CCM, Kuester T, de Miguel AS, Baugh K, Jechow A, Hölker F, Bennie J, Elvidge CD, Gaston KJ, Guanter L. 2017. Artificially lit surface of Earth at night increasing in radiance and extent. *Science Advances*, **3**(11): e1701528. (DOI: 10.1126/sciadv.1701528)
4. Foster JJ, Tocco C, Smolka J, Khaldy L, Baird E, Byrne MJ, Nilsson DE, Dacke M. 2021. Light pollution forces a change in dung beetle orientation behavior. *Current Biology*, **31**(17): 3935-3942. (DOI: 10.1016/j.cub.2021.06.038)
5. Torres D, Tidau S, Jenkins S, Davies T. 2020. Artificial skyglow disrupts celestial migration at night. *Current Biology*, **30**(12): E696-E697. (DOI: 10.1016/j.cub.2020.05.002)
6. Gaston KJ, Davies TW, Nedelec SL, Holt LA. 2017. Impacts of artificial light at night on biological timings. *Annual Review of Ecology, Evolution, and Systematics*, **48**: 49-68. (DOI: 10.1146/annurev-ecolsys-110316-022745)
7. Kyba CCM, Ruhtz T, Fischer J, Hölker F. 2011. Cloud coverage acts as an amplifier for ecological light pollution in urban ecosystems. *PLOS One*, **(6)**3: e17307. (DOI: 10.1371/journal.pone.0017307)
8. Falchi F, Cinzano P, Duriscoe D, Kyba CM, Elvidge CD, Baugh K, Portnov BA, Rybnikova NA, Furgoni R. 2016. The new world atlas of artificial night sky brightness. *Science Advances*, **2**(6): e1600377. (DOI: 10.1126/sciadv.1600377)
9. Cox DTC, Sanchez de Miguel A, Bennie J, Dzurjak SA, Gaston KJ. 2022. Majority of artificially lit Earth surface associated with the non-urban population. *The Science of the total environment*, **841**: 156782. (DOI: 10.1016/j.scitotenv.2022.156782)
10. Davies TW, Duffy JP, Bennie J, Gaston KJ. 2014. The nature, extent, and ecological implications of marine light pollution. *Frontiers in Ecology and the Environment*, **12**(6): 347-355. (DOI: 10.1890/130281)
11. Garrett JK, Donald PF, Gaston KJ. 2020. Skyglow extends into the world's Key Biodiversity Areas. *Animal Conservation*, **23**(2): 153-159. (DOI: 10.1111/acv.12480)
12. Gaston KJ, Duffy JP, Bennie J. 2015. Quantifying the erosion of natural darkness in the global protected area system. *Conservation Biology*, **29**(4): 1132-1141. (DOI: 10.1111/cobi.12462)
13. Davies TW, Duffy JP, Bennie J, Gaston KJ. 2016. Stemming the tide of light pollution encroaching into marine protected areas. *Conservation Letters*, **9**(3): 164-171. (DOI: 10.1111/conl.12191)
14. Hung LW, Anderson SJ, Pipkin A, Fristrup K. 2021. Changes in night sky brightness after a countywide LED retrofit. *Journal of Environmental Management*, **292**: 112776. (DOI: 10.1016/j.jenvman.2021.112776)
15. Robles J, Zamorano J, Pascual S, de Miguel AS, Gallego J, Gaston KJ. 2021. Evolution of brightness and color of the night sky in Madrid. *Remote Sensing*, **13**(8): 1511. (DOI: 10.3390/rs13081511)

16. Kollath Z, Domeny A, Kollath K, Nagy B. 2016. Qualifying lighting remodelling in a Hungarian city based on light pollution effects. *Journal of Quantitative Spectroscopy & Radiative Transfer*, **181**: 46-51. (DOI: 10.1016/j.jqsrt.2016.02.025)
17. Aube M. 2015. Physical behaviour of anthropogenic light propagation into the nocturnal environment. *Philosophical Transactions of the Royal Society B*, **370**: 20140117. (DOI: 10.1098/rstb.2014.0117)
18. Kyba CCM, Ruby A, Kuechly HU, Kinzey B, Miller N, Sanders J, Barentine J, Kleinodt R, Espey B. 2021. Direct measurement of the contribution of street lighting to satellite observations of nighttime light emissions from urban areas. *Lighting Research & Technology*, **53**(3): 189-211. (DOI: 10.1177/1477153520958463)
19. Sciezor T. 2021. Effect of street lighting on the urban and rural night-time radiance and the brightness of the night sky. *Remote Sensing*, **13**(9): 1654. (DOI: 10.3390/rs13091654)
20. Bara S, Rodriguez-Aros A, Perez M, Tosar B, Lima R, de Miguel AD, Zamorano J. 2019. Estimating the relative contribution of streetlights, vehicles, and residential lighting to the urban night sky brightness. *Lighting Research & Technology*, **51**(7): 1092-1107. (DOI: 10.1177/1477153518808337)
21. de Miguel AS, Bennie J, Rosenfeld E, Dzurjak S, Gaston KJ. 2021. First estimation of global trends in nocturnal power emissions reveals acceleration of light pollution. *Remote Sensing*, **13**(16): 3311. (DOI: 10.3390/rs13163311)
22. Luginbuhl CB, Boley PA, Davis DR. 2014. The impact of light source spectral power distribution on sky glow. *Journal of Quantitative Spectroscopy & Radiative Transfer*, **139**: 21-26. (DOI: 10.1016/j.jqsrt.2013.12.004)
23. Bierman A. 2012. Will switching to LED outdoor lighting increase sky glow? *Lighting Research & Technology*, **44**(4): 449-458. (DOI: 10.1177/1477153512437147)
24. Biggs JD, Fouche T, Bilki F, Zadnik MG. 2012. Measuring and mapping the night sky brightness of Perth, Western Australia. *Monthly Notices of the Royal Astronomical Society*, **421**(2): 1450-1464. (DOI: 10.1111/j.1365-2966.2012.20416.x)
25. Pun CSJ, So CW. 2012. Night-sky brightness monitoring in Hong Kong. *Environmental Monitoring and Assessment*, **184**(4): 2537-2557. (DOI: 10.1007/s10661-011-2136-1)
26. Kyba CCM, Tong KP, Bennie J, Birriel I, Birriel JJ, Cool A, Danielsen A, Davies TW, den Outer PN, Edwards W, Ehlert R, Falchi F, Fischer J, Giacomelli A, Giubbilini F, Haaima M, Hesse C, Heygster G, Hölker F, Inger R, Jensen LJ, Kuechly HU, Kuehn J, Langill P, Lolkema DE, Nagy M, Nievas M, Ochi N, Popow E, Posch T, Puschnig J, Ruhtz T, Schmidt W, Schwarz R, Schwope A, Spoelstra H, Tekatch A, Trueblood M, Walker CE, Weber M, Welch DL, Zamorano J, Gaston KJ. 2015. Worldwide variations in artificial skyglow. *Scientific Reports*, **5**: 8409. (DOI: 10.1038/srep12180)
27. Kyba CCM, Ruhtz T, Fischer J, Hölker F. 2012. Red is the new black: how the colour of urban skyglow varies with cloud cover. *Monthly Notices of the Royal Astronomical Society*, **425**(1): 701-708. (DOI: 10.1111/j.1365-2966.2012.21559.x)
28. Baddiley C. 2018. Light pollution modelling, and measurements at Malvern Hills AONB, of county conversion to blue rich LEDs. *Journal of Quantitative Spectroscopy & Radiative Transfer*, **219**: 142-173. (DOI: 10.1016/j.jqsrt.2018.05.011)
29. Pagden M, Ngahane K, Amin SR. 2020. Changing the colour of night on urban streets - LED vs. part-night lighting system. *Socio-Economic Planning Sciences*, **69**: 100692. (DOI: 10.1016/j.seps.2019.02.007)

30. Sedziwy A, Basiura A, Wojnicki I. 2018. Roadway lighting retrofit: Environmental and economic impact of greenhouse gases footprint reduction. *Sustainability*, **10**(11): 3925. (DOI: 10.3390/su10113925)
31. Baddiley C. 2021. Light pollution colour changes at MHAONB, from distant town conversions to blue-rich LED lighting, implications for rural UK skies. *Journal of Quantitative Spectroscopy & Radiative Transfer*, **267**: 107574. (DOI: 10.1016/j.jqsrt.2021.107574)
32. Cronin TW, Johnsen S, Marshall NJ, Warrant EJ. 2014. Light and the optical environment. In: Visual ecology. Princeton University Press, Woodstock, Oxfordshire, UK.
33. van der Kooi CJ, Stavenga DG, Arikawa K, Belušič G, Kelber A. 2021. Evolution of insect color vision: From spectral sensitivity to visual ecology. *Annual Review of Entomology*, **66**: 435-461. (DOI: 10.1146/annurev-ento-061720-071644)
34. Gaston KJ, Davies TW, Bennie J, Hopkins J. 2012. Review: Reducing the ecological consequences of night-time light pollution: options and developments. *Journal of Applied Ecology*, **49**(6): 1256-1266. (DOI: 10.1111/j.1365-2664.2012.02212.x)
35. Longcore T, Rodriguez A, Witherington B, Penniman JF, Herf L, Herf M. 2018. Rapid assessment of lamp spectrum to quantify ecological effects of light at night. *Journal of Experimental Zoology Part A*, **329**(8-9): 511-521. (DOI: 10.1002/jez.2184)
36. Cronin TW, Johnsen S, Marshall NJ, Warrant EJ. 2014. Color vision. In: Cronin TW, Johnsen S, Marshall NJ, Warrant EJ (eds) Visual ecology. Princeton University Press, Woodstock, Oxfordshire, UK.
37. Davies TW, Bennie J, Inger R, De Ibarra NH, Gaston KJ. 2013. Artificial light pollution: are shifting spectral signatures changing the balance of species interactions? *Global Change Biology*, **19**(5): 1417-1423. (DOI: 10.1111/gcb.12166)
38. Boyes DH, Evans DM, Fox R, Parsons MS, Pocock MJO. 2021. Street lighting has detrimental impacts on local insect populations. *Science Advances*, **7**(35): eabi8322. (DOI: 10.1126/sciadv.abi8322)
39. Macgregor CJ, Pocock MJO, Fox R, Evans DM. 2019. Effects of street lighting technologies on the success and quality of pollination in a nocturnally pollinated plant. *Ecosphere*, **20**(1): e02550. (DOI: 10.1002/ecs2.2550)
40. Wakefield A, Broyles M, Stone EL, Harris S, Jones G. 2018. Quantifying the attractiveness of broad-spectrum street lights to aerial nocturnal insects. *Journal of Applied Ecology*, **55**(2): 714-722. (DOI: 10.1111/1365-2664.13004)
41. Pawson SM, Bader MKF. 2014. LED lighting increases the ecological impact of light pollution irrespective of color temperature. *Ecological Applications*, **24**(7): 1561-1568. (DOI: 10.1890/14-0468.1)
42. Boyes DH, Evans DM, Fox R, Parsons MS, Pocock MJO. 2021. Is light pollution driving moth population declines? A review of causal mechanisms across the life cycle. *Insect Conservation and Diversity*, **14**(2): 167-187. (DOI: 10.1111/icad.12447)
43. Grubisic M, van Grunsven RHA. 2021. Artificial light at night disrupts species interactions and changes insect communities. *Current Opinion in Insect Science*, **47**: 136-141. (DOI: 10.1016/j.cois.2021.06.007)
44. Desouhant E, Gomes E, Mondy N, Amat I. 2019. Mechanistic, ecological, and evolutionary consequences of artificial light at night for insects: review and prospective. *Entomologia Experimentalis Et Applicata*, **167**(1): 37-58. (DOI: 10.1111/eea.12754)

45. Owens ACS, Lewis SM. 2018. The impact of artificial light at night on nocturnal insects: A review and synthesis. *Ecology and Evolution*, **8**(22): 11337-11358. (DOI: 10.1002/ece3.4557)
46. Gaston KJ, de Miguel AS. 2022. Environmental impacts of artificial light at night. *Annual Review of Environment and Resources*, **41**(1). (DOI: 10.1146/annurev-environ-112420-014438)
47. Macgregor CJ, Pocock MJO, Fox R, Evans DM. 2015. The dark side of street lighting: impacts on moths and evidence for the disruption of nocturnal pollen transport. *Ecological Entomology*, **40**(3): 187-198. (DOI: 10.1111/een.12174)
48. Gaston KJ, Duffy JP, Gaston S, Bennie J, Davies TW. 2014. Human alteration of natural light cycles: causes and ecological consequences. *Oecologia*, **176**(4): 917-931. (DOI: 10.1007/s00442-014-3088-2)
49. Longcore T, Rich C. 2004. Ecological light pollution. *Frontiers in Ecology and the Environment*, **2**(4): 191-198. (DOI: 10.2307/3868314)
50. Foster JJ, Temple SE, How MJ, Daly IM, Sharkey CR, Wilby D, Roberts NW. 2018. Polarisation vision: overcoming challenges of working with a property of light we barely see. *Science of Nature*, **105**: 27. (DOI: 10.1007/s00114-018-1551-3)
51. Johnsen S. 2014. Polarization. In: Johnsen S. (eds) The optics of life: A biologists guide to light and nature. Princeton University Press, Woodstock, Oxfordshire, UK.
52. Wehner R. 2001. Polarization vision – A uniform sensory capacity? *The Journal of Experimental Biology*, **204**(14): 2589-2596. (DOI: 10.1242/jeb.204.14.2589)
53. Heinze S. 2014. Polarized-light processing in insect brains: Recent insights from the desert locust, the monarch butterfly, the cricket, and the fruit fly. In: Horváth G. (eds) Polarized Light and Polarization Vision in Animal Sciences. Springer Series in Vision Research, vol 2. Springer, Berlin, Heidelberg. (DOI: 10.1007/978-3-642-54718-8_4)
54. Hegedüs R, Barta A, Bernath B, Meyer-Rochow VB, Horvath G. 2007. Imaging polarimetry of forest canopies: how the azimuth direction of the sun, occluded by vegetation, can be assessed from the polarization pattern of the sunlit foliage. *Applied Optics*, **46**(23): 6019-6032. (DOI: 10.1364/ao.46.006019)
55. Hegedüs R, Akesson S, Horvath G. 2007. Polarization patterns of thick clouds: overcast skies have distribution of the angle of polarization similar to that of clear skies. *Journal of the Optical Society of America A*, **24**(8): 2347-2356. (DOI: 10.1364/josaa.24.002347)
56. Cronin TW, Shashar N, Caldwell RL, Marshall J, Cheroske AG, Chiou TH. 2003. Polarization signals in the marine environment. Proceedings of SPIE, **5158**. (DOI: 10.1117/12.507903)
57. Pomozi I, Horvath G, Wehner R. 2001. How the clear-sky angle of polarization pattern continues underneath clouds: full-sky measurements and implications for animal orientation. *Journal of Experimental Biology*, **204**(17): 2933-2942. (DOI: 10.1242/jeb.204.17.2933)
58. Cronin TW, Johnsen S, Marshall NJ, Warrant EJ. 2014. Polarization vision. In: Cronin TW, Johnsen S, Marshall NJ, Warrant EJ. (eds) Visual ecology. Princeton University Press, Woodstock, Oxfordshire, UK.
59. Henze MJ, Labhart T. 2007. Haze, clouds and limited sky visibility: polarotactic orientation of crickets under difficult stimulus conditions. *Journal of Experimental Biology*, **210**(18): 3266-3276. (DOI: 10.1242/jeb.007831)
60. Labhart, T. 2016. Can invertebrates see the e-vector of polarization as a separate modality of light? *Journal of Experimental Biology*, **219**(24): 3844-3856. (DOI: 10.1242/jeb.139899)
61. Heinze S, Reppert SM. 2011. Sun compass integration of skylight cues in migratory monarch butterflies. *Neuron*, **69**(2): 345-58. (DOI: 10.1016/j.neuron.2010.12.025)

62. Reppert SM, Zhu HS, White RH. 2004. Polarized light helps monarch butterflies navigate. *Current Biology*, **14**(2): 155-8. (DOI: 10.1016/j.cub.2003.12.034)
63. Dacke M, Baird E, el Jundi B, Warrant EJ, Byrne M. 2021. How dung beetles steer straight. In: Douglas AE, (eds). *Annual Review of Entomology*, **66**: 243-56. (DOI: 10.1007/s00359-012-0764-8)
64. Dacke M, Doan TA, O'Carroll DC. 2001. Polarized light detection in spiders. *Journal of Experimental Biology*, **204**(14): 2481-90. (DOI: 10.1242/jeb.204.14.2481)
65. Zeil J, Ribi WA, Narendra A. 2014. Polarization vision in ants, bees and wasps. In: Horváth G, (eds), 2nd Ed., Polarized light and polarization vision in animal sciences. Springer Series in Vision Research, vol 2. Springer, Berlin, Heidelberg.
66. Warren TL, Giraldo YM, Dickinson MH. 2019. Celestial navigation in Drosophila. *Journal of Experimental Biology*, **222**(Suppl_1): jeb186148. (DOI: 10.1242/jeb.186148)
67. Goddard SM, Forward RB. 1991. The role of the underwater polarized-light pattern, in sun compass navigation of the grass shrimp, *Palaemonetes vulgaris*. *Journal of Comparative Physiology A*, **169**(4): 479-91.
68. Matsubara N, Okada R, Sakura M. 2021. Possible role of polarized light information in spatial recognition in the cricket *Gryllus bimaculatus*. *Zoological Science*, **38**(4): 297-304. (DOI: 10.2108/zs200081)
69. Patel RN, Cronin TW. 2020. Mantis shrimp navigate home using celestial and idiothetic path integration. *Current Biology*, **30**(11): 1981-7. (DOI: 10.1016/j.cub.2020.03.023)
70. Land MF, Nilsson D-E. 2012. Light and vision. In: Land MF, Nilsson D-E. (eds), 2nd Ed., Animal eyes. Oxford University Press, Oxford, Oxfordshire, UK.
71. Montell C. 2012. Drosophila visual transduction. *Trends in Neurosciences*, **35**(6): 356-363. (DOI: 10.1016/j.tins.2012.03.004)
72. Labhart T, Meyer EP. 1999. Detectors for polarized skylight in insects: A survey of ommatidial specializations in the dorsal rim area of the compound eye. *Microscopy Research and Technique*, **47**(6): 368-379. (DOI: 10.1002/(sici)1097-0029(19991215)47:6<368::aid-jemt2>3.3.co;2-h)
73. Labhart T, Meyer EP. 2002. Neural mechanisms in insect navigation: polarization compass and odometer. *Current Opinion in Neurobiology*, **12**(6): 707-714. (DOI: 10.1016/s0959-4388(02)00384-7)
74. el Jundi B, Pfeiffer K, Heinze S, Homberg U. 2014. Integration of polarization and chromatic cues in the insect sky compass. *Journal of Comparative Physiology A*, **200**(6): 575-589. (DOI: 10.1007/s00359-014-0890-6)
75. Dacke M, Nilsson DE, Warrant EJ, Blest AD, Land MF, O'Carroll DC. 1999. Built-in polarizers form part of a compass organ in spiders. *Nature*, **401**(6752): 470-473. (DOI: 10.1038/46773)
76. Freas CA, Narendra N, Lemesle C, Cheng K. 2017. Polarized light use in the nocturnal bull ant, *Myrmecia midas*. *Royal Society Open Science*, **4**: 170598. (DOI: 10.1098/rsos.170598)
77. Reid SF, Narendra A, Hemmi JM, Zeil J. 2011. Polarised skylight and the landmark panorama provide night-active bull ants with compass information during route following. *Journal of Experimental Biology*, **214**(3): 363-370. (DOI: 10.1242/jeb.049338)
78. Mappes M, Homberg U. 2004. Behavioral analysis of polarization vision in tethered flying locusts. *Journal of Comparative Physiology A*, **190**(1): 61-8. (DOI: 10.1007/s00359-003-0473-4)

79. Antonerxleben F, Langer H. 1988. Functional morphology of the ommatidia in the compound eye of the moth, *Antheraea polyphemus* (Insecta, Saturniidae). *Cell and Tissue Research*, **252**(2): 385-396. (DOI: 10.1007/BF00214381)
80. Hammerle B, Kolb G. 1996. Retinal ultrastructure of the dorsal eye region of *Pararge aegeria* (Linne) (Lepidoptera: Satyridae). *International Journal of Insect Morphology & Embryology*, **25**(3): 305-315. (DOI: 10.1016/0020-7322(96)00003-7)
81. Hammerle B, Kolb G. 1987. Structure of the dorsal eye region of the moth, *Adoxophyes reticulana HB* (Lepidoptera, Tortricidae). *International Journal of Insect Morphology & Embryology*, **16**(2): 121-129. (DOI: 10.1016/0020-7322(87)90012-2)
82. Kolb G. 1986. Retinal ultrastructure in the dorsal rim and large dorsal area of the eye of *Aglais urticae* (Lepidopteran). *Zoomorphology*, **106**(4): 244-246. (DOI: 10.1007/bf00312045)
83. Meinecke, C. C. 1981. The fine structure of the compound eye of the African armyworm moth, *Spodoptera exempta* walk (Lepidoptera, Noctuidae). *Cell and Tissue Research*, **216**(2): 333-347. (DOI: 10.1007/BF00233623)
84. Stalleicken J, Mukhida M, Labhart T, Wehner R, Frost B, Mouritsen H. 2005. Do monarch butterflies use polarized skylight for migratory orientation? *Journal of Experimental Biology*, **208**(12): 2399-2408. (DOI: 10.1242/jeb.01613)
85. Stalleicken J, Labhart T, Mouritsen H. 2006. Physiological characterization of the compound eye in monarch butterflies with focus on the dorsal rim area. *Journal of Comparative Physiology A*, **192**(3): 321-331. (DOI: 10.1007/s00359-005-0073-6)
86. Kyba CCM, Ruhtz T, Fischer J, Hölker F. 2011. Lunar skylight polarization signal polluted by urban lighting. *Journal of Geophysical Research-Atmospheres*, **116**: D24106. (DOI: 10.1029/2011JD016698)
87. Foster JJ, Kirwan JD, el Jundi B, Smolka J, Khaldy L, Baird E. Byrne MJ, Nilsson DE, Johnsen S, Dacke M. 2019. Orienting to polarized light at night - matching lunar skylight to performance in a nocturnal beetle. *Journal of Experimental Biology*, **222**(2): jeb188532. (DOI: 10.1242/jeb.188532)
88. Frisch von K. 1967. Orientation on long-distance flights. In: Frisch von K. (eds) The dance language and orientation of bees. Harvard University Press, Cambridge, MA, US.
89. Khaldy L, Foster JJ, Yilmaz A, Belušič G, Gagnon Y, Tocco C, Byrne MJ, Dacke M. 2022. The interplay of directional information provided by unpolarised and polarised light in the heading direction network of the diurnal dung beetle *Kheper lamarcki*. *Journal of Experimental Biology*, **225**(3): jeb243734. (DOI: 10.1242/jeb.243734)
90. Dreyer D, Frost B, Mouritsen H, Gunther A, Green K, Whitehouse M, Johnsen S, Heinze S, Warrant E. 2018. The Earth's magnetic field and visual landmarks steer migratory flight behaviour in the nocturnal Australian bogong moth. *Current Biology*, **28**: 2160-2166. (DOI: 10.1016/j.cub.2018.05.030)
91. el Jundi B, Smolka J, Baird E, Byrne MJ, Dacke M. 2014. Diurnal dung beetles use the intensity gradient and the polarization pattern of the sky for orientation. *Journal of Experimental Biology*, **217**: 2422-2429. (DOI: 10.1242/jeb.101154)
92. Wehner R. 1997. The ant's celestial compass system: spectral and polarization channels. In: Lehrer M, (eds). Orientation and communication in arthropods. Birkhäuser Verlag, Basel, Switzerland.

93. Dacke M, Byrne M, Smolka J, Warrant E, Baird E. 2013. Dung beetles ignore landmarks for straight-line orientation. *Journal of Comparative Physiology A*, **199**(1): 17-23. (DOI: 10.1007/s00359-012-0764-8)
94. Dovey KM, Kemfort JR, Towne WF. 2013. The depth of the honeybee's backup sun-compass systems. *Journal of Experimental Biology*, **216**(11): 2129-39. (DOI: 10.1242/jeb.084160)
95. Cui Y, Zhang XG, Zhou XC, Liu YF, Chu JK. 2019. Effect of aerosol on polarization distribution of sky light. *Acta Optica Sinica*, **39**(6): 0601001. (DOI: 10.3788/aos201939.0601001)
96. Kreuter A, Emde C, Blumthaler M. 2010. Measuring the influence of aerosols and albedo on sky polarization. *Atmospheric Research*, **98**(2-4): 363-367. (DOI: 10.1016/j.atmosres.2010.07.010)
97. Cavazzani S, Ortolani S, Bertolo A, Binotto R, Fiorentin P, Carraro G, Zitelli V. 2020. Satellite measurements of artificial light at night: aerosol effects. *Monthly Notices of the Royal Astronomical Society*, **499**(4): 5075-5089. (DOI: 10.1093/mnras/staa3157)
98. Liu YP, Wu JG, Yu DY, Hao RF. 2018. Understanding the patterns and drivers of air pollution on multiple time scales: The case of Northern China. *Environmental Management*, **61**(6): 1048-1061. (DOI: 10.1007/s00267-018-1026-5)
99. Foster RG, Kreitzman L. 2017. Circadian rhythms: A 24-hour phenomenon. In: Foster RG, Kreitzman L. (eds) Circadian rhythms: A very short introduction. Oxford University Press, Oxford, Oxfordshire, UK.
100. Yan S, Zhu JL, Zhu WL, Zhang XF, Li Z, Liu XX, Zhang QW. 2014. The expression of three opsin genes from the compound eye of *Helicoverpa armigera* (Lepidoptera: Noctuidae) is regulated by a circadian clock, light conditions and nutritional status. *PLOS One*, **9**(10): e111683. (DOI: 10.1371/journal.pone.0111683)
101. Hardin PE. 2011. Molecular Genetic Analysis of circadian timekeeping in *Drosophila*. *Genetics of Circadian Rhythms*, **74**: 141-173. (DOI: 10.1016/b978-0-12-387690-4.00005-2)
102. Bumgarner R, Nelson J. 2021. Light at night and disrupted circadian rhythms alter physiology and behavior. *Integrative and Comparative Biology*, **61**(3): 1160-1169. (DOI: 10.1093/icb/icab017)
103. Schlichting M, Grebler R, Menegazzi P, Helfrich-Förster C. 2015. Twilight dominates over moonlight in adjusting *Drosophila's* activity pattern. *Journal of Biological Rhythms*, **30**(2): 117-128. (DOI: 10.1177/0748730415575245)
104. Norgaard T, Henschel JR, Wehner R. 2006. The night-time temporal window of locomotor activity in the Namib Desert long-distance wandering spider, *Leucorchestris arenicola*. *Journal of Comparative Physiology A*, **192**(4): 365-372. (DOI: 10.1007/s00359-005-0072-7)
105. Persson B. 1971. Influence of light on flight activity of Noctuids (Lepidoptera) in South Sweden. *Insect Systematics & Evolution*, **2**: 215–232. (DOI: 10.1163/187631271X00220)
106. Bennie J, Davies TW, Cruse D, Inger R, Gaston KJ. 2018. Artificial light at night causes top-down and bottom-up trophic effects on invertebrate populations. *Journal of Applied Ecology*, **55**(6): 2698-2706. (DOI: 10.1111/1365-2664.13240)
107. Kistenpfennig C, Hirsh J, Yoshii T, Helfrich-Förster C. 2012. Phase-shifting the fruit fly clock without cryptochrome. *Journal of Biological Rhythms*, **27**(2): 117-125. (DOI: 10.1177/0748730411434390)
108. Helfrich-Förster C, Winter C, Hofbauer A, Hall JC, Stanewsky R. 2001. The circadian clock of fruit flies is blind after elimination of all known photoreceptors. *Neuron*, **30**(1): 249-261. (DOI: 10.1016/s0896-6273(01)00277-x)

109. Stanewsky R, Kaneko M, Emery P, Beretta B, Wager-Smith K, Kay SA, Rosbash M, Hall J.C. 1998. The cry(b) mutation identifies cryptochrome as a circadian photoreceptor in *Drosophila*. *Cell*, **95**(5): 681-692. (DOI: 10.1016/s0092-8674(00)81638-4)
110. Zantke J, Ishikawa-Fujiwara T, Arboleda E, Lohs C, Schipany K, Hallay N, Straw AD, Todo T, Tessmar-Raible K. 2013. Circadian and circalunar clock interactions in a marine annelid. *Cell Reports*, **5**(1): 99-113. (DOI: 10.1016/j.celrep.2013.08.031)
111. Häfker NS, Meyer B, Last KS, Pond DW, Hueppe L, Teschke M. 2017. Circadian clock involvement in zooplankton diel vertical migration. *Current Biology*, **27**(14): 2194-2201. (DOI: 10.1016/j.cub.2017.06.025)
112. Zhan S, Merlin C, Boore JL, Reppert SM. 2011. The monarch butterfly genome yields insights into long-distance migration. *Cell*, **147**(5): 1171-1185. (DOI: 10.1016/j.cell.2011.09.052)
113. Merlin C, Gegear RJ, Reppert SM. 2009. Antennal circadian clocks coordinate sun compass orientation in migratory monarch butterflies. *Science*, **325**(5948): 1700-1704. (DOI: 10.1126/science.1176221)
114. Xu J, Gao B, Shi M-R, Yu H, Huang L-Y, Chen P, Li Y-H. 2019. Copulation exerts significant effects on mRNA expression of cryptochrome genes in a moth. *Journal of Insect Science*, **19**(2): 3;1-8. (DOI: 10.1093/jisesa/iez016)
115. Kozak GM, Wadsworth CB, Kahne SC, Bogdanowicz SM, Harrison RG, Coates BS, Dopman EB. 2019. Genomic basis of circannual rhythm in the European corn borer moth. *Current Biology*, **29**(20): 3501-3509. (DOI: 10.1016/j.cub.2019.08.053)
116. Meuti ME, Denlinger DL. 2013. Evolutionary links between circadian clocks and photoperiodic diapause in insects. *Integrative and Comparative Biology*, **53**(1): 131-143. (DOI: 10.1093/icb/ict023)
117. Ikeno T, Tanaka SI, Numata H, Goto SG. 2010. Photoperiodic diapause under the control of circadian clock genes in an insect. *BMC Biology*, **8**: 116. (DOI: 10.1186/1741-7007-8-116)
118. Horn M, Mitesser O, Hovestadt T, Yoshii T, Rieger D, Helfrich-Förster C. 2019. The circadian clock improves fitness in the fruit fly, *Drosophila melanogaster*. *Frontiers in Physiology*, **10**. (DOI: 10.3389/fphys.2019.01374)
119. Schlichting M, Helfrich-Förster C. 2015. Photic entrainment in *Drosophila* assessed by locomotor activity recordings. In: Circadian rhythms and biological clocks, Part B. *Methods in enzymology*, **552**: 105-203. (DOI: 10.1016/bs.mie.2014.10.017)
120. Chen F, Shi J, Keena M. 2016. Evaluation of the effects of light intensity and time interval after the start of scotophase on the female flight propensity of Asian gypsy moth (Lepidoptera: Erebidae). *Environmental Entomology*, **45**(2): 404-409. (DOI: 10.1093/ee/nvv222)
121. Charlton RE, Carde RT, Wallner WE. 1999. Synchronous crepuscular flight of female Asian gypsy moths: Relationships of light intensity and ambient and body temperatures. *Journal of Insect Behaviour*, **12**(4): 517-531. (DOI: 10.1023/a:1020918924471)
122. Dreisig H. 1980. The importance of illumination level in the daily onset of flight activity in nocturnal moths. Physiological Entomology, **5**: 327–342. (DOI: 10.1111/j.1365-3032.1980.tb00243.x)
123. Riley JR, Armes NJ, Reynolds DR, Smith AD. 1992. Nocturnal observations on the emergence and flight behaviour of *Helicoverpa armigera* (Lepidoptera, Noctuidae) in the post-rainy season in central India. *Bulletin of Entomological Research*, **82**(2): 243-256. (DOI: 10.1017/s0007485300051798)

124. Li X-W, Jia X-T, Xiang H-M, Diao HL, Yan Y, Wang Y, Ma RY. 2019. The effect of photoperiods and light intensity on mating behavior and reproduction of *Grapholita molesta* (Lepidoptera: Tortricidae). *Environmental Entomology*, **48**(5): 1035-1041. (DOI: 10.1093/ee/nvz066)
125. Schal C, Carde RT. 1986. Effects of temperature and light on calling in the tiger moth *Holomelina lamae* (Freeman) (Lepidoptera, Arctiidae). *Physiological Entomology*, **11**(1): 75-87. (DOI: 10.1111/j.1365-3032.1986.tb00392.x)
126. Mah A, Ayoub N, Toporikova N, Jones TC, Moore D. 2020. Locomotor activity patterns in three spider species suggest relaxed selection on endogenous circadian period and novel features of chronotype. *Journal of Comparative Physiology A*, **206**(4): 499-515. (DOI: 10.1007/s00359-020-01412-y)
127. Jones TC, Wilson RJ, Moore D. 2018. Circadian rhythms of locomotor activity in Metazygia wittfeldae (Araneae: Araneidae). *Journal of Arachnology*, **46**(1): 26-30. (DOI: 10.1636/JoA-S-17-036.1)
128. Ortega J, Ruiz M, Fernandezmontraveta C. 1992. Daily patterns of locomotor activity in a Lycosid spider. *Journal of Interdisciplinary Cycle Research*, **23**(4): 295-301. (DOI: 10.1080/09291019209360188)
129. Moore D, Watts JC, Herrig A, Jones TC. 2016. Exceptionally short-period circadian clock in *Cyclosa turbinata*: regulation of locomotor and web-building behavior in an orb-weaving spider. *Journal of Arachnology*, **44**(3): 388-396. (DOI: 10.1636/JoA-S-16-014.1)
130. Ortega-Escobar J. 2002. Circadian rhythms of locomotor activity in *Lycosa tarentula* (Araneae, Lycosidae) and the pathways of ocular entrainment. *Biological Rhythm Research*, **33**(5): 561-576. (DOI: 10.1076/brhm.33.5.561.13934)
131. Liu JA, Melendez-Fernandez OH, Bumgarner JR, Nelson RJ. 2022. Effects of light pollution on photoperiod-driven seasonality. *Hormones and Behavior*, **141**: 105150. (DOI: 10.1016/j.yhbeh.2022.105150)
132. Levy K, Wegrzyn Y, Efronny R, Barnea A, Ayali A. 2021. Lifelong exposure to artificial light at night impacts stridulation and locomotion activity patterns in the cricket *Gryllus bimaculatus*. *Proceedings of the Royal Society B*, **288**: 20211626. (DOI: 10.1098/rspb.2021.1626)
133. Duarte C, Quintanilla-Ahumada D, Anguita C, Manriquez PH, Widdicombe S, Pulgar J, Silva-Rodriguez EA, Miranda C, Manriquez K, Quijon PA. 2019. Artificial light pollution at night (ALAN) disrupts the distribution and circadian rhythm of a sandy beach isopod. *Environmental Pollution*, **248**: 565-573. (DOI: 10.1016/j.envpol.2019.02.037)
134. Holt CS, Waters TF. 1967. Effect of light intensity on the drift of stream invertebrates. *Ecology*, **48**(2): 225-234. (DOI: 10.2307/1933104)
135. van Geffen KG, van Eck E, de Boer RA, van Grunsven RHA, Salis L, Berendse F, Veenendaal EM. 2015. Artificial light at night inhibits mating in a geometrid moth. *Insect Conservation and Diversity*, **8**(3): 282-287. (DOI: 10.1111/icad.12116)
136. Czarnecka M, Kobak J, Grubisic M, Kakareko T. 2021. Disruptive effect of artificial light at night on leaf litter consumption, growth and activity of freshwater shredders. *Science of the Total Environment*, **786**: 147407. (DOI: 10.1016/j.scitotenv.2021.147407)
137. Lynn KD, Quintanilla-Ahumada D, Anguita C, Widdicombe S, Pulgar J, Manriquez PH, Quijon PA, Duarte C. 2021. Artificial light at night alters the activity and feeding behaviour of sandy beach amphipods and pose a threat to their ecological role in Atlantic Canada. *Science of the Total Environment*, **780**: 146568. (DOI: 10.1016/j.scitotenv.2021.146568)

138. Luarte T, Bonta CC, Silva-Rodriguez EA, Quijon PA, Miranda C, Farias AA, Duarte C. 2016. Light pollution reduces activity, food consumption and growth rates in a sandy beach invertebrate. *Environmental Pollution*, **218**: 1147-1153. (DOI: 10.1016/j.envpol.2016.08.068)
139. Kehoe R, Sanders D, Cruse D, Silk M, Gaston KJ, Bridle JR, van Veen F. 2020. Longer photoperiods through range shifts and artificial light lead to a destabilizing increase in host-parasitoid interaction strength. *Journal of Animal Ecology*, **89**(11): 2508-2516. (DOI: 10.1111/1365-2656.13328)
140. Suk JY, Walter RJ. 2019. New nighttime roadway lighting documentation applied to public safety at night: A case study in San Antonio, Texas. *Sustainable Cities and Society*, **46**: 101459. (DOI: 10.1016/j.scs.2019.101459)
141. European Standards EN 13201-2. 2003. Road lighting – Part 2: Performance requirements. Brussels: European Committee for Standardization.
142. Jechow A, Kyba CCM, Hölker F. 2020. Mapping the brightness and color of urban to rural skyglow with all-sky photometry. *Journal of Quantitative Spectroscopy & Radiative Transfer*, **250**: 106988. (DOI: 10.1016/j.jqsrt.2020.106988)
143. Land MF, Nilsson, D-E. 2012. What makes a good eye? In: Land MF, Nilsson, D-E. (eds) Animal eyes. Oxford, Oxford University Press.
144. Brehm G, Niermann J, Nino LMJ, Enseling D, Justel T, Axmacher JC, Warrant E, Fiedler K. 2021. Moths are strongly attracted to ultraviolet and blue radiation. *Insect Conservation and Diversity*, **14**(2): 188-198. (DOI: 10.1111/icad.12476)
145. Plummer KE, Hale JD, O'Callaghan MJ, Sadler JP, Siriwardena GM. 2016. Investigating the impact of street lighting changes on garden moth communities. *Journal of Urban Ecology*, **2**(1): juw004. (DOI: 10.1093/jue/juw004)
146. Somers-Yeates R, Hodgson D, McGregor PK, Spalding A, Ffrench-Constant RH. 2013. Shedding light on moths: shorter wavelengths attract noctuids more than geometrids. *Biology Letters*, **9**(4): 20130376. (DOI: 10.1098/rsbl.2013.0376)
147. van Langevelde, F, Ettema JA, Donners M, WallisDeVries MF, Groenendijk D. 2011. Effect of spectral composition of artificial light on the attraction of moths. *Biological Conservation*, **144**(9): 2274-2281. (DOI: 10.1016/j.biocon.2011.06.004)
148. van Langevelde F, van Grunsven RHA, Veenendaal EM, Fijen TPM. 2017. Artificial night lighting inhibits feeding in moths. *Biology Letters*, **13**(3): 20160874. (DOI: 10.1098/rsbl.2016.0874)
149. Soteras F, Camps A, Costas M, Giaquinta A, Peralta G, Cocucci AA. 2022. Fragility of nocturnal interactions: Pollination intensity increases with distance to light pollution sources but decreases with increasing environmental suitability. *Environmental Pollution*, **292**: 118350. (DOI: 10.1016/j.envpol.2021.118350)
150. Wakefield A, Broyles M, Stone EL, Harris S, Jones G. 2017. Quantifying the attractiveness of broad-spectrum streetlights to aerial nocturnal insects. *Journal of Applied Ecology*, **55**(2): 714-722. (DOI: 10.1111/1365-2664.13004)
151. Fitt GP. 1989. The ecology of Heliothis species in relation to agroecosystems. *Annual Review of Entomology*, **34**: 17-52. (DOI: 10.1146/annurev.en.34.010189.000313)
152. Shimizu K, Fujisaki K. 2006. Geographic variation in diapause induction under constant and changing conditions in *Helicoverpa armigera*. *Entomologia Experimentalis Et Applicata*, **121**(3): 253-260. (DOI: 10.1111/j.1570-8703.2006.00483.x)
153. Shimizu K, Fujisaki K. 2006. Timing of diapause induction and overwintering success in the cotton bollworm *Helicoverpa armigera* (Hb.) (Lepidoptera: Noctuidae) under outdoor

conditions in temperate Japan. *Applied Entomology and Zoology*, **41**(1): 151-159. (DOI: 10.1303/aez.2006.151)

154. Jones CM, Parry H, Tay WT, Reynolds DR, Chapman JW. 2019. Movement ecology of pest *Helicoverpa*: Implications for ongoing spread. *Annual Review of Entomology*, **64**: 277-295. (DOI: 10.1146/annurev-ento-011118-111959)
155. Jyothi P, Aralimarad P, Wali V, Dave S, Bheemanna M, Ashoka J, Shivayogiyappa P, Lim KS. 2021. Evidence for facultative migratory flight behavior in *Helicoverpa armigera* (Noctuidae: Lepidoptera) in India. *PLOS One*, **16**(1): e0245665. (DOI: 10.1371/journal.pone.0245665)
156. Satterfield DA, Sillett TS, Chapman JW, Altizer S, Marra PP. 2020. Seasonal insect migrations: massive, influential, and overlooked. *Frontiers in Ecology and the Environment*, **18**(6): 335-344. (DOI: 10.1002/fee.2217)
157. Coombs M. 1997. Tethered-flight and age-related reproductive performance of *Helicoverpa punctigera* (Wallengren) and *H. armigera* (Hubner) (Lepidoptera: Noctuidae). *Australian Journal of Zoology*, **45**(4): 409-422. (DOI: 10.1071/zo96064)
158. Colvin J, Gatehouse AG. 1993. Migration and genetic regulation of the pre-reproductive period in the cotton bollworm moth, *Helicoverpa armigera*. *Heredity*, **70**: 407-412. (DOI: 10.1038/hdy.1993.57)
159. Colvin J, Gatehouse AG. 1993. Migration and the effect of 3 environmental factors on the pre-reproductive period of the cotton bollworm moth, *Helicoverpa armigera*. *Physiological Entomology*, **18**(2): 109-113. (DOI: 10.1111/j.1365-3032.1993.tb00456.x)
160. Chapman JW, Reynolds DR, Mouritsen H, Hill JK, Riley JR, Sivell D, Smith AD, Woiwod IP. 2008. Wind selection and drift compensation optimize migratory pathways in a high-flying moth. *Current Biology*, **18**(7): 514-518. (DOI: 10.1016/j.cub.2008.02.080)
161. Feng HQ, Wu XF, Wu B, Wu KM. 2009. Seasonal Migration of *Helicoverpa armigera* (Lepidoptera: Noctuidae) over the Bohai Sea. *Journal of Economic Entomology*, **102**(1): 95-104. (DOI: 10.1603/029.102.0114)
162. Feng HQ, Wu KM, Cheng DF, Guo YY. 2004. Northward migration of *Helicoverpa armigera* (Lepidoptera: Noctuidae) and other moths in early summer observed with radar in northern China. *Journal of Economic Entomology*, **97**(6): 1874-1883. (DOI: 10.1093/jee/97.6.1874)
163. Saito, O. 2000. Flight activity changes of the cotton bollworm, *Helicoverpa armigera* (Hubner) (Lepidoptera: Noctuidae), by aging and copulation as measured by flight actograph. *Applied Entomology and Zoology*, **35**(1): 53-61. (DOI: 10.1303/aez.2000.53)
164. Dent DR, Pawar CS. 1988. The influence of moonlight and weather on catches of *Helicoverpa armigera* (Hübner) (Lepidoptera, Noctuidae) in light and pheromone traps. *Bulletin of Entomological Research*, **78**(3): 365-377. (DOI: 10.1017/s0007485300013146)
165. Nowinszky L, Puskas J, Barczikay G. 2015. The relationship between polarized moonlight and the number of pest microlepidoptera specimens caught in pheromone traps. *Polish Journal of Entomology*, **84**(3): 163-176. (DOI: 10.1515/pjen-2015-0014)
166. Sotthibandhu S, Baker RR. 1979. Celestial orientation by the large yellow underwing moth, *Noctua pronuba* L. *Animal Behaviour*, **27**: 786-800. (DOI: 10.1016/0003-3472(79)90015-0)
167. Belušič G, Sporar K, Meglic A. 2017. Extreme polarisation sensitivity in the retina of the corn borer moth *Ostrinia*. *Journal of Experimental Biology*, **220**(11): 2047-2056. (DOI: 10.1242/jeb.153718)

168. Labhart T, Baumann F, Bernard GD. 2009. Specialized ommatidia of the polarization-sensitive dorsal rim area in the eye of monarch butterflies have non-functional reflecting tapeta. *Cell and Tissue Research*, **338**(3): 391-400. (DOI: 10.1007/s00441-009-0886-7)
169. Dacke M, Nordstrom P, Scholtz CH, Warrant EJ. 2002. A specialized dorsal rim area for polarized light detection in the compound eye of the scarab beetle *Pachysoma striatum*. *Journal of Comparative Physiology A*, **188**(3): 211-216. (DOI: 10.1007/s00359-002-0295-9)
170. Labhart T. 1986. The electrophysiology of photoreceptors in different eye regions of the desert ant, *Cataglyphis bicolour*. *Journal of Comparative Physiology A*, **158**(1): 1-7. (DOI: 10.1007/bf00614514)
171. Labhart T, Hodel B, Valenzuela I. 1984. The physiology of the crickets compound eye with particular reference to the anatomically specialized dorsal rim area. *Journal of Comparative Physiology*, **155**(3): 289-296. (DOI: 10.1007/bf00610582)
172. Labhart T. 1980. Specialized photoreceptors at the dorsal rim of the honeybees compound eye – Polarization and angular sensitivity. *Journal of Comparative Physiology*, **141**(1): 19-30. (DOI: 10.1007/bf00611874)
173. Bee L, Oxford G, Smith H. 2020. Gnaphosidae. In: Bee L, Oxford G, Smith H. (eds), 2nd Ed., Britain's spiders – A field guide. Princeton University Press, Woodstock, Oxfordshire, UK.
174. Azevedo GHF, Griswold CE, Santos AJ. 2018. Systematics and evolution of ground spiders revisited (Araneae, Dionycha, Gnaphosidae). *Cladistics*, **34**(6): 579-626. (DOI: 10.1111/cla.12226)
175. Michálek O, Petrakova L, Pekar S. 2017. Capture efficiency and trophic adaptations of a specialist and generalist predator: A comparison. *Ecology and Evolution*, **7**(8): 2756-2766. (DOI: 10.1002/ece3.2812)
176. Morehouse NI, Buschbeck EK, Zurek DB, Steck M, Porter ML. 2017. Molecular evolution of spider vision: new opportunities, familiar players. *Biological Bulletin*, **233**(1): 21-38. (DOI: 10.1086/693977)

2

Light pollution and the skylight polarization pattern

This chapter contains measurements of the temporal and spatial characteristics of the skylight polarization pattern taken using photographic polarimetry at several sites across Europe. This work describes major differences in the polarization pattern between dark and light-polluted skies across four moon phases and explores the relationship between light pollution radiance and the availability of the lunar polarization pattern as a navigational cue. These findings are placed in the context of *Helicoverpa armigera* and *Drassodes* sp. visual systems as species that use navigation for long distance migrations and central place foraging walks, respectively. These results inform the experiments described in chapters 3-5 to test the effects of light pollution on the activity and navigation of *Helicoverpa armigera* and *Drassodes* sp.

Contributions: Myself and my supervisors, Nicholas Roberts (University of Bristol) and Lauren Sumner-Rooney (Leibniz Institute for Biodiversity and Evolution Research), collected the data. I collected and embedded the heads of *Drassodes* sp. and *H. armigera* in resin to be scanned by myself and Lauren Sumner-Rooney at beamline I13-2 of Diamond Light Source. Nicholas Roberts produced the photographic polarimetry images and modelled the photoreceptor contrast. I performed the data analysis and authored the chapter in discussion with my supervisors.

2.1 Background

The skylight polarization pattern is a 'band' of polarized light created by the Rayleigh scattering of sunlight or moonlight in the Earth's atmosphere[1]. The distribution of both the angles and degrees of polarization of the scattered light creates a pattern that depends on the position of the sun or moon. This pattern is used by many polarization-sensitive arthropods as a wide-field visual landmark or for the acquisition of compass information for orientation during nocturnal journeys (see chapter 1, section 1.2.1). The pattern is a reliable visual cue as the physical characteristics that inform orientation persist under a range of meteorological conditions, under canopy cover, and in water[2-5]. However, at night, urban skyglow caused by light pollution reduces the degree of polarization (DoP) of the lunar

polarization pattern[6]potentially compromising navigation in nocturnal arthropods, with subsequent implications for species fitness and dispersal[7-11]. Such impacts are likely to worsen as light pollution increases in both geographic range and intensity[6].

At dusk, the relative contribution of sunlight and moonlight to the polarization pattern changes. The solar polarization pattern is dominant in the sky until the sun drops >12^{o} below the horizon at sunset, when it is superseded by the lunar polarization pattern[12,13]. At sunrise the same sequence happens in reverse. The lunar contribution is a strong function of the phases in the lunar cycle which defines the percentage of illumination, azimuth, and time of moon rise[6,12,13]. If the moon is not illuminated, does not rise during the night, or is occluded by overcast conditions, no skylight polarization pattern will be present following sunset. However, the behaviour of the lunar polarization pattern is relatively unexplored, particularly in the context of species-dependent considerations. Given that any nocturnal navigation using the skylight polarization pattern cannot occur in the absence of moonlight, determining the relationship between the lunar polarization pattern and moon phase is fundamental to our understanding of nocturnal navigation.

Similarly, urban skyglow caused by anthropogenic light pollution reduces the DoP of the lunar polarization pattern by depolarizing the skylight through the addition of unpolarized (or marginally polarized) artificial light[6], which may affect navigational performance in nocturnal arthropods (see chapter 1, section 1.2.1.5). As the radiance of light pollution increases, so does the magnitude of the effect on the DoP[6]. However, the relationship between light pollution radiance and the DoP of the skylight polarization pattern is unknown. Furthermore, previous photographic polarimetry measurements did not image the whole sky and were taken at single times and locations[6], giving no insight to the temporal and spatial impacts of light pollution or the relationship with radiance. Characterising these fundamental relationships, with consideration of the parallel effect of lunar phase, is crucial for the accurate assessment of the impacts of light pollution on polarization-guided navigation.

The absolute DoP and angle of polarization (AoP) of the skylight polarization pattern do not directly inform the navigational maps and compasses of arthropods[14]. Arthropod visual systems can only detect the relative signal strength from two or more visual channels tuned to differing angles of polarization, e.g., from two eyes or populations of photoreceptors orientated perpendicular to each other. These are compared downstream using neural opponency mechanisms and ultimately the information relevant to an animal that is provided by the polarization of light relies on the polarization contrast between the two populations of photoreceptors (see chapter 1, section 1.2.1.3)[14,15,16]. Assuming the visual system is monochromatic[15], or can discriminate polarization from intensity and

chromatic visual channels (i.e., true polarization vision)[17,18], this opponent processing gives information on the DoP, AoP, and overall intensity of the skylight polarization pattern that the animal can use to determine its trajectory[14]. Modelling this signal opponency mechanism is more ecologically relevant than measuring absolute DoP and AoP alone, as it can provide species-specific measurements on the impacts of light pollution on the use of the skylight polarization pattern for navigation. However, such models for the detection of the lunar polarization pattern are limited, and it is unclear how the output of theoretical modelling relates to absolute DoP and AoP values. Comparative investigations using both theoretical and experimental methods will help to determine the validity and true ecological relevance of polarization contrast models of the lunar polarization pattern.

2.1.1 Aims and hypotheses

This work aims to identify the major impacts of light pollution on the spatial and temporal characteristics of the skylight polarization pattern, and to measure the relationship between light pollution radiance and the availability of the lunar polarization pattern as a navigational cue. Using photographic polarimetry, we first compared the characteristics of the polarization pattern between an area of high light pollution and low light pollution in two simultaneous time-series measurements from sunset to true night, across four moon phases. We then took single photographic polarimetry measurements along a light pollution gradient across Europe to establish the relationship between the characteristics of the skylight polarization pattern and light pollution radiance. These measurements were then used to calculate photoreceptor contrast for *Drassodes* sp. and *Helicoverpa armigera* for each of the sampled sites across Europe. Photoreceptor contrast is a metric that considers the DoP and AoP of the polarization pattern and the field of view (FoV) of a given visual system to represent how the polarization pattern is perceived by an animal.

2.2 Materials and methods

2.2.1 Zenith light pollution radiance

Light pollution radiance values for all the sites included in this investigation were acquired from www.lightpollution.info, an online mapping application that displays the light pollution data collected from the Visible Infrared Imaging Radiation Suite Day-Night Band (VIIRS DNB) on the Suomi National Polar-Orbiting Partnership satellite (Table.2.1)[19]. All zenith radiance values were calculated using the mean of the monthly values per site taken from the 2013-2018 VIIRS DNB dataset. The VIIRS DNB sensor is the first to provide globally calibrated radiance measurements of the night sky and has been

pivotal for the measuring and modelling of ecological light pollution[20,21]. However, when considering data obtained from the VIIRS DNB, it is important to note its limitations: 1) the sensor cannot detect wavelengths of <500 nm (i.e. the human perception of blue light), a large component of LED light, and therefore may underestimate light pollution radiance; 2) it is also sensitive to infrared light (IR) and therefore to emissions from fires and HPS sodium lamps which may bias radiance estimates; 3) the spatial resolution of the sensor is ~750 m and cannot be used to estimate emissions from isolated light sources; 4) the sensor only captures upward emitted radiation during non-cloudy conditions and therefore should only be considered as an approximation of the light conditions on the ground and; 5) the data are consistently acquired at particular local times and does not give an indication of daily variation[20].

2.2.2 Photographic polarimetry

Measurements of the skylight polarization pattern were taken using DSLR digital cameras (Nikon D810 and D850, Nikon) equipped with a fisheye lens (Sigma 8mm f3.5 Circular Fisheye EX DG) and polaroid filter (Rosco UV Polaroid 730011 – set into the rear lens filter slot). The cameras were mounted on a tripod and images of the sky were taken at four 45° rotations of the camera i.e., with the transmission axis of the polaroid at 0, 45, 90, and 135°. All four images were digitally reregistered and blue channel normalised intensity differences between the pixels of the four images were used to calculate Stoke's parameters[22]. Stoke's parameters are defined as

$$S_0 = (I_0 + I_{90})/(I_0 + I_{90})$$

$$S_1 = (I_0 - I_{90})/(I_0 + I_{90})$$

$$S_2 = (I_{45} - I_{135})/(I_{45} + I_{135}),$$

where *I* is the total light intensity and I_i is the light intensity transmitted with the camera orientated at i degrees. Assuming that there is no circular polarization, which is valid for Rayleigh scattering, the AoP and DoP can then be calculated by

$$\text{AoP} = \frac{1}{2} arctan\left(\frac{S_2}{S_1}\right)$$

$$\text{DoP} = \frac{\sqrt{{S_1}^2 + {S_2}^2}}{S_0}.$$

Polarization information was then processed into false colour map images that visualize the characteristics of the skylight polarization pattern, with each pixel assigned a DoP and AoP value. All image processing was completed using R (R Studio v. 4.1.2, R Development Core Team 2021).

2.2.3 The effects of moon phase and light pollution radiance on DoP

To compare the temporal and spatial characteristics of the DoP of the skylight polarization pattern in areas of high and low light pollution across the lunar cycle, two sites were sampled simultaneously between June and August 2018: Clifton, Bristol, UK (high light pollution: 42.77 nW/cm^{2}sr, Lat=51.459148, Lon=-2.601233) and the Mendips AONB, Somerset, UK (low light pollution: 0.48 nW/cm^{2}sr, Lat=51.219332, Lon=-2.601234), during four moon phases: new (0.3% illuminated), first quarter (53.6% illuminated), full (99.9% illuminated), and third quarter (33.4% illuminated). Measurements were taken at 15-minute intervals beginning at sunset and finishing ~3 hours after sunset.

To establish the change in DoP of the lunar polarization pattern with light pollution radiance, 14 sites across Europe were sampled between June 2018 and August 2019, under clear sky conditions around the full moon (>80% illumination). Sites were selected to represent a gradient of light pollution radiance from 48.85 (high) to 0.36 nW/cm^{2}sr (low) (Table.2.1). One measurement was taken per sampling site between 1 and 4 hours after sunset. The AoP of the skylight polarization pattern is not affected by light pollution or moon phase[13], instead being defined by the azimuth and elevation of the sun or moon, and thus was not considered here.

Table 2.1. The sites sampled to investigate the effect of light pollution radiance on the DoP of the skylight polarization pattern.

Location	Date	Coordinates (Lat, Lon)	Radiance (nW/cm^{2}sr)
Worcester College, UK	14/05/2019	51.755998, -1.267212	48.55
Oxford Business Park, UK	14/05/2019	51.733143, -1.203624	41.83
Tesco Superstore Wolverhampton, UK	21/04/2109	52.575667, -2.134707	35.36
St Anne's College, UK	14/05/2019	51.761839, -1.261790	29.04
MINI Plant Oxford, UK	14/05/2019	51.736334, -1.192975	25.19
Oxford University Department of Zoology, UK	14/05/2019	51.757260, -1.250925	19.61
Church Hill, Wolverhampton, UK	20/04/2019	52.555609, -2.156873	13.60
Penn Cricket Club, UK	22/04/2019	52.558887, -2.145724	10.09
Ounsdale, UK	20/04/2019	52.536202, -2.194967	7.12
Skillinge, Sweden	21/08/2018	55.473980, 14.283457	5.56
South Horrington, UK	21/05/2019	51.214399, -2.619168	2.89
Gavarnie, France	27/09/2018	42.742301, -0.017742	0.56
East Horrington, UK	21/05/2019	51.217176, -2.600550	0.51
Borrby Strandbad, Sweden	21/09/2018	55.426041, 14.231644	0.36

2.2.4 Photoreceptor contrast

We modelled the photoreceptor contrast (PRC) in the visual systems of *Helicoverpa armigera* and *Drassodes* sp. for the 14 sites sampled across Europe (Table 2.1). The PRC model is based on the mechanism of polarization analysis common to many visual systems; opponent processing of signals from two groups of photoreceptors that have high polarization sensitivity but different polarization axes[15]. To calculate the PRC for all 14 sites, the processed polarimetry images were restricted to the FoV (30°) of the ~100 ommatidia of the dorsal rim area (DRA) of a single eye in *H. armigera*[23] (Fig.2.1a_i,b_i), and a single posterior median eye (PME) of *Drassodes* sp. with a lensless FoV of 60° (Fig.2.1a_{ii},b_{ii})[24], and the median DoP and AoP values were calculated.

The AoP and DoP values were used to calculate the strength of the polarization signal detected by a two-channel orthogonal photoreceptor visual system, wherein one set of photoreceptors is aligned parallel with the polarization pattern and the other is perpendicular[15]

$$R_{par}(\emptyset, d) = [1 + \left(\frac{d(S_p - 1)}{S_p + 1}\right)\cos 2\emptyset - 2\emptyset_0]$$

$$R_{per}(\emptyset, d) = [1 + \left(\frac{d(S_p - 1)}{S_p + 1}\right)\cos 2\emptyset - 2\emptyset_{90}],$$

where $\emptyset$ is the AoP of the skylight polarization pattern, $\emptyset_0$ and $\emptyset_{90}$ are the two photoreceptor orientations of maximum sensitivity (parallel and perpendicular, respectively), d is the median DoP of the polarization pattern, and S_p is the effective polarization sensitivity of each photoreceptor. A value of 10 was assigned to S_p in both photoreceptor contrast models, which matches experimentally measured polarization sensitivities of the many arthropod DRAs[25,26]. The relative signals from the two sets of photoreceptors are then combined through opponent connections to an interneuron[15], theoretically represented as photoreceptor contrast,

$$\mathrm{PRC} = \ln\left(\frac{R_{par}}{R_{per}}\right).$$

PRC information for each species at all 14 sites were then used to produce false colour map images with each pixel assigned a contrast value between -2 and 2 (Fig.2.1c). The PRC scale runs from negative to positive to reflect the opponent nature of the processing. The PMEs of *Drassodes* sp. are non-image-forming due to a lack of focusing optics and therefore integrate polarization information across the FoV of the whole eye, producing a single PRC value representing the strength of the signal received from the skylight polarization pattern (Fig.2.1c_{ii})[24]. The ommatidia of the DRA of *H. armigera,* however, do have focusing optics and perceive polarization information as an array of signals across

the DRA, with each group of ommatidia receiving information on the DoP and AoP of the skylight polarization pattern for processing in the brain (Fig.2.1c_i). For subsequent analysis and comparison of the two visual systems, the maximum PRC value of the DRA of *H. armigera* at each site were compared to the single PRC value of the *Drassodes* sp. PMEs. The relationship between light pollution radiance and PRC signal strength in both species could then be visualised using non-linear least-square analyses. All image processing and analysis was completed using the R package 'imager'[27] (R Studio v. 4.1.2).

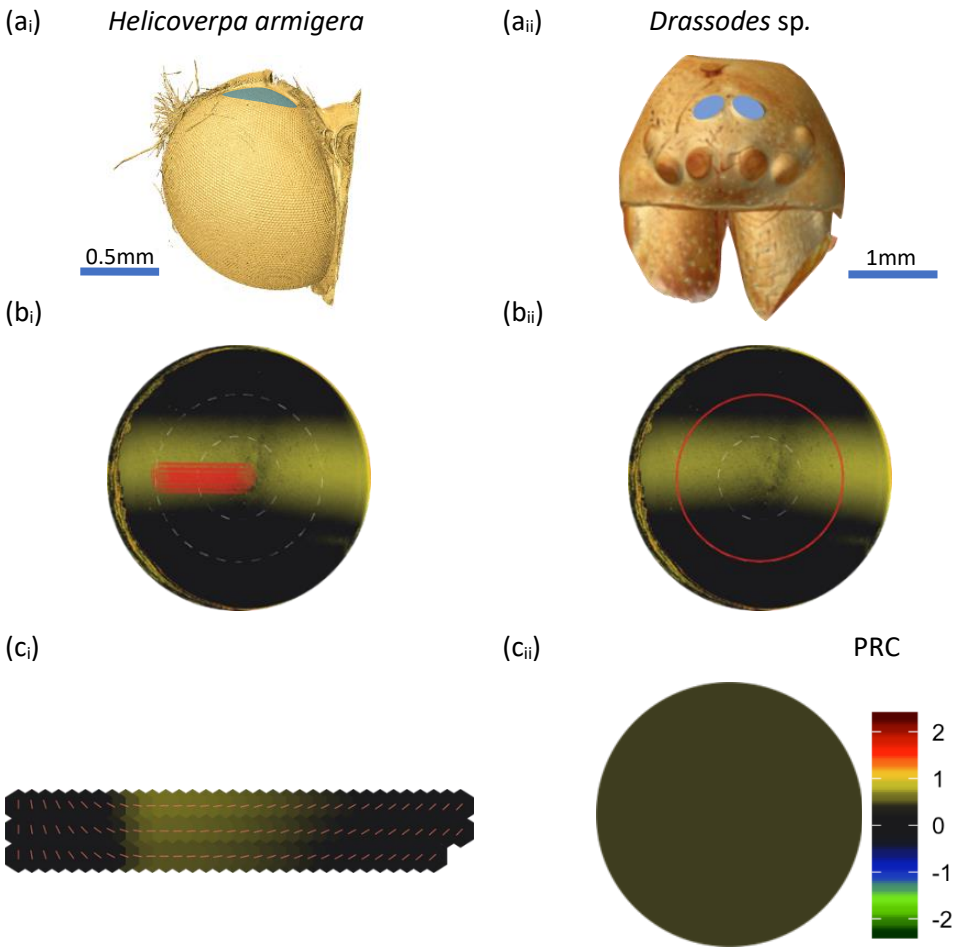

Figure 2.1. (a) 3D models of the right eye of *Helicoverpa armigera* (a_i) and the head of *Drassodes* sp. (a_{ii}) produced from synchrotron scans (taken at beamline I13-2 of Diamond Light Source, Harwell, UK) using Avizo Lite v9.4 (Thermo Fisher). The approximate locations of polarization-sensitive DRA and PMEs are highlighted in blue. (b) The FoV of the ~100 ommatidia of the DRA (b_i) and the PMEs (b_{ii}) of *H. armigera* and *Drassodes* sp. (red circles) overlaid on a processed PRC colour map image, at camera resolution, of the skylight polarization pattern at Borrby Strandbad, Sweden. (c) Examples of photoreceptor contrast information processed by the DRA of *H. armigera* (c_i) and the PMEs of *Drassodes* sp. (c_{ii}). Red lines in c_i indicate the polarization axes of the ommatidia in *H. armigera*.

2.3 Results

2.3.1 Impacts of light pollution and moon phase on the skylight polarization pattern

Both moon phase and the presence of light pollution affected the spatial and temporal distribution of the skylight polarization pattern, as well as its maximum DoP (Table.2.2).

Dark skies

In the absence of light pollution, the maximum DoP of the skylight polarization pattern remained constant at 0.5-0.75 throughout the night. Similarly, the spatial distribution of the pattern was maximal at around 50% of the area of the night sky and remained between 25-50% of the sky throughout the night. The temporal distribution of the pattern extended well into the night during nights of a full moon but began to dissipate ~135 minutes after sunset during nights of partially illuminated moons, even when the moon was above the horizon.

Generally, the solar polarization pattern waned when the sun dropped between 13 and 15^{o} below the horizon. Under a full moon, the lunar polarization pattern succeeded the solar pattern during this transition, being only marginally smaller in spatial extent across the sky and ~25% lower in maximum DoP than the solar polarization pattern (Table 2.2, full moon, 75 minutes after sunset). During quarter moon phases, the lunar pattern was scarcely visible following the waning of the solar polarization pattern, the characteristic 'band' not present and instead two small areas of polarized light at ~0.25 DoP at opposite horizons, perpendicular to the position of the moon (Table 2.2, 1st and 3rd quarter moons, 105 minutes after sunset). The transition to the lunar polarization patterns can be identified by the 90^{o} rotation of the pattern occurring at 120-135 minutes after sunset during the 1st quarter moon and 195 minutes after sunset during the 3rd quarter moon. This change in rotation occurred due to the position of the moon being roughly perpendicular to that of the sun during quarter moon phases, therefore making their relative polarization patterns perpendicular. Under a new moon, the moon rises and sets with the sun and does not produce a lunar polarization pattern[28]. The solar pattern is the only available source of skylight polarization during a new moon, until it disappears when the sun drops >12^{o} below the horizon (Table 2.2, new moon, 120 minutes after sunset).

Light-polluted skies

Light pollution dramatically reduced the spatial and temporal distribution and DoP of the solar and lunar polarization patterns. Generally, the maximum DoP of the skylight pattern was reduced to <0.25 from >0.5 by high light pollution and the spatial extent was reduced from ~50% to <30% of the area of the night sky. The temporal distribution of the pattern did not extend into the night under light

pollution, the reductive effects beginning before the solar pattern had waned (Table 2.2, all moons, between 30-60 minutes after sunset) and reducing to the above stated values around 90 minutes after sunset across all moon phases. Similarly, the shape of the polarization pattern was distorted by light pollution. The characteristic 'band' losing its symmetry, particularly at the zenith where the pattern began to distort rapidly following the transition to the lunar polarization pattern (Table 2.2, all moons, ~105-120 minutes after sunset).

Under a full moon, the effects of light pollution occurred 30 minutes after sunset and increased in magnitude throughout the night, peaking following the transition to the lunar polarization pattern which was reduced in DoP and spatial extent by ~50% compared to non-light polluted skies (Table 2.2, full moon). During the 1st quarter moon (53.6% illumination), light pollution visibly reduced the extent and DoP of the pattern around 75 minutes after sunset compared to non-light polluted skies, an effect that may have occurred earlier but was imperceptible due to small clouds moving across the hemisphere and obscuring the imaging of the pattern(Table 2.2, 1st quarter moon row). During the 3rd quarter moon (33.4% illumination), similar effects occurred at sunset (Table 2.2, 3rd quarter moon). Light pollution effectively removed the lunar polarization pattern of both quarter moons following the transition from the solar pattern at 105 minutes after sunset (Table 2.2, 1st and 3rd quarter moons). Under a new moon, light pollution began to affect the extent of the solar polarization pattern at 90 minutes after sunset and effectively eliminated the pattern at 120 minutes after sunset (Table 2.2, new moon). Although, again, there was some interference in the imaging caused by cloud cover.

DoP

0 1

Sun elevation (s^o) Moon elevation (m^o)

Minutes after sunset	0	15	30	45	60	75	90	105	120	135	150
	New moon (0.3% illumination) 13/06/18 Sunset=21:27 | Moonrise=04:56 | Moonset=20:57										
Low pollution	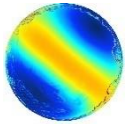		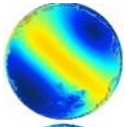		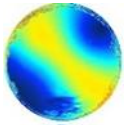		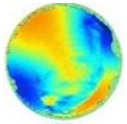		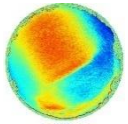		
High pollution	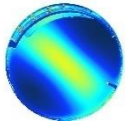		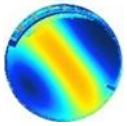		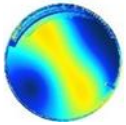		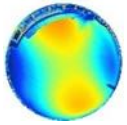				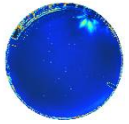
	s^o=0 m^o=-5		s^o=-5 m^o=-8		s^o=-7 m^o=-11		s^o=-10 m^o=-14		s^o=-12 m^o=-16		s^o=-14 m^o=-18
	1st quarter (53.6% illumination) 20/06/18 Sunset=21:30 | Moonrise=13:02 | Moonset=01:52										
Low pollution	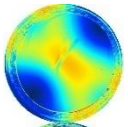	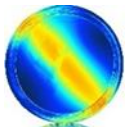	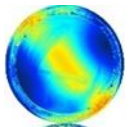	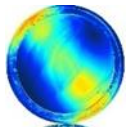	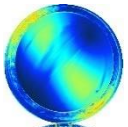	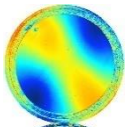	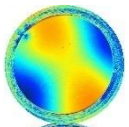	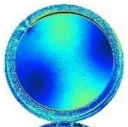	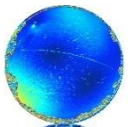	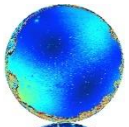	
High pollution	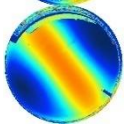	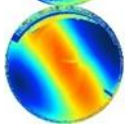	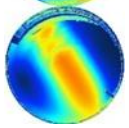	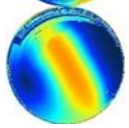	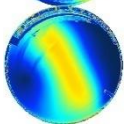	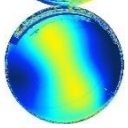	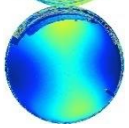				
	s^o=0 m^o=35	s^o=-2 m^o=33	s^o=-4 m^o=33	s^o=-6 m^o=30	s^o=-7 m^o=28	s^o=-9 m^o=26	s^o=-10 m^o=22	s^o=-11 m^o=18	s^o=-12 m^o=12	s^o=-13 m^o=10	
Minutes after sunset	0	15	30	45	60	75	90	105	120	135	150

Full moon (99.9% illumination)

28/06/18

Sunset=21:31 | Moonrise=21:38 | Moonset=06:07

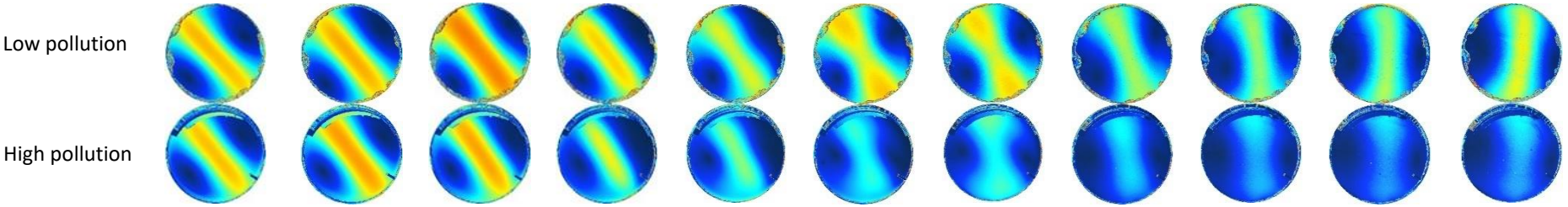

s^o=0	s^o=-2	s^o=-4	s^o=-5	s^o=-6	s^o=-8	s^o=-10	s^o=-11	s^o=-12	s^o=-13	s^o=-14
m^o=-1	m^o=1	m^o=2	m^o=4	m^o=6	m^o=7	m^o=9	m^o=10	m^o=12	m^o=13	m^o=15

3rd quarter (33.4% illumination)

06/08/18

Sunset=19:45 | Moonrise=16:47 | Moonset=01:21

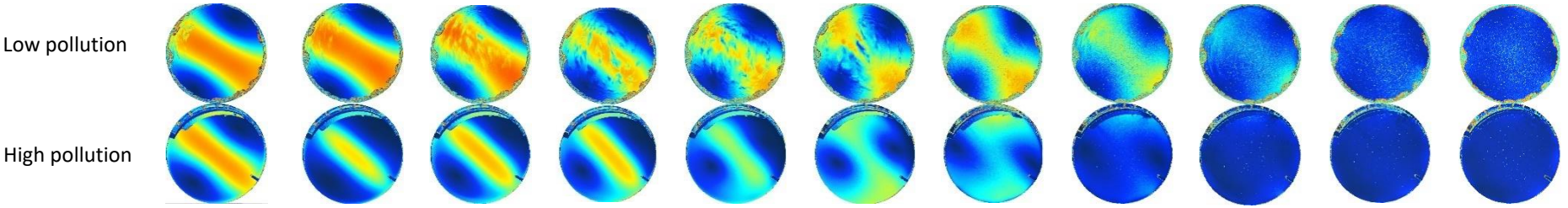

s^o=0	s^o=-1	s^o=-4	s^o=-6	s^o=-8	s^o=-10	s^o=-11	s^o=-13	s^o=-15	s^o=-16	s^o=-18
m^o=-22	m^o=-22	m^o=-21	m^o=-21	m^o=-21	m^o=-20	m^o=-19	m^o=-18	m^o=-17	m^o=-16	m^o=-14

Minutes after sunset	165	180	195	210
	Full moon (99.9% illumination) 28/06/18 Sunset=21:31 | Moonrise=21:38 | Moonset=06:07			
Low pollution	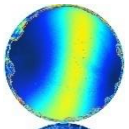	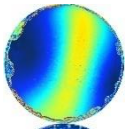		
High pollution				
	s^o=-14 m^o=15	s^o=-15 m^o=16		
	3rd quarter (33.4% illumination) 06/08/18 Sunset=19:45 | Moonset=16:47 | Moonrise=01:21			
Low pollution		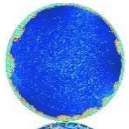		
High pollution				
	s^o=-19 m^o=-13	s^o=-20 m^o=-11	s^o=-22 m^o=-6	s^o=-22 m^o=-3

Figure 2.2. Changes in the spatial and temporal distribution and DoP of the skylight polarization pattern under low and high light pollution and across four moon phases. Irregularities in the pattern in the new moon and quarter moon measurements were due to local cloud cover. Note that the 3rd quarter moon did not rise above the horizon during the experiment.

2.3.2 Light pollution radiance and the skylight polarization pattern

Both the maximum DoP and spatial extent of the polarization pattern reduces with increasing light pollution radiance (Fig.2.3). At extremely low levels of light pollution (<6 nW/cm^{2}sr), the maximum DoP of the polarization pattern was between 0.4 and 0.6 and its spatial extent covered between 50-60% of the area of the night sky (Fig.2.3, Gavarnie-South Horrington). Conversely, at high radiance (>20 nW/cm^{2}sr), the diluting effect of light pollution was enough to almost reduce the pattern to extinction (Fig.2.3, MINI plant-Worcester College) by obscuring its shape, reducing its spatial extent to <50% of the sky, and reducing the DoP to <0.25. Light pollution of moderate radiance (6-20 nW/cm^{2}sr, Fig.2.2, Ounsdale-University of Oxford) reduced the maximum DoP of the pattern to between 0.25 and 0.4 with the spatial distribution of the pattern reducing only marginally, but with significant reduction in the total area of the pattern at DoP of >0.25 compared to sites of extremely low radiance.

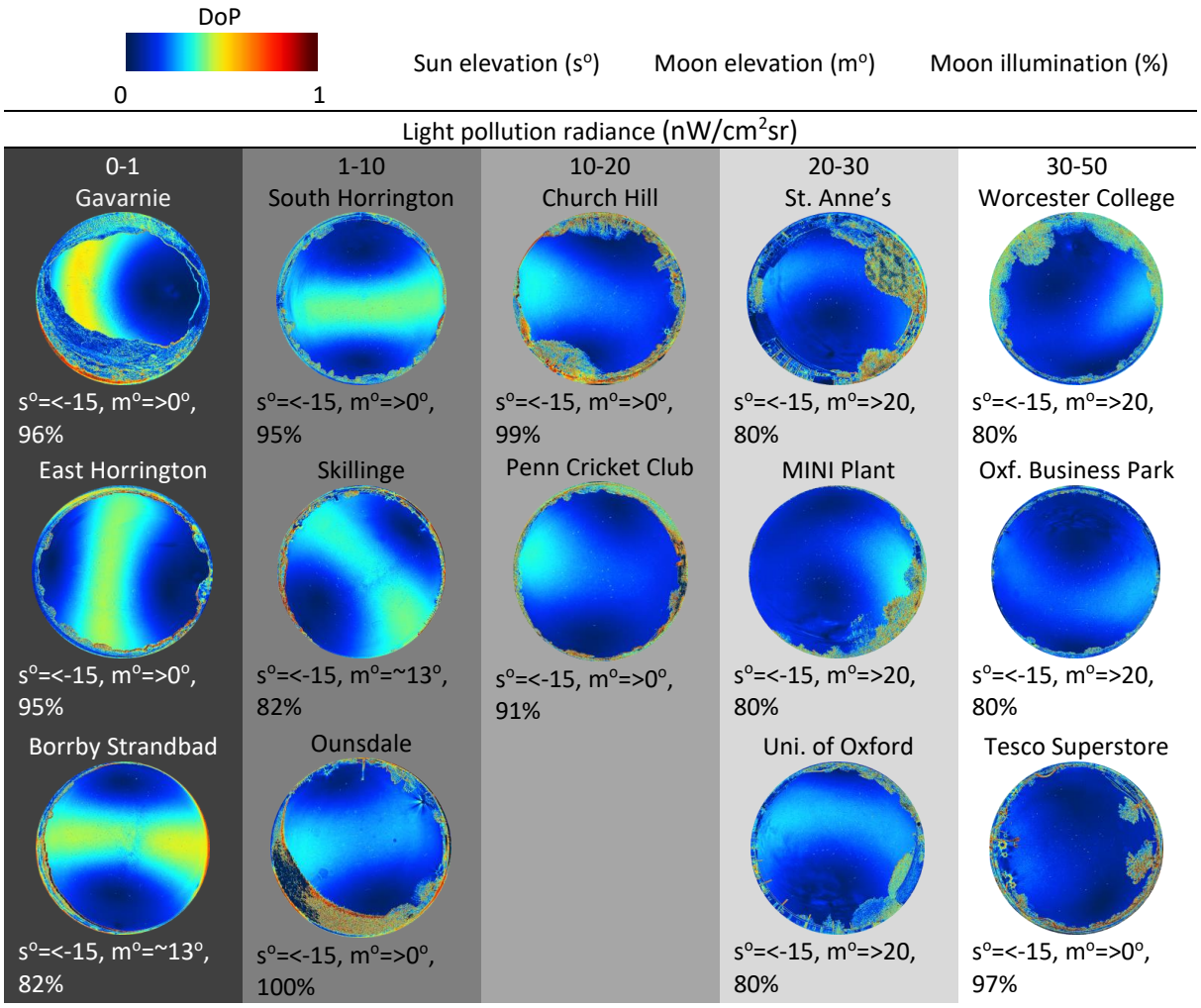

Figure 2.3. The spatial distribution and DoP of the lunar polarization pattern across a light pollution radiance gradient from 0-50 nW/cm^{2}sr. All measurements were taken on or near the full moon (>80% illumination) when the moon was above the horizon and the sun was >15° below the horizon.

2.3.3 Light pollution radiance and photoreceptor contrast in *H. armigera* and *Drassodes* sp.

Photoreceptor contrast in the visual systems of both *H. armigera* and *Drassodes* sp. reduced exponentially with increasing levels of light pollution radiance (R^2: *H. armigera*=0.95; *Drassodes* sp.=0.93) (Fig.2.4. With almost no light pollution (<5 nW/cm^{2}sr), maximum PRC was calculated to be 0.69 for *H. armigera* and 0.46 for *Drassodes* sp. Under high levels of light pollution, equivalent to those typically found in large cities (>30 nW/cm^{2}sr), the PRC was reduced by almost an order of magnitude to 0.11 for *H. armigera* and to 0.12 for *Drassodes* sp. This negative relationship is strongest between 0-30 nW/cm^{2}sr, an effect that is exaggerated in *H. armigera* due to larger PRC values at lower radiances than *Drassodes* sp.. At radiance values above 30 nW/cm^{2}sr, when the lunar polarization

pattern is obscured to near extinction, PRC in the two species overlaps and begins to stabilise between 0.1-0.2 (Fig.2.4).

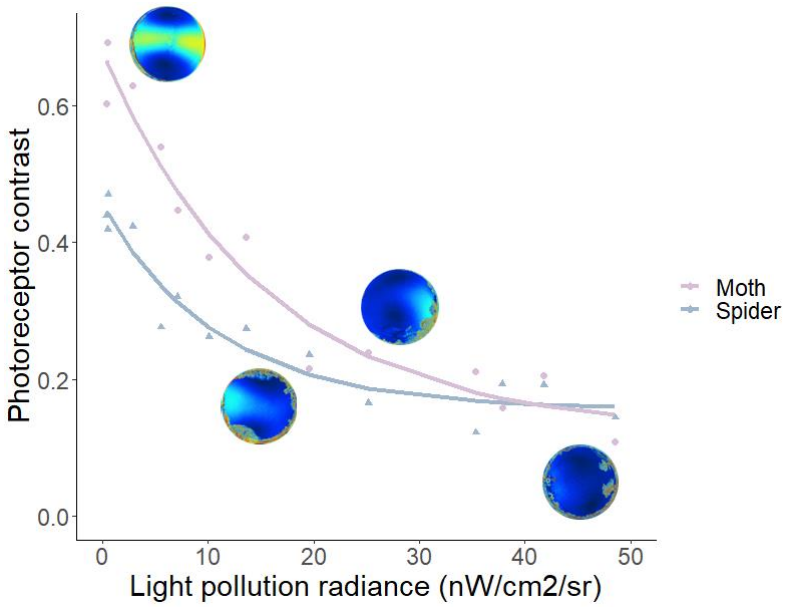

Figure 2.4. Modelled photoreceptor contrast across a light pollution radiance gradient in the visual systems of *Helicoverpa armigera* (purple circles) and *Drassodes* sp. (grey triangles). The exponentially decaying relationships between PRC and radiance were fitted using non-linear least squares. The exemplary photographic polarimetry images of the polarization pattern from left to right show: Borrby Strandbad (0.36 nW/cm^{2}sr), Ounsdale (7.12 nW/cm^{2}sr), MINI plant (25.19 nW/cm^{2}sr), and Tesco superstore (35.36 nW/cm^{2}sr).

2.4 Discussion

2.4.1 Light pollution radiance, moon phase, and the skylight polarization pattern

Both the solar and lunar polarization patterns are reduced in DoP and in spatial and temporal distribution by artificial light pollution, reducing the pattern to extinction 30-240 minutes earlier in the evening, depending on moon phase. Our results show for the first time that radiance values as low as 5 nW/cm^{2}sr have diminishing effects on several characteristics of the solar and lunar patterns, and that such effects change in magnitude over time. Radiance values of 5 nW/cm^{2}sr are representative of zenith skyglow illumination created by human settlements the size of a typical European village. Therefore, light pollution from modestly sized settlements, not just large cities that have previously

been investigated[6], has the potential to reduce the reliability of the skylight polarization pattern for navigation and in turn, affect the navigational efficiency of nocturnal arthropods.

Moon phase also has an important effect on the characteristics of the skylight polarization pattern. Moon illuminations of <50% (i.e., quarter moons or less) reduced the availability of the lunar polarization pattern spatially, temporally, and in DoP following the transition from the solar pattern. However, the DoP of the lunar polarization pattern, particularly during a full moon, remained >0.25 and is visible in the sky longer into the night, in contrast to the more extreme effects of light pollution. Under natural conditions, only a new moon, when the sun is >12° below the horizon, or a completely overcast sky would mean that the lunar polarization pattern is unavailable throughout the night[7]. Such natural variability across moon phases brings into question the reliability of the lunar polarization as a navigational cue in comparison to the more consistent and prevalent solar polarization pattern. Indeed, Foster *et al.* (2019) suggests that the lunar polarization pattern of a crescent moon, at a median DoP of 0.23, was close to the polarization detection threshold of a nocturnal dung beetle (0.11-0.31 DoP)[7]. Thus, the lunar polarization pattern may be an unreliable visual cue during both the new moon and crescent moons, i.e., nearly half of the lunar cycle. Light pollution is a persistent anthropogenic stressor that exacerbates the effects of moon phase, but it is important to consider the inherent variability of the skylight polarization pattern at night as a naturally occurring barrier to polarization-guided navigation.

2.4.2 Effects of light pollution radiance and moon phase on the skylight polarization pattern as a navigational cue

Calculated photoreceptor contrast reduced dramatically with increasing light pollution radiance in the visual systems of both *H. armigera* and *Drassodes* sp.. PRC decreased most rapidly between 0-30 nW/cm^{2}sr and stabilised at ~30nW/cm^{2}sr, indicating that human settlements of modest size and population density may produce light pollution at intensities that are detrimental to the detection of the lunar polarization pattern. In both species, PRC stabilised at minimum values of ~0.1-0.2 in areas of the highest light pollution. However, the initial decrease between sites of 0-30 nW/cm^{2}sr was larger in *H. armigera* due to a greater disparity in PRC between the two species at low radiance. This suggests that the visual system of *H. armigera*, and possibly other nocturnal lepidopterans, responsible for the detection of the skylight polarization pattern is more susceptible to the effects of light pollution.

The critical question is whether a PRC of ~0.1-0.2, correlating with a DoP of <0.25, represents a perceivable contrast to moths and spiders. In the context of known behavioural thresholds of polarized light detection in nocturnal dung beetle and locust orientation, which are estimated to be 0.11-0.32 and 0.05-0.07, respectively. These animals are still likely to be able to orientate with and

use the polarization pattern for navigation, but less reliably[7,25]. Alternatively, in the absence of a detectable polarization pattern, this cue may be abandoned in favour of a more available and stable cue such as a visual landmark[8Error! Reference source not found.]. Given the natural variability in the lunar p olarization pattern, and the critical importance of navigation to survival, it is likely that nocturnal arthropods have evolved mechanisms to cope with the loss of skylight polarization. This could involve reduced activity (see Chapter 5), the use of an alternative 'compass', or synchronising behaviour with the presence of other visual cues such as the moon. For example, when exposed to light pollution, nocturnal dung beetles switch their orientation strategy from the use of celestial cues to using the visible artificial light as landmarks[8]. In a uniform arena, *Drassodes* spp. becomes disorientated when an artificial polarization pattern is removed[24], but this is in the absence of other visual cues. However, it is unknown how moths and spiders respond to a weakened skylight polarization pattern, or whether navigational success is linked to a particular threshold of cue availability. Such information could enhance our understanding of the observed species declines in arthropods caused, at least in part, by light pollution[9]. The need for behavioural evidence to investigate such questions is addressed in chapters 3 and 4.

2.5 Conclusions

Both the solar and lunar polarization patterns are significantly affected by anthropogenic light pollution at night due to the depolarizing effect of unpolarized artificial light combining with polarized skylight. This not only affects the DoP of the polarization pattern, but its spatial and temporal extent, reducing its availability as a nocturnal visual cue in all three. These impacts can occur even at low levels of light pollution, representative of human settlements of modest size. Moon phase has similar effects on the characteristics of the lunar polarization pattern, with smaller illuminations being analogous to greater levels of light pollution, but with a less extreme effect. Truly nocturnal polarization-guided navigation must be flexible given the natural monthly variation of the lunar polarization pattern. Therefore, nocturnal arthropods may have evolved mechanisms that compensate for loss or changes in polarized celestial cues, but whether this affects navigational performance is unclear.

The next chapters will investigate the effects of DoP reduction and loss on orientation in *H. armigera* and *Drassodes* sp.. The results of this chapter highlight the importance of establishing behavioural thresholds and characterising the variation in navigational performance between the two species when exposed to a proxy of light pollution. Questions also remain on the timing and initiation of navigational behaviour between the two species and how this relates to polarized cues and exposure to light pollution. These questions will be addressed in chapter 5.

References

1. Johnsen S. 2012. Polarization. In: Johnsen S. (eds) The optics of life: A biologist's guide to light in nature. Princeton University Press, Woodstock, Oxfordshire, UK
2. Hegedüs R, Barta A, Bernath B, Meyer-Rochow VB, Horvath G. 2007. Imaging polarimetry of forest canopies: how the azimuth direction of the sun, occluded by vegetation, can be assessed from the polarization pattern of the sunlit foliage. *Applied Optics*, **46**(23): 6019-6032. (DOI: 10.1364/ao.46.006019)
3. Hegedüs R, Akesson S, Horvath G. 2007. Polarization patterns of thick clouds: overcast skies have distribution of the angle of polarization similar to that of clear skies. *Journal of the Optical Society of America A*, **24**(8): 2347-2356. (DOI: 10.1364/josaa.24.002347)
4. Cronin TW, Shashar N, Caldwell RL, Marshall J, Cheroske AG, Chiou TH. 2003. Polarization signals in the marine environment. Proc. SPIE 5158, *Polarization Science and Remote Sensing*, (12 December 2003). (DOI: 10.1117/12.507903)
5. Pomozi I, Horvath G, Wehner R. 2001. How the clear-sky angle of polarization pattern continues underneath clouds: full-sky measurements and implications for animal orientation. *Journal of Experimental Biology*, **204**(17): 2933-2942. (DOI: 10.1242/jeb.204.17.2933)
6. Kyba CCM, Ruhtz T, Fischer J, Hölker F. 2011. Lunar skylight polarization signal polluted by urban lighting. *Journal of Geophysical Research - Atmospheres*, **116**: D24106. (DOI: 10.1029/2011JD016698)
7. Foster JJ, Kirwan JD, el Jundi B, Smolka J, Khaldy L, Baird E. Byrne MJ, Nilsson DE, Johnsen S, Dacke M. 2019. Orienting to polarized light at night - matching lunar skylight to performance in a nocturnal beetle. *Journal of Experimental Biology*, **222**(2): jeb188532. (DOI: 10.1242/jeb.188532)
8. Foster JJ, Tocco C, Smolka J, Khaldy L, Baird E, Byrne MJ, Nilsson DE, Dacke M. 2021. Light pollution forces a change in dung beetle orientation behavior. *Current Biology*, **31**(17): 3935-3942. (DOI: 10.1016/j.cub.2021.06.038)
9. Owens ACS, Cochard P, Durrant J, Farnworth B, Perkin EK, Seymoure B. 2020. Light pollution is a driver of insect declines. *Biological Conservation*, **241**: 108259. (DOI: 10.1016/j.biocon.2019.108259)
10. el Jundi B, Pfeiffer K, Heinze S, Homberg U. 2014. Integration of polarization and chromatic cues in the insect sky compass. *Journal of Comparative Physiology A*, **200**(6): 575-589. (DOI: 10.1007/s00359-014-0890-6)
11. Ugolini A, Boddi V, Mercatelli L, Castellini C. 2005. Moon orientation in adult and young sandhoppers under artificial light. *Proceedings of the Royal Society B*, **272**(1577): 2189-2194. (DOI: 10.1098/rspb.2005.3199)
12. Cronin TW, Warrant EJ, Greiner B. 2006. Celestial polarization patterns during twilight. *Applied Optics*, **45**(22): 5582-5589. (DOI: 10.1364/ao.45.005582)
13. Barta A, Farkas A, Szaz D, Egri A, Barta P, Kovacs J, Csak B, Jankovics I, Szabo G, Horvath G. 2014. Polarization transition between sunlit and moonlit skies with possible implications for animal orientation and Viking navigation: anomalous celestial twilight polarization at partial moon. *Applied Optics*, **53**(23): 5193-5204. (DOI: 10.1364/ao.53.005193)
14. Cronin TW, Johnsen S, Marshall NJ, Warrant EJ. 2014. Polarization vision. In: Cronin TW, Johnsen S, Marshall NJ, Warrant EJ. (eds) Visual ecology. Princeton University Press, Woodstock, Oxfordshire, UK

15. How MJ, Marshall NJ. 2014. Polarization distance: a framework for modelling object detection by polarization vision systems. *Proceedings of the Royal Society B*, **281**(1776): 20131632. (DOI: 10.1098/rspb.2013.1632)
16. Land MF, Nilsson D-E. 2012. Light and vision. In: Land MF, Nilsson D-E. (eds), 2nd Ed., Animal eyes. Oxford University Press, Oxford, Oxfordshire, UK
17. Labhart T. 2016. Can invertebrates see the e-vector of polarization as a separate modality of light? *Journal of Experimental Biology*, **219**(24): 3844-3856. (DOI: 10.1242/jeb.139899)
18. Roberts NW, How MJ, Porter ML, Temple SE, Caldwell RL, Powell SB, Gruev V, Marshall NJ, Cronin TW. 2014. Animal polarization imaging and implications for optical processing. *Proceedings of the Ieee*, **102**(10): 1427-1434. (DOI: 10.1109/jproc.2014.2341692)
19. Falchi F, Cinzano P, Duriscoe D, Kyba CCM, Elvidge CD, Baugh K, Portnov BA, Rybnikova NA, Furgoni R. 2016. The new world atlas of artificial night sky brightness. *Science Advances*, **2**(6): e1600377. (DOI: 10.1126/sciadv.1600377)
20. Gaston KJ, Ackermann S, Bennie J, Cox DTC, Phillips BB, de Miguel AS, Sanders D. 2021. Pervasiveness of biological impacts of artificial light at night. *Biology*, **61**(3): 1098-1110. (DOI: 10.1093/icb/icab145)
21. Kyba CCM, Kuester T, de Miguel AS, Baugh K, Jechow A, Hölker F, Bennie J, Elvidge CD, Gaston KJ, Guanter L. 2017. Artificially lit surface of Earth at night increasing in radiance and extent. *Science Advances*, **3**(11): e1701528. (DOI: 10.1126/sciadv.1701528)
22. Foster JJ, Temple SE, How MJ, Daly IM, Sharkey CR, Wilby D, Roberts NW. 2018. Polarisation vision: overcoming challenges of working with a property of light we barely see. *Science of Nature*, **105:** 27. (DOI: 10.1007/s00114-018-1551-3)
23. Belušič G, Šporar K, Meglič A. 2017. Extreme polarisation sensitivity in the retina of the corn borer moth Ostrinia. *Journal of Experimental Biology*, **220**(11): 2047-2056. (DOI: 10.1242/jeb.153718)
24. Dacke M, Nilsson DE, Warrant EJ, Blest AD, Land MF, O'Carroll DC. 1999. Built-in polarizers form part of a compass organ in spiders. *Nature*, **401**(6752): 470-473. (DOI: 10.1038/46773)
25. Henze MJ, Labhart T. 2007. Haze, clouds and limited sky visibility: polarotactic orientation of crickets under difficult stimulus conditions. *Journal of Experimental Biology*, **210**(18): 3266-76. (DOI: 10.1242/jeb.007831)
26. Dacke M, Nordstrom P, Scholtz CH, Warrant EJ. 2002. A specialized dorsal rim area for polarized light detection in the compound eye of the scarab beetle *Pachysoma striatum*. *Journal of Comparative Physiology A*, **188**(3): 211-216. (DOI: 10.1007/s00359-002-0295-9)
27. Barthelmé S, Tschumperlé, D. 2019. imager: an R package for image processing based on CImg. *Journal of Open Source Software*, **4**(38): 1012. (DOI: 10.21105/joss.01012)
28. Cronin TW, Johnsen S, Marshall NJ, Warrant EJ. 2014. Light and the optical environment. In: Cronin TW, Johnsen S, Marshall NJ, Warrant EJ. (eds) Visual ecology. Princeton University Press, Woodstock, Oxfordshire, UK

3

Light pollution and nocturnal navigation in Helicoverpa armigera

The detrimental effects of light pollution on the strength and spatio-temporal distribution of the night-time skylight polarization pattern are clear, but how might these affect the nocturnal arthropods that use the pattern as a navigational aid? This chapter reports a series of tethered flight experiments on the long-distance migratory moth *Helicoverpa armigera*. The aim was to test the effect of the presence and absence of skylight polarization on orientation and use the same experimental set-up to establish behavioural thresholds of polarization sensitivity in *H. armigera* to determine the link between light pollution radiance and successful polarization-guided navigation in a nocturnal lepidopteran. However, the design underwent several iterations, spanning across three field seasons, until it produced a reliable dataset. As a result, there was insufficient time to address thresholds. The tethered behavioural experiments with *Drassodes* sp. were more successful and were able to progress both phases of the experiment to completion, details of which are described in chapter 4.

Contributions: Myself, my supervisors Nicholas Roberts (University of Bristol) and Lauren Sumner-Rooney (Leibniz Institute for Biodiversity and Evolution Research), and my collaborators Karl Wotton (University of Exeter), Toby Doyle (University of Exeter), Will Hawkes (University of Exeter), Richard Massy (University of Exeter), Seb Lloyd, Christian Drerup (University of Cambridge), and Siân Vincent Venables collected the animals. I, Seb Lloyd, Christian Drerup and Siân Vincent prepared the moths for the flight simulator. Richard Massy adapted a small LED light into the fake moon used in the flight simulator. Ilse Daly wrote the Raspberry Pi program for video monitoring. Myself, my supervisors, Seb Lloyd, Christian Drerup, and Siân Vincent, and Richard Massy undertook data collection. I completed the tracking and data analysis and authored the chapter in discussion with my supervisors.

3.1 Background

Successful navigation typically involves the combination of learned spatial maps, sensory cues, and path integration[1]. In nocturnal arthropods, some or all these strategies are used simultaneously during seasonal and daily journeys[2]. The skylight polarization pattern is a common visual cue used for

navigation in diurnal, crepuscular, and nocturnal arthropods[3-8], but light pollution reduces its spatial and temporal availability across the lunar cycle (see chapter 2). Research on insect orientation shows performance impairment when certain celestial cues are removed, reduced, or misaligned[3,9-12]. The Australian bogong moth (*Agrotis infusa*) combines visual landmarks with the Earth's magnetic field to steer its migratory flight but becomes disorientated when the two cues are placed in conflict[10]. When homing, the nocturnal bull ant (*Myrmecia midas*) increases the weighted importance of the polarization pattern against other cues as it gets further from the nest[3]. Dung beetles show similarly high plasticity, placing weighted importance on directional information with the highest certainty at a given moment, the position of the sun being dominant in the cue hierarchy[12,13]. The loss of the skylight polarization pattern caused by light pollution may therefore impact arthropod orientation precision through misdirected migration and homeward trajectories, with implications for dispersal, energy expenditure, predation risk, and reproductive and foraging success[9,14-19].

The polarization pattern can function as a navigational cue in two distinct ways: 1) as a wide-field visual landmark for straight-line orientation[11,20,21] and, 2) through providing compass information during true navigation, by integrating polarization information with the solar/lunar location, even if either celestial body is occluded[22-27]. The pattern is considered to be reliable cue due to its persistence under a range of meteorological conditions, under canopy cover, and underwater[28,29,30]. However, as shown in chapter 2, light pollution can dramatically reduce the degree of polarization (DoP) and the spatial and temporal distribution of the skylight polarization pattern.

The direct impacts of light pollution on the use of the polarization pattern as a cue during navigation are unknown. When exposed to outdoor lighting, nocturnal dung beetles switch their orientation strategy from the use of celestial compass cues to landmark orientation, using the bright light sources as beacons[15]. Similarly, urban skyglow disrupts the lunar orientation of sandhoppers during their nightly foraging journeys[31]. However, these investigations did not isolate polarized cues from other celestial cues and therefore do not directly address the impacts related to the removal of skylight polarization by light pollution. Behavioural evidence suggests that reductions in the DoP of skylight polarization can disrupt successful navigation, causing individuals to use an alternative cue, follow an erroneous trajectory, or become disorientated[9,11,13,14,31,32]. Given the available evidence on navigational impairment, the effect of light pollution on the skylight polarization pattern has the potential to significantly impact nocturnal navigation in polarization-sensitive arthropods.

3.1.1 Aims and hypotheses

The following experiments aimed to investigate the impact of skylight polarization on orientation performance in *Helicoverpa armigera*. More specifically, we wanted to investigate two aspects of

orientation performance: 1) Does *H. armigera* use skylight polarization to select a particular heading direction? and, 2) Does *H. armigera* use skylight polarization to maintain a particular heading direction? Tethered moths within a flight simulator were exposed to an artificially polarized and unpolarized 'sky' at the zenith, to simulate the polarization pattern under natural and light-polluted skies, respectively, with the unpolarized 'sky' also serving as a control. The ability of individuals to maintain a chosen orientation was tracked during 90° rotations of both light treatments and the responses to both were compared. Individuals were predicted to change orientation direction or become disorientated following the rotation of the polarized treatment and no change in orientation performance was predicted following the rotation of the unpolarized treatment.

3.2 Materials and methods

A modified Mouritsen-Frost flight simulator was used to test the effect of the presence and absence of artificially polarized skylight on orientation of magneto-tethered, flying moths[6]. Adult *H. armigera* were captured in the Hautes-Pyrénées at the Port de Boucharo pass, France (Lat=42.703950, Long=-0.063988, mean zenith sky radiance between 2013-2018 from lightpollutionmap.info=0.56 nW/cm^{2}sr) in September 2021. Individuals were caught at night during their southward, autumn migration using Skinner traps illuminated with one of two light sources: LED light arrays powered by external battery banks (LepiLED mini, LepiLED maxi, and LepiLED maxi switch)[33], or a fluorescent bulb powered by external car batteries (UV-A 20W Mini-Lynx backlight compact fluorescent). Captured moths were collected from the traps at or before sunrise to minimise heat-stress and transported to a field location in Gavarnie, France. Individuals were held in mesh cages containing egg boxes for refuge (between 30 and 60 moths per cage depending on cage size). The cages were covered in white fabric to minimise visual disturbance and placed in a quiet room, exposed to natural temperatures and indirect natural light. The moths were fed with cotton balls soaked in 33% honey solution every three days. Animals were kept for the minimum time possible to complete experiments (1-5 days). All experiments and capture of animals in the Hautes-Pyrénées were conducted under the authorisation of the Parc National des Pyrénées (permit 2021-253).

Experiments took place outside, around 5.3km from the site of capture (Lat=42.745952, Lon=-0.033586). Testing occurred during evenings of clear skies and low wind between one and five hours after sunset, from the 16th to the 30th of September 2021. The moon was between its first and final quarter phase throughout the testing period.

3.2.1 Preparation of *Helicoverpa armigera*

The moths were immobilised with weighted mesh and their scales on the dorsal metathorax were removed using a fine paintbrush. The exposed exoskeleton was scored using sandpaper to promote glue adhesion and a small drop of contact adhesive was applied to the area (Evo Stik, Bostik Ltd.). Using tweezers, the head of a dressmaker pin was dipped in the same contact adhesive and placed on top of the glue on the exposed metathorax and allowed to cure for 24 hours. With the pinhead adhered to the dorsal thorax, the moths could then be magnetically tethered inside the flight simulator. Before transfer to the location of the simulator experiment, the prepared moths were placed outside at dusk for exposure to natural environmental cues that initiate migratory flight.

3.2.2 The modified Mouritsen-Frost flight simulator

The flight simulator consisted of a 500x800mm cylindrical arena, lined with white felt and sealed with a UV-transmissive Perspex lid (Fig.3.1a). Prepared moths were connected to an optical encoder (RE12D-300-201-1, Nidec Copal Electronics) in the centre of the Perspex lid by a custom plastic collar that attached to its shaft (Fig.3.2b). A dressmaker pin, with a small disc magnet glued to the pinhead, extended from the ventral face of the plastic collar and magnetically tethered the metal pinhead on the moths' metathorax to the optical encoder (Fig.3.2a,b). This held the moths in a central position inside the simulator, allowing them to freely wingbeat, but rotate along the yaw axis only. The optical encoder was not used for data collection, only to allow the rotation of the moths. Instead, moths were illuminated using infrared LED spotlights invisible to the moths[34-36] and recorded from below using an infrared video camera (Raspberry Pi Night Vision Camera and Raspberry Pi Module 4, Raspberry Pi Foundation). The camera was obscured from the moth's ventral field of view using white felt with a small circular hole to allow unobstructed recording (Fig.3.1a).

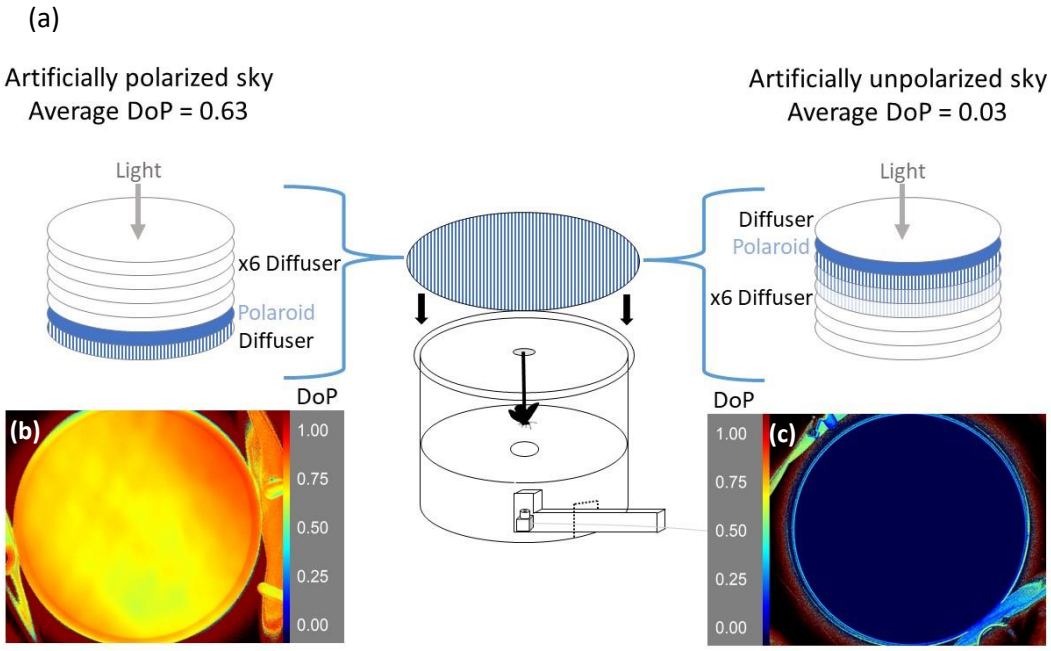

Figure 3.1. (a) The modified Mouritsen-Frost flight simulator for testing orientation under different simulations of skylight polarization. Outdoors, with the moon obstructed from view, moths were magneto-tethered inside the simulator and exposed to the real night sky and two artificially polarized treatments overhead while a video camera recorded behavioural responses in infrared. (b) Photographic polarimetry image of the polarized side of the filter stack that represented skylight polarization under optimal conditions. (c) Photographic polarimetry image of the unpolarized side of the filter stack that represented skylight polarization under extreme light pollution. Photographic polarimetry images taken using a polarization camera (Triton 5.0 MP Polarization Model, Lucid Vision Labs Inc.).

To aid flight stabilisation and create a more realistic visual scene inside the flight simulator, an artificial moon and artificial mountains were added using a single cool-white LED and four identical black triangles, respectively (Fig.3.2b). The single, cool-white LED had a visual angle of 0.68°, slightly larger than the 0.5° of the real moon[21], and an intensity of 0-0.1lux. The LED was placed behind the white felt lining to diffuse the light and hide any electrical wires. The four black triangles were made from black card and were symmetrical in size, shape, and position inside the simulator. The artificial moon was aligned with the real moon at the start of testing and remained at this position throughout the testing period. The real moon was obscured using a large umbrella.

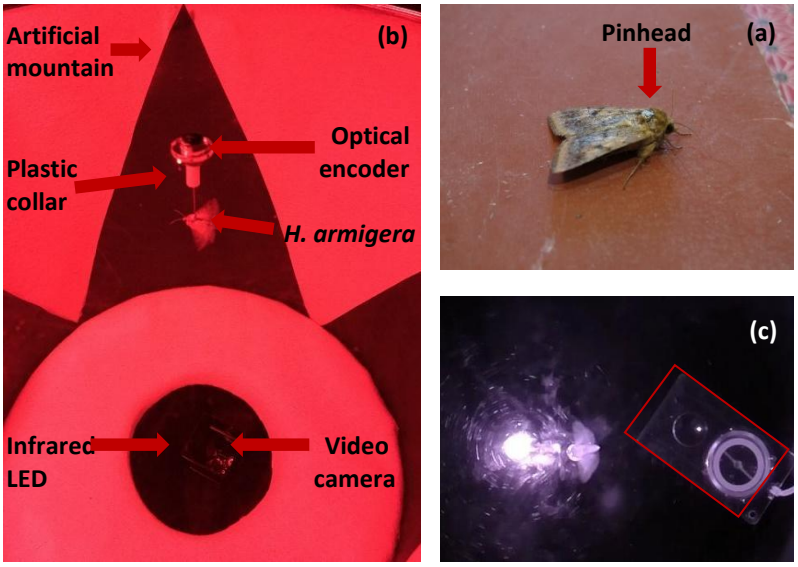

Figure 3.2. (a) Photograph of *Helicoverpa armigera* prepared for the flight simulator with a dressmaker pinhead glued to the dorsal metathorax. (b) Photograph of a tethered *H. armigera* inside the modified Mouritsen-Frost flight simulator. The moths were magnetically tethered to an optical encoder in the centre of a Perspex lid to allow for stationary flight and rotation in the yaw-axis only. Polarized treatments (not shown) were presented above the animal while a video camera recorded behavioural responses in infrared. An artificial moon (not shown) and artificial, symmetrical mountains provided additional visual cues for flight stabilisation, self-monitoring of rotation, and a more realistic visual scene. (c) Example image from an infrared video recording of *H. armigera* inside the flight simulator alongside a navigational compass used for calibrating polar degrees shown by the red box.

3.2.3 Experimental protocol

A total of 41 moths were exposed to a series of five treatments in a pseudo-random order inside the flight simulator: 1) the real night sky, an artificially polarized sky oriented at 2) 0° and 3) 90°, and an artificially unpolarized sky oriented at 4) 0° and 5) 90°. Experiments typically started with a two-minute burn-in period under the artificially polarized or unpolarized sky at 0°. The sky was then rotated manually through 90° and back to 0°, before switching to the other treatment, which was also rotated through 90° and back. The final experimental treatment involved the removal of the polarized filters to reveal the real night sky. Individuals were recorded for two minutes before and after the 90° rotations of the polarization treatments and during the real night sky treatment (total minutes inside the flight simulator=14). Individuals that did not turn throughout the 14 minutes or stopped flying more than three times were excluded from the experiment (n=4).

The polarized treatments were created using a circular filter stack (45 cm diameter) of seven layers of ¼ diffuser (251 Quarter white diffusion, LEE Filters, Hampshire, UK) and one layer of UV-transmissive polarizing filter (Rosco, London, UK; Fig.3.1). The diffuser layers and polarizing filter were arranged such that one face of the filter stack transmitted polarized light (x1 layer of diffuser below the polarizing filter and x6 layers of diffuser above, mean DoP=0.63) and, when inverted, the opposite face of the filter stack transmitted uniform, unpolarized light (x6 layers of diffuser below the polarizing filter and x1 layer of diffuser above, mean DoP=0.03; Fig.3.1). All DoP values were an average of three polarimetry measurements taken manually at different locations across the filter stack using a Glann-Thompson polarizing prism, a QE65000 spectrometer and a P200-UV-VIS optical fibre (Ocean Insight Inc.). Intensity measurements were taken with the prism at 0, 45, 90 and 135° rotations and intensity differences between the four rotations could then be used to calculate Stoke's parameters to give a measure of DoP (see chapter 2, section 2.2.2). The two DoP values were selected to represent the skylight polarization pattern under optimal natural conditions (DoP=0.63) and under extreme light pollution (DoP=0.03). The angle of polarization (AoP) of the transmitted polarized light was uniform across the diameter of the filter stack, and fixed relative to the transmission angle of the polarizing filter. The filter stack was manually aligned to be perpendicular to the position of the moon (thereby roughly aligned to the natural polarization pattern).

The deep neural network software, DeepLabCut[37] was used to track the head and tail position of the moths per video frame (30 frames per second). The orientation of the moths in radians (θ) were calculated using the given x,y coordinates of the head and tail locations and the atan2 base function in the statistical software, R (R Studio v. 4.1.2, R Development Core Team 2021):

$$\theta = atan2((y^2 - y^1) - (x^2 - x^1))$$

where x^1 and y^1 are the coordinates of the head position and x^2 and y^2 are the coordinates of the tail position. Thus, giving a dataset of the orientation directions of the moths over time. Only orientations with an estimated tracking error of <10% were included in the analysis.

3.2.4 Statistical analysis

The following analyses were chosen to explore two central questions to this investigation: 1) does *H. armigera* use the polarization of light for orientation (turning responses) and heading selection (circular distributions), and 2) does the polarization of light affect the ability of *H. armigera* to maintain a selected heading (directedness)? Turning response and directedness were calculated and analysed in individuals and heading selection was calculated for the population of moths tested.

The mean orientation direction θ (mean vector direction in radians) and *r* value (mean resultant vector length or directedness ranging from 0 to 1, with 1 representing strong directedness) of individuals were calculated using the package 'CircStats' in R[38]. Mean directions were corrected to true north using a navigational compass captured within the frame of each infrared video (Fig.3.2c) in MatLab (MatLab v. R2018a, The MathWorks Inc.).

Turning responses

To establish whether individuals changed orientation following the rotations of the polarized treatments, changes in θ of individuals between the 2 minutes before and after treatment rotation were categorised as a turning response if the absolute difference was >45° and analysed using a binomial generalised linear mixed model (GLMM). The binary turning response of the moths were treated as the response variable; treatment, order of presentation, direction of treatment rotation, whether the individual began the experiment under the artificially polarized or unpolarized treatment, and the interaction between treatment and order of presentation were treated as fixed factors; and moth ID as a random term. The model had a logit link function. Model structure and link functions with the best model fit was selected using the Akaike information criterion (AIC) values and model diagnostic information[39]. Variance components were estimated using restricted maximum likelihood (REML) method. Models were selected using manual backwards-stepwise model refinement and the significance of fixed terms was determined using analysis of variance tests (ANOVA) and associated p-values[39]. Residual diagnostics of all models were done using the 'DHARMa'[40] package in R. All statistical analysis was conducted in R.

Directedness

To establish if individuals became disorientated (decrease in *r*) with the rotation/removal of the polarized treatments, differences in *r* were compared between treatment rotations using non-parametric Kruskal-Wallis tests with pairwise post-hoc Bonferroni adjustments. Comparisons were also made between the mean *r* of individuals and the order of treatment presentation and the direction of treatment rotation.

Circular distributions

To establish whether treatment groups clustered around specific directions and whether they changed distribution between treatments, the R package 'CircMLE'[41] was used to compare the θ vectors of each treatment (forced into 20° bins) to the ten models of animal orientation proposed by Schnute and Groot[42] using maximum likelihood. These models are built upon the von Mises (uniform), unimodal, bimodal, and mixed distribution models of orientation (Table.3.1). Each distribution is

described by up to five parameters: up to two mean directions (θ_1, θ_2), and concentration parameters (reciprocal of the variance, K_1, K_2), and the proportional size of the first distribution (λ). The minimum difference in orientation direction for bimodal models was 45° and the minimum proportion size of the first distribution was 25%.

Table 3.1. Schnute and Groot's (1992) ten models of animal orientation[42].

Model code	Modes	Name	Free parameters ($\theta_1, K_1, \lambda, \theta_2, K_2$)
M1	0	Uniform (von Mises)	(na, 0, 1, na, na)
M2A	1	Unimodal	(θ_1, K_1, 1, na, na)
M2B	1	Symmetric modified unimodal	(θ_1, K_1, 0.5, na, 0)
M2C	1	Modified unimodal	(θ_1, K_1, λ, na, 0)
M3A	2	Homogenous symmetric bimodal	$(\theta_1, K_1, 0.5, \theta_1 + \pi, K_1)$
M3B	2	Symmetric bimodal	$(\theta_1, K_1, 0.5, \theta_1 + \pi, K_2)$
M4A	2	Homogenous axial bimodal	$(\theta_1, K_1, \lambda, \theta_1 + \pi, K_1)$
M4B	2	Axial bimodal	$(\theta_1, K_1, \lambda, \theta_1 + \pi, K_2)$
M5A	2	Homogenous bimodal	$(\theta_1, K_1, \lambda, \theta_2, K_1)$
M5B	2	Bimodal	$(\theta_1, K_1, \lambda, \theta_2, K_2)$

The best fitting models were selected based on the delta Akaike Information Criterion corrected for smaller sample sizes (ΔAICc)[43]. The model with the smallest ΔAICc value, binned orientation directions of the moths, and mean resultant length of the vectors (R*) per treatment were visualised using circular histograms. Fitted models are approximations and it is therefore unlikely that a single model can explain a set of real-world observations[44]. As such, all fitted models (up to three) with an ΔAICc of <2[45] are given for each treatment as well as the ΔAICc of the uniform model (M1) for comparison.

Rayleigh tests for non-uniformity were also performed on the mean vectors of the moths per treatment. The Rayleigh test compares the likelihood of the data fitting a uniform distribution (*K*=0) against the likelihood of a non-uniform distribution (*K*=>0) with the null hypothesis assuming uniformity[41]. All statistical analyses were performed using R.

3.3 Results

For ease, the following section categorises the moths into two groups according to the sequence of treatments experienced in the flight simulator: group P (polarized treatment followed by unpolarized

and the real night sky) and group UP (unpolarized treatment followed by polarized and the real night sky).

3.3.1 Polarization and orientation performance in individuals

Turning responses

Polarization did not affect the turning responses of individuals (binomial GLMM, d.f.=1, χ^2=0.02, p=0.12) (Fig.3.3), nor did the sequence of treatments experienced in the flight simulator (binomial GLMM, d.f.=1, χ^2=0.02, p=0.87). The number of turning individuals consistently increased following the second rotation of both treatments (by 13% in the unpolarized treatment and 9% in the polarized treatment). Following the removal of both artificial treatments to reveal the real night sky, 50% of the individuals in group P (Fig.3.3b) and group UP (Fig.3.3a) turned >45°. The direction of treatment rotation (binomial GLMM, d.f.=1, χ^2=0.28, p=0.59) and the order of treatment presentation (binomial GLMM, d.f.=1, χ^2=0.44, p=0.50) did not affect the turning responses of individuals.

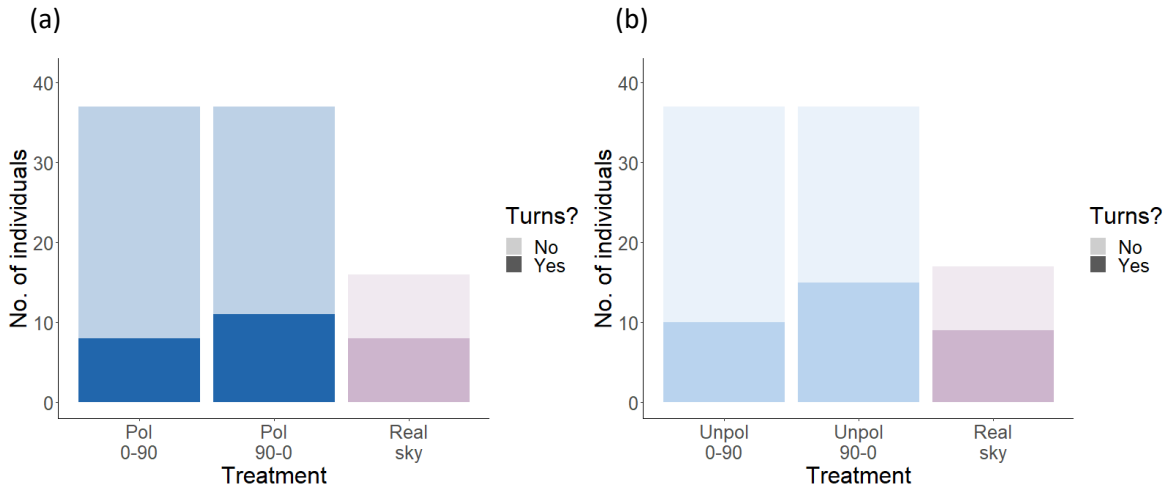

Figure 3.3. The proportion of moths that turned >45° following back-and-forth 90° rotations of (a) the artificially polarized sky and (b) the artificially unpolarized sky (dark and light blue columns, respectively) and, following the removal of both artificial treatments to reveal the real night sky (purple columns).

Directedness

The mean directedness of individuals did not differ between clockwise or anticlockwise rotations of the treatments (Kruskal-Wallis Test, χ^2=0.10, d.f.=2, p=0.94). Therefore, directedness was pooled across the two rotation directions in the following analyses.

Polarization did not influence the directedness of individuals (Kruskal-Wallis Test, χ^2=4.05, d.f.=7, p=0.77), which remained relatively high throughout the experiment (mean *r*: polarized

treatments=0.73, unpolarized treatments=0.60) (Fig.3.4). Directedness decreased in the moths that experienced the unpolarized treatment prior to the real night sky (mean change in r=0.01) and increased in the moths that experienced the polarized treatment prior to the real night sky (mean change in r=0.05), but this difference was not significant (Kruskal-Wallis Test, χ^2=0.03, d.f.=1, p=0.85). Directedness did not change as a function of order of treatment presentation (Kruskal-Wallis Test, χ^2=5.77, d.f.=6, p=0.44).

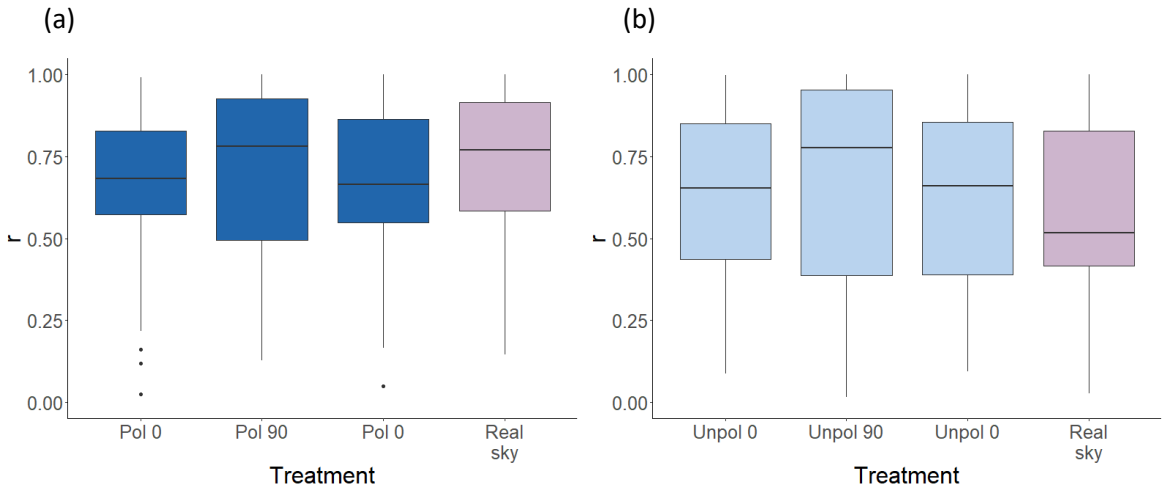

Figure 3.4. The directedness of the moths following two minutes of exposure to (a) the artificially polarized sky (dark blue boxes) and (b) artificially unpolarized sky (light blue boxes) at 0-90-0° rotations followed by two minutes of exposure to the real night sky (purple boxes).

3.3.2 Polarization and orientation performance in populations

When oriented in a non-uniform distribution, the moths preferred to fly in a south-southwest direction, independent of polarization (Fig.3.5-8). In the unpolarized treatments, overall directedness (R*) was stable or decreased across the rotations (group P=0.37, 0.27, 0.12; group UP=0.39, 0.37, 0.36) (Fig.3.5 and 3.7). In the polarized treatments, R* increased following the first rotation and decreased following the second rotation in both groups (group P=0.34, 0.52, 0.29; group UP=0.45, 0.54, 0.33) (Fig.3.5 and 3.7). When exposed to the night sky, the directedness of all moths remained low (R*=0.24) increasing by 0.12 in group P (from unpolarized) and decreasing by 0.09 in group UP (from polarized) (Fig.3.8).

Circular distributions: Rotations of the first treatments

At the start of the experiment, prior to any rotations or changes of treatment, the moths of group UP displayed a more unimodal south-southwest distribution (models with ΔAICc <2=M2B; Rayleigh Test

R*=0.39, p=0.06) than group P (models with ΔAICc <2=M1, M2A, M2B; Rayleigh Test R*=0.34, p=0.11) but neither were significantly different from uniform (Fig.3.5a_i,a_{ii}).

Group P (n=19)		Group UP (n=18)	
(a_i) (1) Pol 0°		(a_{ii}) (1) Unpol 0°	
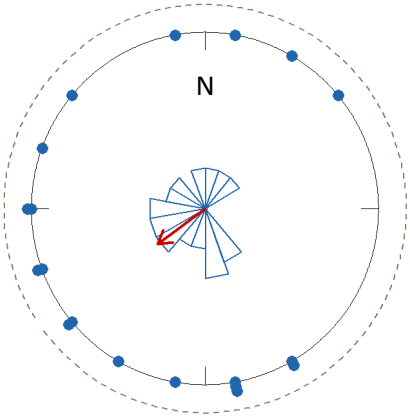		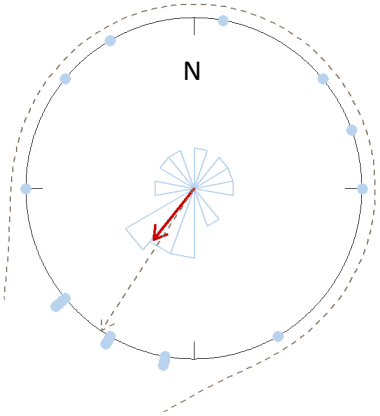	
Rayleigh Test R*=0.34 p=0.11	ΔAICc M1, 0(26%) M2A, 0.19(23%) M2B, 0.25(23%)	Rayleigh Test R*=0.39 p=0.06	ΔAICc M2B: 0(52%) M1: 5.75(5%)
(b_i) (2) Pol 90°		(b_{ii}) (2) Unpol 90°	
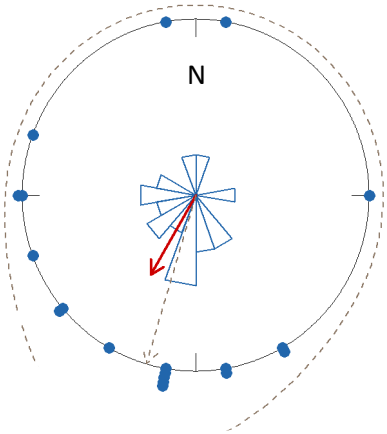		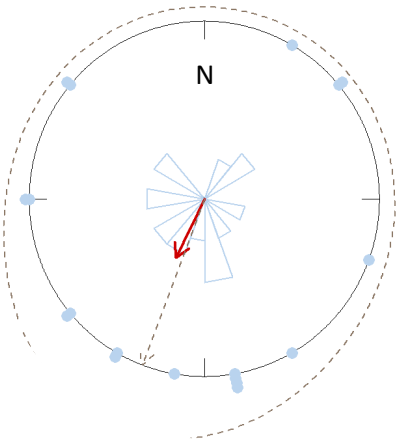	
Rayleigh Test R*=0.52 p=0.05	ΔAICc M2B: 0(39%) M2A: 0.55(29%) M1: 6.92(1%)	Rayleigh Test R*=0.37 p=0.09	ΔAICc M2B: 0(32%) M2A: 0.92(20%) M1: 1.176(18%)

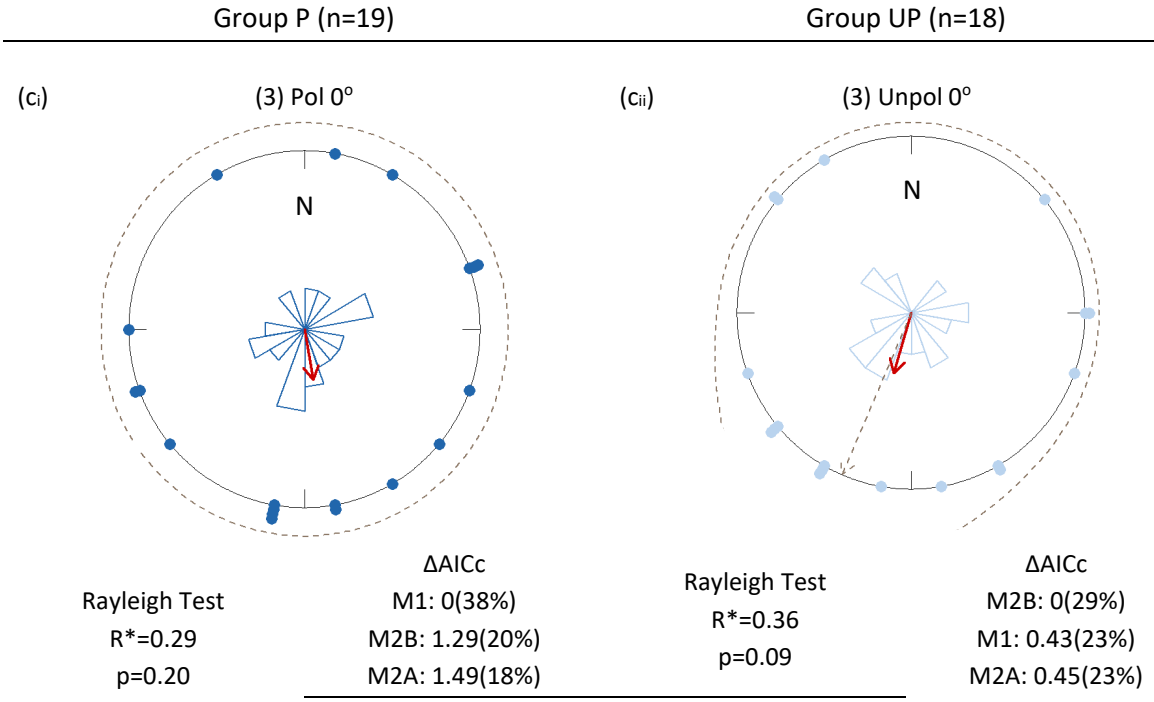

Figure 3.5. The observed and modelled orientations of group P (left) and group UP (right) across the first (a) 0° to (b) 90° to (c) 0° rotations of the polarized treatment (dark blue) and unpolarized treatment (light blue). Mean directions (red arrows) and circular histograms (blue and purple bars and dots) represent observed orientation of *Helicoverpa armigera* in 20° bins. The density (dashed line) and mean direction(s) (dashed arrows) of the model with the lowest ΔAICc value are shown. The ΔAICc and probability (%) of the models with a ΔAICc of <2 and the uniform M1 model are given, as are the test statistic (R*) and p-value of the Rayleigh Tests for each treatment.

Following the first rotation of the polarized treatment of group P from 0-90° (Fig.3.5b_i), the moths converged around the mean south-southwest direction, with a near-significant difference from uniform (models with ΔAICc <2=M2B, M2A; Rayleigh Test R*=0.52, p=0.05). In the unpolarized treatment of group UP (Fig.3.5b_{ii}) minimal changes occurred to the direction and distribution of the moths (models with ΔAICc <2=M2B, M2A, M1; Rayleigh Test R*=0.37, p=0.09).

Following the second rotation of the polarized treatment from 90-0° (Fig.3.5c_i), the moths lost unimodality and became more scattered (models with ΔAICc <2=M1, M2B, M2A; Rayleigh Test R*=0.29, p=0.20). Again, minimal changes were observed in the direction and distribution of the moths in the unpolarized treatment following the second rotation from 90-0° (Fig.3.5c_{ii}; models with ΔAICc <2=M2B, M1, M2A; Rayleigh Test R*=0.36, p=0.09).

Circular distributions: Treatment inversion

The inversion of the filter stack from polarized to unpolarized did not cause any substantial changes in the moths of group P (Fig.3.6a_i,b_i) which became marginally more concentrated around the mean (models with ΔAICc <2=M2A, M1, M2B; Rayleigh Test R*=0.37, p=0.07). In group UP (Fig.3.6a_{ii},b_{ii}), the inversion of the filter stack from the unpolarized to polarized treatment caused the circular distribution of the moths to diverge significantly in two directions from the mean: southwest and southeast (models with ΔAICc <2= M5A, M3B, M2A, Rayleigh Test, R*=0.45, p=0.02).

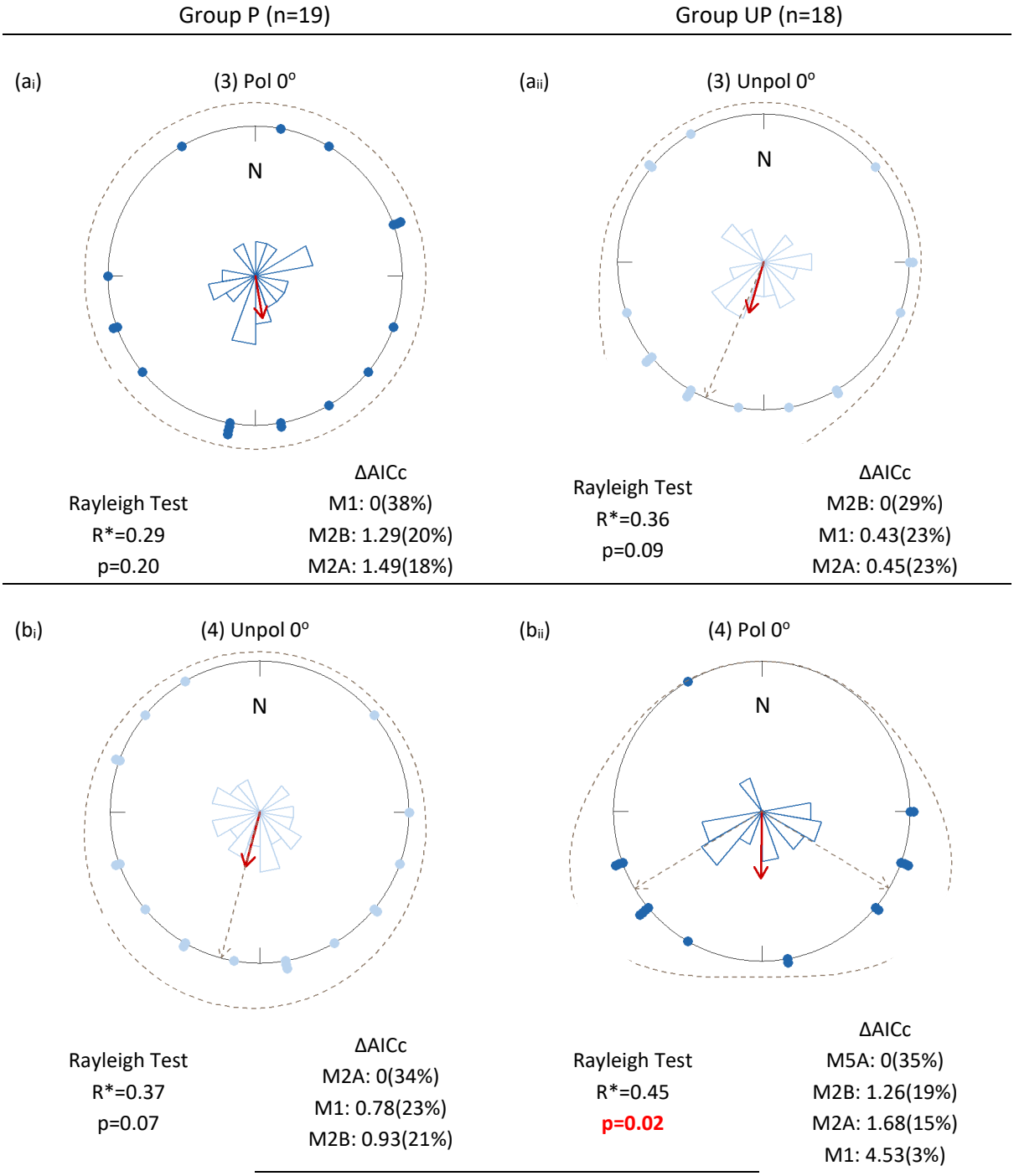

Figure 3.6. The observed and modelled orientations of group P (left) and group UP (right) following the inversion of the filter stack from (a_i) the polarized (dark blue) to (b_i) the unpolarized face (light blue) (group P), and from (a_{ii}) the unpolarized to (b_{ii}) the polarized face (group UP). Red arrows, circular histograms, dashed lines, and dashed arrows are as described in Figure 3.5. The ΔAICc and probability (%) of the models with a ΔAICc of <2 and the uniform M1 model are given, as are the test

statistic (R*) and p-value of the Rayleigh Tests for each treatment. Statistically significant values are highlighted in red. Note that (a) is the same data as Fig.3.5c.

Circular distributions: Rotations of the second treatments

The weak unimodal structure observed in group P following the filter inversion was lost upon the first 90° rotation of the unpolarized treatment (models with ΔAICc <2=M1, M2B, M2A; Rayleigh Test R*=0.27, p=0.25) (Fig.3.7a_i,b_i). In group UP, the moths converged in a strong unimodal south-southwest direction following the first rotation of the polarized treatment (models with ΔAICc <2=M2A, M2B, M2C; Rayleigh Test R*=0.54, p=0.004) (Fig.3.7a_{ii},b_{ii}).

The distributions of both groups of moths lost all structure following the final rotation of the treatments from 90-0° (group P: models with ΔAICc <2=M1, M3A, M2B; Rayleigh Test R*=0.12, p=0.77, group UP: models with ΔAICc <2=M1, M2A, M2B; Rayleigh Test R*=0.33, p=0.14), but still maintained a weak mean direction towards the south-southwest (Fig.3.7b,c).

Group P (n=19)		Group UP (n=18)	
(a_i) (4) Unpol 0°		(a_{ii}) (4) Pol 0°	
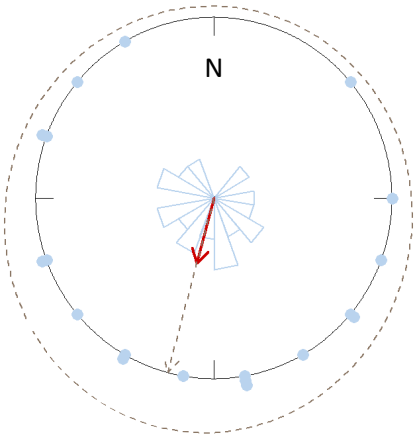		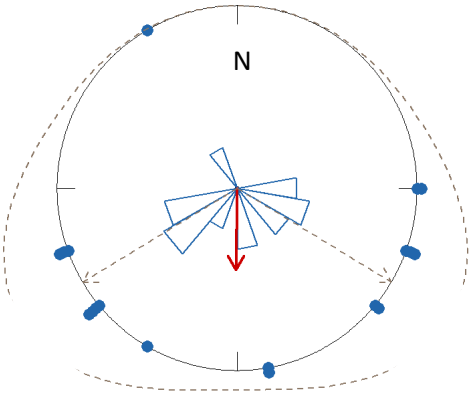	
Rayleigh Test R*=0.37 p=0.07	ΔAICc M2A: 0(34%) M1: 0.78(23%) M2B: 0.93(21%)	Rayleigh Test R*=0.45 **p=0.02**	ΔAICc M5A: 0(35%) M2B: 1.26(19%) M2A: 1.68(15%) M1: 4.53(3%)
(b_i) (5) Unpol 90°		(b_{ii}) (5) Pol 90°	
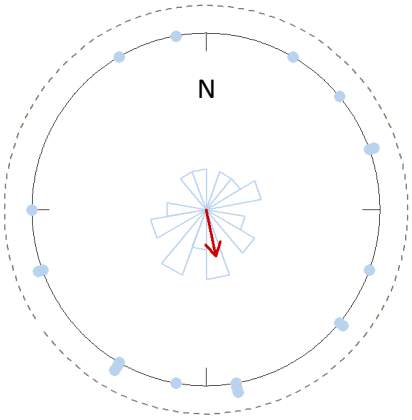		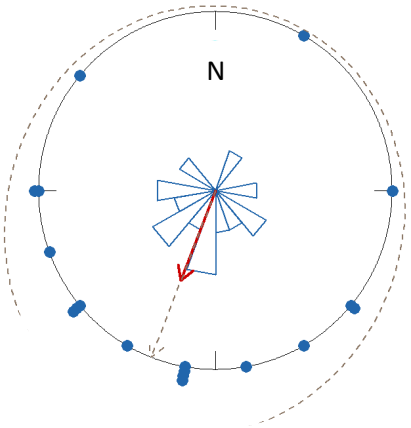	
Rayleigh Test R*=0.27 p=0.25	ΔAICc M1: 0(42%) M2B: 1.72(18%) M2A: 1.92(16%)	Rayleigh Test R*=0.54 **p=0.004**	ΔAICc M2A: 0(54%) M2B: 1.67(23%) M2C: 3.22(11%) M1: 6.64(1%)

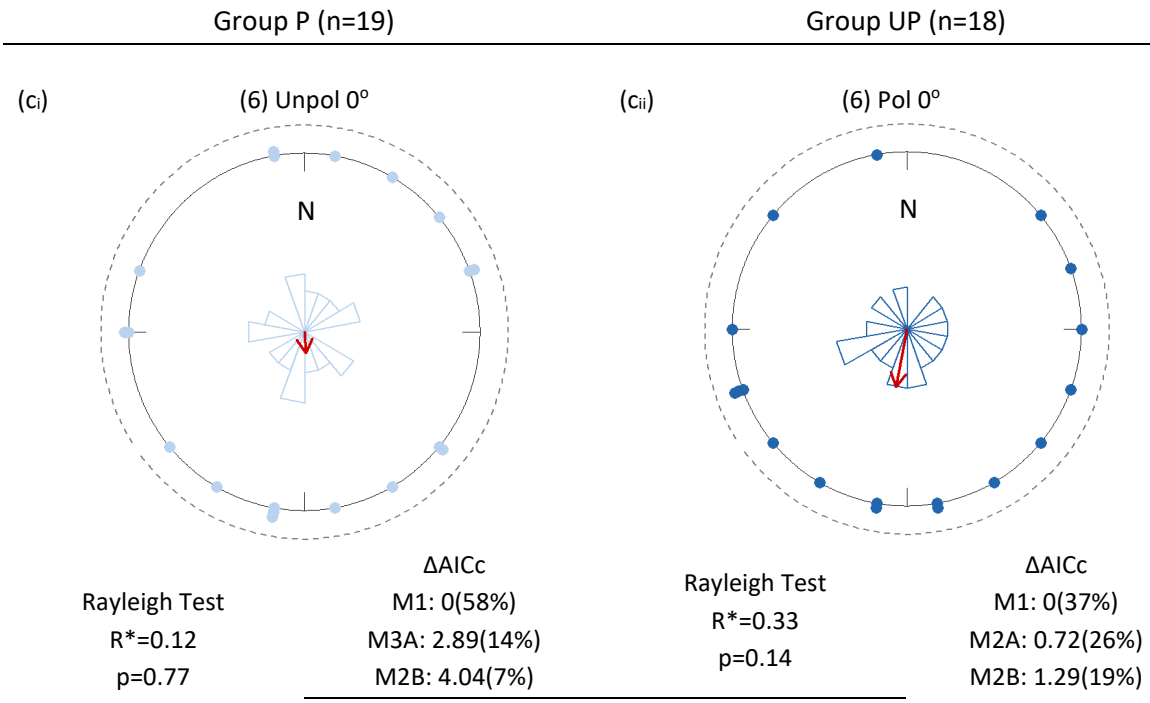

Figure 3.7. The observed and modelled orientations of group P (left) and group UP (right) across the second (a) 0° to (b) 90° to (c) 0° rotations of the polarized treatment (dark blue) and unpolarized treatment (light blue). Red arrows, circular histograms, dashed lines, and dashed arrows are as described in Figure 3.5. The ΔAICc and probability (%) of the models with a ΔAICc of <2 and the uniform M1 model are given, as are the test statistic (R*) and p-value of the Rayleigh Tests for each treatment. Statistically significant values are highlighted in red. Note that (a) is the same data as Fig.3.6b.

Circular distributions: Real night sky

Moths in group UP (that were exposed to the polarized treatment immediately prior to the real night sky) exhibited uniform distributions both before (models with ΔAICc <2=M1, M2A, M2B, Rayleigh Test, R*=0.33, p=0.14) and after the switch (models with ΔAICc <2=M1, M2B, M3A, Rayleigh Test, R*=0.24, p=0.41) (Fig.3.8a_{ii},b_{ii}). Those in group P, that had previously experienced the unpolarized treatment, changed from a uniform distribution (models with ΔAICc <2=M1, M3A, M2B, Rayleigh Test, R*=0.12, p=0.7) to a weakly bimodal northwest-southeast distribution (models with ΔAICc <2=M3A, M2B, M3B, Rayleigh Test, R*=0.24, p=0.37) (Fig.3.8a_{i},b_{i}). However, this change in distribution was not statistically significant from uniform.

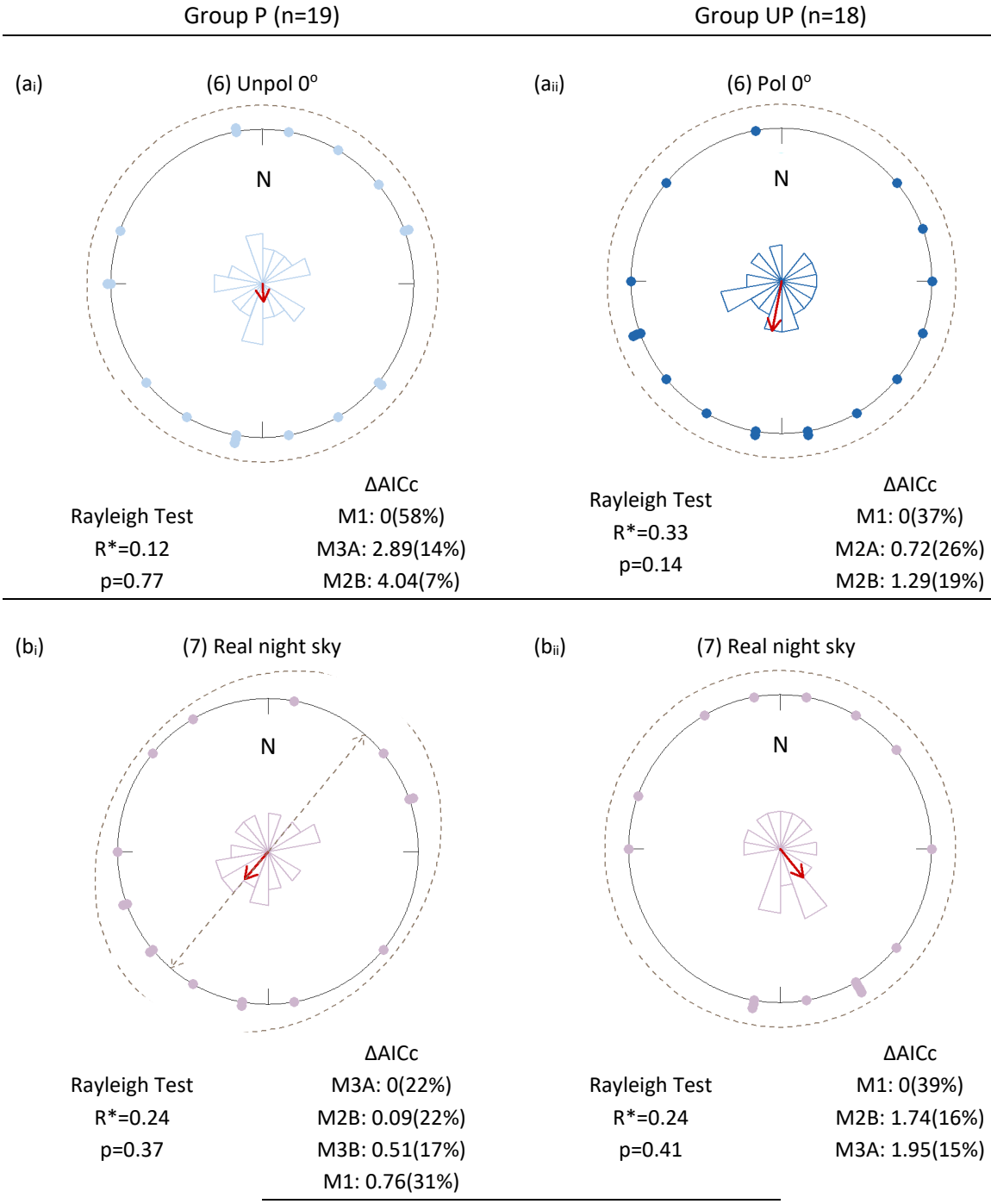

Figure 3.8. The observed and modelled orientations of group P (left) and group UP (right) (a) prior to and (b) following the removal of the filter stack to reveal the real night sky (purple) after exposure to the unpolarized treatment (light blue) and the polarized treatment (dark blue). Red arrows, circular histograms, dashed lines, and dashed arrows are as described in Figure 3.5. The ΔAICc and probability (%) of the models with a ΔAICc of <2 and the uniform M1 model are given, as are the test statistic (R*) and p-value of the Rayleigh Tests for each treatment. Statistically significant values are highlighted in red. Note that (a) is the same data as Fig.3.7c.

3.4 Discussion

This investigation explored the effect of the polarization of light on orientation, heading selection, and directedness in *H. armigera* at the individual and group level. We found limited evidence that polarization consistently and reliably influenced the orientation behaviour of individuals. However, at the population level, we found that *H. armigera* generally flew in a south-westerly direction and that the distributions of the selected headings and directedness of the moth's flight paths were only ever significant when exposed to polarization. Furthermore, the moths were more likely to change orientation and/or the concentration around a mean direction following rotations of the polarized treatment, and these same parameters were more likely to be lost or reduced without polarization. The introduction of the real sky polarization pattern also caused a small change in these parameters. This is the first time polarization-guided navigation has been shown behaviourally in a nocturnal lepidopteran.

We also found an interesting effect of order of presentation on the grouped flight behaviour of *H. armigera*. The moths that began flight with polarization lost their ability to orientate when it was removed, while moths that began flight without polarization were able to maintain orientation but became briefly disorientated when it was introduced. These results lead to interesting conclusions on the migratory performance of *H. armigera* when flying through larges areas of intermittently high levels of light pollution.

3.4.1 Skylight polarization and orientation in individuals

Turning responses and directedness

The polarization of light did not affect the directedness of the flight paths of individual *H. armigera*, nor did a change in AoP cause a direction change of >45°. We could not replicate the turning responses of monarch butterflies following the rotation of an overhead polarizer observed by Reppert *et al*. (2004)[46]. Rather, our results agree with the opposing observation by Stalleicken *et al*. (2005)[47], who found limited evidence of turning responses in individuals to the same stimulus. Overall, directedness was high with and without polarization (mean *r*: polarized treatments=0.73, unpolarized treatments=0.60). This was expected, and indeed desired, given that the supplementary visual cues of an artificial moon and mountains were given to the moths to intentionally increase flight stability. That being said, a decrease in directedness was expected following the rotation of the polarized treatment, which would have set the visual landmarks within the flight simulator into conflict with the directional information given by the polarized cue[10]. Reppert *et al*. (2004)[46] did not report

observations of directedness in individuals but Stalleicken *et al*. (2005) also found limited effects of polarization on the directedness of individual butterflies.

However, our grouped observations of mean orientation direction, the distributions around the mean, and directedness of *H. armigera* in response to changes in an overhead polarized cue do not reflect that observed in individuals. This contrasts with the grouped observations of Stalleicken *et al*. (2005), who found no effect of polarization on mean group orientation or directedness[47]. Our results suggest that skylight polarization does indeed promote orientation performance in populations of a migratory lepidopteran.

3.4.2 Skylight polarization and orientation in populations

Group direction

Helicoverpa armigera fly through the Port de Boucharo pass in a south-south-westerly direction during their autumn migrations (Fig.3.9). *H. armigera* flew in this direction independent of polarization when inside the flight simulator, probably due to the presence of an artificial moon and mountains providing consistent directional information, as mentioned above, but also potentially the result of magnetic cues from the tether or the Earth's magnetic field providing directional information[10].

Despite no evidence of large directional changes, group direction did shift from west-southwest to south-southwest following the first rotation of the polarized treatment of group P (Fig.3.5), and then again from south-southwest to south-southeast following the second rotation. An effect that was not observed during the same rotations of the unpolarized treatment in group UP. This contrasts with the observations made at the individual-level and could be explained, in part, by the small number of individuals that did turn >45° effectively shifting overall mean direction. Or perhaps individuals that turned <45° but converged on the same direction may also have significantly shifted the mean direction of the groups. Under natural skies, the lunar polarization pattern will rotate over time as the moon moves across the horizon[41] and navigating arthropods will adjust their trajectories accordingly to maintain a desired heading[9,23]. When in the flight simulator, the moths may be correcting their trajectories in response to the change in the artificial polarization pattern as they would in the wild, although these changes occur over several hours in the wild unlike several seconds in the flight simulator. However, these differential shifts in group direction between treatment rotations in the first half of the experiment (Fig.3.5) were not repeated in the second half (Fig.3.7). Wherein which, group P were observed to change direction following rotations of the unpolarized treatment alongside similar changes, albeit much lower in strength, in group UP following rotations of the polarized treatment. This effect can be attributed to the loss of unimodality within group P, which begin the

second half of the experiment in a unimodal distribution that became more uniform with each rotation, rather than a response to the unpolarized treatment. Thus, suggesting a loss of orientation direction in the group over time following the removal of the polarized cue.

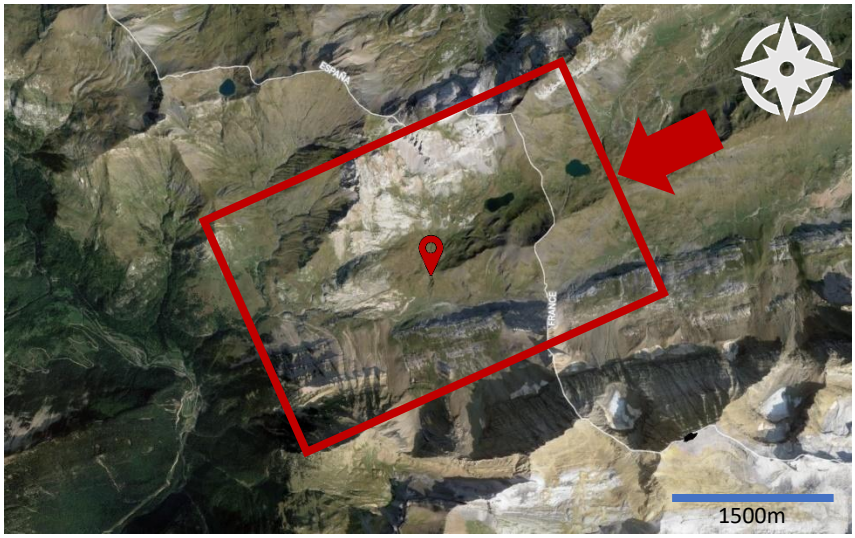

Figure 3.9. Aerial image of the valley in the Hautes-Pyrénées (red box) where *Helicoverpa armigera* were collected during their autumn migration through Europe (red marker shows site of collection). The red arrow indicates the south-westerly direction of the moths during this migration which aligns with the mean group directions of the moths observed during the flight simulator experiment. Aerial image taken from Google Earth (v.9.163.0.0, Gavarnie, France, Lat=42.703950, Long=-0.063988, eye altitude= 2381m).

Larger directional changes were observed in both groups in the final two minutes of the experiment, when the moths were exposed to real sky polarization pattern (Fig.3.8). Prior to exposure to the real sky polarization pattern, both groups of moths were flying in a weakly southern direction (Fig.3.8a). Group P shifted to a south-westerly direction following the removal of the unpolarized treatment and group UP shifted to a south-easterly direction following the removal of the polarized treatment (Fig.3.8b). We would expect the moths of group P to change direction towards the southwest given that they experienced a change from no polarization to the true skylight polarization pattern. In group UP, perhaps the artificial polarization pattern and the real polarization pattern where manually misaligned, creating a cue conflict and subsequent confusion in some individuals following the removal of the artificial polarization. However, distributions and directness of both groups of moths were weak, and large directional changes where not observed upon exposure to artificial polarization following the inversion of the filter stack in group UP (Fig.3.6b_{ii}), so it is difficult to interpret ecological meaning from these observations.

Circular distributions

H. armigera significantly clustered around a particular mean direction when exposed to artificial polarization only (Fig.3.7). Similarly, in the first half of the experiment, the circular distributions of the moths changed with the rotation of the polarized treatment only (Fig.3.5). The moths in group UP maintained a unimodal south-southwest distribution throughout both rotations of the unpolarized treatment, whereas the moths in group P changed from a uniform distribution to a unimodal south-south-west distribution and back to a uniform distribution following the two rotations of the polarized treatment. In the second half of the experiment, significant changes to the distribution of the moths were observed following rotations of the polarized cue, which were not observed after rotations of the unpolarized cue (Fig.3.7). The former changing from a significant bi-modal distribution to a significant unimodal distribution before becoming uniform, and the latter changing from a weakly unimodal distribution to an increasingly uniform distribution. This loss of directionality over time under the unpolarized treatment was weakly observed in the first half of the experiment in group UP and more strongly (although not significantly) observed in the second half of the experiment in group P. Furthermore, the addition of artificial (Fig3.6) and real sky polarization (Fig.3.8) caused the moths to change their heading distributions, significantly in the case of the former, which was not observed to the same magnitude when artificial polarization was removed (Fig.3.6b).

This suggests that polarization is a) detectable and b) relevant to orientation in *H. armigera*. It also suggests that skylight polarization is a dominant cue within the hierarchy of visual navigational cues, being placed above large visual landmarks like the moon and mountains which did not prevent changes in distribution and losses in directionality following the presence or absence of polarization, respectively. This contrasts with diurnal monarch butterflies, which use the sun as the dominant celestial cue when migrating[47]. However, we did not use the real moon as a navigational cue so we cannot be certain of its dominance in the compass of *H. armigera*. Nonetheless, given that the behaviour of the moon and its polarization pattern is dynamic (see chapter 2), it is surprising that the moon would be a dominant visual cue within the compass hierarchy. Perhaps the moths account for this by timing their migrations with the lunar cycle, much like how some migratory moths delay migratory flight until the occurrence of favourable winds[48]. Further evidence on the hierarchical importance of a suite of navigational cues will help us better predict the impacts of the obscuring effect of light pollution on the skylight polarization pattern.

Directedness

Group directedness (R*) was highest during the polarization treatments, particularly in the second half of the experiment (Fig.3.5 and Fig.3.7). Directedness improved following the first rotation of the

polarized treatment and decreased after the second rotation in groups P and UP, suggesting an initial adjustment to the new orientation of the polarized treatment and subsequently becoming confused and scattered following a second change shortly after. In contrast, directedness was stable in the initial rotations of the unpolarized treatment in group UP but reduced dramatically during the rotations of the same treatment in group P in the latter half of the experiment. The moths in group UP potentially used visual landmarks or other cues to orientate at the start of the experiment, as mentioned above, and thus were unaffected by the unpolarized overhead cue. The gradual reduction in directedness in group P during the unpolarized treatment echoes the weak change in mean direction and concentration around the mean described above. Again, suggesting that the removal of polarization for even short lengths of time causes a loss of orientation. Temporary loss of skylight polarization can occur in nature during overcast conditions[14], highlighting the need for flexible navigation in nocturnal arthropods, but in lepidopterans the flexibility of this system may be time sensitive. Inside the flight simulator, *H. armigera* were able to maintain their directedness and direction in the first few minutes following cue loss, but this was gradually lost it over time. In nature, this could be highly problematic for individuals travelling through large areas of urbanization where the polarization pattern could be lost for long stretches of time. Even brief losses of orientation in urban areas could increase the risk of 'flight-to-light' behaviour luring individuals towards bright sources of light[49] and subsequently becoming trapped beneath them (see chapter 5). Additionally, as an economically important agricultural pest, erroneous trajectories and disorientation could affect the densities of individuals feeding and breeding on agricultural land with implications for productivity and profitability[50,51,52].

The addition of artificial (Fig3.6) and real sky polarization (Fig.3.8) caused a disparity in the changed directedness of the moths. Those that experienced a transition from artificial polarization to no polarization (Fig.3.6) lost some directedness, and the same effect occurred in those that experienced the opposite. However, when introducing the real sky polarization pattern (Fig.3.8), the moths experiencing a transition from artificial to real polarization lost some directedness, whereas those that experienced a transition from no polarization to the real sky polarization pattern gained directedness. The discrepancy between grouped directedness following the introduction of the real skylight polarization pattern was expected as one group gained a directional cue (group P) whilst the other possibly experienced some cue conflict (group UP). The shared increase in directedness following the transitions between artificially polarized treatments is more difficult to interpret. However, only the transition from the unpolarized to polarized treatments was significantly non-uniformly distributed, thus supporting the conclusion that polarization did indeed affect directedness and heading selection.

3.5 Conclusions

H. armigera were more concentrated around biologically meaningful headings and maintained this orientation over time under artificial skylight polarization. When migrating, this could aid successful and more efficient migration. Without skylight polarization, the moths were still able to maintain a weak heading direction, but trajectories were more scattered, and directedness degraded considerably following the removal of polarization. Thus, light pollution threatens the navigational efficiency of *H. armigera* during their seasonal migrations by obscuring an important visual input of their navigational compass. These results also hint at the importance of context: animals that began their flight in the absence of polarization (e.g., in polluted areas) were somewhat able to identify and maintain the 'correct' heading but may then experience cue conflicts when they are exposed to polarization (e.g., entering dark areas). Conversely, animals initiating flight with polarization cues available may be less able to maintain their orientation if these cues are lost. Questions remain about specific behavioural polarization sensitivity thresholds in lepidopteran and where these fall in relation to light pollution radiance and skylight polarization dilution.

References

1. Webb B. 2019. The internal map of insects. *Journal of Experimental Biology*, **222**(Suppl_1): jeb188094. (DOI: 10.1242/jeb.188094)
2. Warrant E, Dacke M. 2016. Visual navigation in nocturnal insects. *Physiology*, **31**: 182-192. (DOI: 10.1152/physiol.00046.2015)
3. Freas CA, Narendra N, Lemesle C, Cheng K. 2017. Polarized light use in the nocturnal bull ant, *Myrmecia midas*. *Royal Society Open Science*, **4**: 170598. (DOI: 10.1098/rsos.170598)
4. Zeil J, Ribi WA, Narendra A. 2014. Polarization vision in ants, bees and wasps. In: Horváth G, editor, 2nd Ed., Polarized light and polarization vision in animal sciences. Springer Series in Vision Research, vol 2. Springer, Berlin, Heidelberg, pp. 41-60.
5. Dacke M, Nordstrom P, Scholtz CH. 2003. Twilight orientation to polarised light in the crepuscular dung beetle *Scarabaeus zambesianus*. *Journal of Experimental Biology*, **206**(9): 1535-1543. (DOI: 10.1242/jeb.00289)
6. Mouritsen H, Frost BJ. 2002. Virtual migration in tethered flying monarch butterflies reveals their orientation mechanisms. *Proceedings of the National Academy of Sciences*, **99**(15): 10162-10166. (DOI: 10.1073/pnas.152137299)
7. Wehner, R. 2001. Polarization vision – A uniform sensory capacity? *Journal of Experimental Biology*, **204**(14): 2589-2596. (DOI: 10.1242/jeb.204.14.2589)
8. Dacke M, Nilsson DE, Warrant EJ, Blest AD, Land MF, O'Carroll DC. 1999. Built-in polarizers form part of a compass organ in spiders. *Nature*, **401**(6752): 470-473. (DOI: 10.1038/46773)
9. Foster JJ, Kirwan JD, el Jundi B, Smolka J, Khaldy L, Baird E. Byrne MJ, Nilsson DE, Johnsen S, Dacke M. 2019. Orienting to polarized light at night - matching lunar skylight to performance in a nocturnal beetle. *Journal of Experimental Biology*, **222**(2): jeb188532. (DOI: 10.1242/jeb.188532)
10. Dreyer D, Frost B, Mouritsen H, Gunther A, Green K, Whitehouse M, Johnsen S, Heinze S, Warrant E. 2018. The Earth's magnetic field and visual landmarks steer migratory flight behaviour in the nocturnal Australian bogong moth. *Current Biology*, **28**: 2160-2166. (DOI: 10.1016/j.cub.2018.05.030)
11. el Jundi B, Smolka J, Baird E, Byrne MJ, Dacke M. 2014. Diurnal dung beetles use the intensity gradient and the polarization pattern of the sky for orientation. *Journal of Experimental Biology*, **217**: 2422-2429. (DOI: 10.1242/jeb.101154)
12. Wehner R. 1997. The ant's celestial compass system: spectral and polarization channels. In: Lehrer M. (eds) Orientation and communication in arthropods. Birkhäuser Verlag, Basel, Switzerland, pp. 145–185.
13. Khaldy L, Foster JJ, Yilmaz A, Belušič G, Gagnon Y, Tocco C, Byrne MJ, Dacke M. 2022. The interplay of directional information provided by unpolarised and polarised light in the heading direction network of the diurnal dung beetle *Kheper lamarcki*. *Journal of Experimental Biology*, **225**(3): jeb243734. (DOI: 10.1242/jeb.243734)
14. Henze MJ, Labhart T. 2007. Haze, clouds and limited sky visibility: Polarotactic orientation of crickets under difficult stimulus conditions. *Journal of Experimental Biology*, **210**(18): 3266-76. (DOI: 10.1242/jeb.007831)
15. Foster JJ, Tocco C, Smolka J, Khaldy L, Baird E, Byrne MJ, Nilsson DE, Dacke M. 2021. Light pollution forces a change in dung beetle orientation behavior. *Current Biology*, **31**(17): 3935-3942. (DOI: 10.1016/j.cub.2021.06.038)

16. Owens ACS, Cochard P, Durrant J, Farnworth B, Perkin EK, Seymoure B. 2020. Light pollution is a driver of insect declines. *Biological Conservation*, **241**: 108259. (DOI: 10.1016/j.biocon.2019.108259)
17. Owens ACS, Lewis SM. 2018. The impact of artificial light at night on nocturnal insects: A review and synthesis. *Ecology and Evolution*, **8**(22): 11337-11358. (DOI: 10.1002/ece3.4557)
18. el Jundi B, Pfeiffer K, Heinze S, Homberg U. 2014. Integration of polarization and chromatic cues in the insect sky compass. *Journal of Comparative Physiology A*, **200**(6): 575-589. (DOI: 10.1007/s00359-014-0890-6)
19. Ugolini A, Boddi V, Mercatelli L, Castellini C. 2005. Moon orientation in adult and young sandhoppers under artificial light. *Proceedings of the Royal Society B*, **272**(1577): 2189-2194. (DOI: 10.1098/rspb.2005.3199)
20. el Jundi B, Foster JJ, Khaldy L, Byrne MJ, Dacke M, Baird E. 2016. A snapshot-based mechanism for celestial orientation. *Current Biology*, **26**(11): 1456-62. (DOI: 10.1016/j.cub.2016.03.030)
21. Smolka J, Baird E, el Jundi B, Reber T, Byrne MJ, Dacke M. 2016. Night sky orientation with diurnal and nocturnal eyes: Dim-light adaptations are critical when the moon is out of sight. *Animal Behaviour*, **111**: 127-146. (DOI: 10.1016/j.anbehav.2015.10.005)
22. Heinze S, Reppert SM. 2011. Sun compass integration of skylight cues in migratory monarch butterflies. *Neuron*, **69**(2): 345-58. (DOI: 10.1016/j.neuron.2010.12.025)
23. Dacke M, Doan TA, O'Carroll DC. 2001. Polarized light detection in spiders. *Journal of Experimental Biology*, **204**(14): 2481-90. (DOI: 10.1242/jeb.204.14.2481)
24. Patel RN, Cronin TW. 2020. Mantis shrimp navigate home using celestial and idiothetic path integration. *Current Biology*, **30**(11): 1981-7. (DOI: 10.1016/j.cub.2020.03.023)
25. Lebhardt F, Ronacher B. 2015. Transfer of directional information between the polarization compass and the sun compass in desert ants. *Journal of Comparative Physiology A*, **201**(6): 599-608. (DOI: 10.1007/s00359-014-0928-9)
26. Weir PT, Dickinson MH. 2012. Flying drosophila orient to sky polarization. *Current Biology*, **22**(1): 21-7. (DOI: 10.1016/j.cub.2011.11.026)
27. Homberg U, Heinze S, Pfeiffer K, Kinoshita M, El Jundi B. 2011. Central neural coding of sky polarization in insects. *Philosophical Transactions of the Royal Society B*, **366**(1565): 680-7. (DOI: 10.1098/rstb.2010.0199)
28. Hegedüs R, Barta A, Bernath B, Meyer-Rochow VB, Horvath G. 2007. Imaging polarimetry of forest canopies: How the azimuth direction of the sun, occluded by vegetation, can be assessed from the polarization pattern of the sunlit foliage. *Applied Optics*, **46**(23): 6019-6032. (DOI: 10.1364/ao.46.006019)
29. Hegedüs R, Akesson S, Horvath G. 2007. Polarization patterns of thick clouds: Overcast skies have distribution of the angle of polarization similar to that of clear skies. *Journal of the Optical Society of America A*, **24**(8): 2347-2356. (DOI: 10.1364/josaa.24.002347)
30. Cronin TW, Shashar N, Caldwell RL, Marshall J, Cheroske AG, Chiou TH. 2003. Polarization signals in the marine environment. Proc. SPIE 5158, *Polarization Science and Remote Sensing*, (12 December 2003). (DOI: 10.1117/12.507903)
31. Torres D, Tidau S, Jenkins S, Davies T. 2020. Artificial skyglow disrupts celestial migration at night. *Current Biology*, **30**(12): E696-E7. (DOI: 10.1016/j.cub.2020.05.002)
32. Dacke M, Byrne M, Smolka J, Warrant E, Baird E. 2013. Dung beetles ignore landmarks for straight-line orientation. *Journal of Comparative Physiology A*, **199**(1): 17-23. (DOI: 10.1007/s00359-012-0764-8)

33. Brehm G. 2017. A new LED lamp for the collection of nocturnal Lepidoptera and a spectral comparison of light-trapping lamps. *Nota lepidopterological*, **40**: 87–108. (DOI: 10.3897/nl.40.11887)
34. Sondhi Y, Ellis EA, Bybee SM, Theobald JC, Kawahara AY. 2021. Light environment drives the evolution of color vision genes in butterflies and moths. *Integrative and Comparative Biology*, **4**(61): 177. (DOI: 10.1038/s42003-021-01688-z)
35. Feuda R, Marletaz F, Bentley MA, Holland PWH. 2016. Conservation, duplication, and divergence of five opsin genes in insect evolution. *Genome Biology and Evolution*, **8**(3): 579-587. (DOI: 10.1093/gbe/evw015)
36. Eguchi E, Watanabe K, Hariyama T, Yamamoto K. 1982. A comparison of electrophysiologically determined spectral responses in 35 species of Lepidotopera. *Journal of Insect Physiology*, **28**(8): 675-682. (DOI: 10.1016/0022-1910(82)90145-7)
37. Mathis A, Mamidanna P, Cury KM, Abe T, Murthy VN, Mathis MW, Bethge M. 2018. DeepLabCut: markerless pose estimation of user-defined body parts with deep learning. *Nature Neuroscience,* **21**(9): 1281–1289. (DOI: 10.1038/s41593-018-0209-y)
38. Agostinelli C. 2018. CircStats: Circular statistics, from "Topics in circular statistics" (2001). R package version 0.2-6. (https://CRAN.R-project.org/package=CircStats)
39. Thomas R, Lello J, Medeiros R, Pollard A, Robinson P, Seward A, Smith J, Vafidis J, Vaughan I. 2017. Statistical Models: Model selection. In: Thomas R. (eds), 2nd Ed., Data analysis with R statistical software – A guidebook for scientists. Eco-explore, Cardiff, UK, pp. 69-71.
40. Hartig F. 2022. DHARMa: Residual diagnostics for hierarchical (multi-level / mixed) regression models. R package version 0.4.5. (https://CRAN.R-project.org/package=DHARMa)
41. Fitak RR, Johnsen S. 2017. Bringing the analysis of animal orientation data full circle: Model-based approaches with maximum likelihood. *Journal of Experimental Biology*, **220**(21): 3878-3882. (DOI: 10.1242/jeb.167056)
42. Schnute JT, Groot K. 1992. Statistical analysis of animal orientation data. *Animal Behaviour*, **43**(1): 15-33. (DOI: 10.1016/s0003-3472(05)80068-5)
43. Brewer MJ, Butler A, Cooksley SL. 2016. The relative performance of AIC, AIC(C) and BIC in the presence of unobserved heterogeneity. *Methods in Ecology and Evolution*, **7**(6): 679-692. (DOI: 10.1111/2041-210x.12541)
44. Burnham KP, Anderson DR, Huyvaert KP. 2011. AIC model selection and multimodel inference in behavioral ecology: Some background, observations, and comparisons. *Behavioral Ecology and Sociobiology*, **65**(1): 23-25. (DOI: 10.1007/s00265-010-1029-6)
45. Kingston ACN, Chappell DR, Speiser DI. 2018. Evidence for spatial vision in *Chiton tuberculatus*, a chiton with eyespots. *Journal of Experimental Biology*, **221**(19): jeb183632. (DOI: 10.1242/jeb.183632)
46. Reppert SM, Zhu HS, White RH. 2004. Polarized light helps monarch butterflies navigate. *Current Biology*, **14**(2): 155-8. (DOI: 10.1016/j.cub.2003.12.034)
47. Stalleicken J, Mukhida M, Labhart T, Wehner R, Frost B, Mouritsen H. 2005. Do monarch butterflies use polarized skylight for migratory orientation? *Journal of Experimental Biology*, **208**(12): 2399-2408. (DOI: 10.1242/jeb.01613)
48. Chapman JW, Reynolds DR, Mouritsen H, Hill JK, Riley JR, Sivell D, Smith AD, Woiwod IP. 2008. Wind selection and drift compensation optimize migratory pathways in a high-flying moth. *Current Biology*, **18**(7): 514-518. (DOI: 10.1016/j.cub.2008.02.080)

49. Donners M, van Grunsven RHA, Groenendijk D, van Langevelde F, Bikker JW, Longcore T, Veenendaal E. 2018. Colors of attraction: Modeling insect flight to light behavior. *Journal of Experimental Zoology Part A*, **329**(8-9): 434-440. (DOI: 10.1002/jez.2188)
50. Jones CM, Parry H, Tay WT, Reynolds DR, Chapman JW. 2019. Movement ecology of pest *Helicoverpa*: Implications for ongoing spread. *Annual Review of Entomology*, **64**: 277-295. (DOI: 10.1146/annurev-ento-011118-111959)
51. Nowinszky L, Puskas J, Barczikay G. 2015. The relationship between polarized moonlight and the number of pest microlepidoptera specimens caught in pheromone traps. *Polish Journal of Entomology*, **84**(3): 163-176. (DOI: 10.1515/pjen-2015-0014)
52. Fitt GP. 1989. The ecology of *Heliothis* species in relation to agroecosystems. *Annual Review of Entomology*, **34**: 17-52. (DOI: 10.1146/annurev.en.34.010189.000313)

4

Light pollution and nocturnal navigation in Drassodes *sp.*

The previous chapter provided evidence to link light pollution and the impairment of polarization-guided navigation in *Helicoverpa armigera*. This chapter has a similar aim and reports two behavioural experiments using a tethered walking system to test for the effect of diminished skylight polarization on orientation in *Drassodes* sp.. The first experiment was an adaptation of the tethered flight experiment described in chapter 3 and was designed to test for the effect of the presence and absence of skylight polarization on orientation. The second experiment was designed to identify behavioural thresholds of polarization sensitivity that might help to establish the link between light pollution radiance, the dilution of the skylight polarization pattern, and the limits of detectability of *Drassodes* sp. polarization-guided navigation.

Contributions: Vun Wen Jie built the trackball and helped to develop the tethering method. I, Vun Wen Jie, Susan Meah, and Rebecca Meah collected the animals. I undertook data collection, data analysis, and authored the chapter in discussion with my supervisors, Nicholas Roberts (University of Bristol) and Lauren Sumner-Rooney (Leibniz Institute for Biodiversity and Evolution Research).

4.1 Background

Drassodes spp. are known to use skylight polarization to navigate during central-place foraging. The weighted importance of skylight polarization to its navigational compass is unknown but anatomical and behavioural evidence suggests that the PMEs are adapted exclusively for the detection of skylight polarization[1]. Such investment in a single functionality suggests that polarization-guided navigation is of high importance to fitness[1]. Therefore, the reduction of the polarization pattern by light pollution is expected to significantly degrade navigational performance in *Drassodes* spp..

The magnitude of this effect will be directly related to the sensitivity of the PMEs to the polarization of light which is estimated to be relatively high compared to other arthropods[1]. However, measurements of polarization sensitivity can vary between experimental paradigms and there are

often discrepancies between measurements obtained by electrophysiology, behavioural techniques, and modelling[2,3,4]. Generally, behavioural techniques estimate thresholds of detection by measuring changes in a robust behavioural response to an incrementally reducing or increasing external stimuli. This provides a more direct insight into the ecological impacts of stimulus strength. A behavioural threshold of polarization detection has yet to be determined in any spider. If *Drassodes* sp. does indeed have high polarization sensitivity then polarization-guided navigation may be able to occur in all but the most light-polluted areas. However, light pollution of radiances between 0-30 nW/cm^{2}sr had a strong negative relationship with the modelled photoreceptor contrast (PRC) of the PMEs of *Drassodes* sp., suggesting that even modest levels of light pollution could affect navigation (see chapter 2). Determining the behavioural thresholds of polarization sensitivity, and its correlation with light pollution radiance and skylight polarization, will give a more accurate picture of the severity of light pollution impacts on nocturnal arthropod movements.

4.1.1 Aims and hypotheses

The following experiments aimed to investigate the impact of the loss of the skylight polarization pattern on orientation performance in *Drassodes* sp. using an adaptation of the trackball design used by Dacke (2001) to test polarized-guided navigation in wolf spiders[5]. This first experiment is analogous to the tethered flight experiment given in the previous chapter but used a tethering system appropriate for walking arthropods. The aim of the experiment was to replicate Dacke (2001)[5] by investigating the use of skylight polarization for heading selection and maintenance in *Drassodes* sp.. Tethered individuals within an arena were exposed to an artificially polarized and unpolarized 'sky' at the zenith to simulate the polarization pattern under natural and light-polluted skies, with the unpolarized 'sky' also serving as a control. Individuals' movement along a fictive path was tracked during 90^o rotations of both treatments to establish whether polarization influenced their ability to maintain a chosen orientation and/or a straight path. Individuals were expected to change orientation direction or become disorientated following the rotation of the polarized treatment and no change in orientation performance was predicted following the rotation of the unpolarized treatment.

The same tethering system was used to determine a behavioural threshold of polarization sensitivity in *Drassodes* sp. and establish the link between light pollution radiance and navigational performance. This was achieved using four polarized treatments with DoP values between 0.3 and 0.9. These conservative values were selected to include: a positive control for comparison with the negative control of the first experiment, and a range of DoP values representative of the measured light pollution radiance given in chapter 2. No more than four treatments were used to limit the duration of the experiment thereby reducing the likelihood of order effects and limiting stress in the spiders.

The fictive paths of individuals were tracked during 90° rotations of the four treatments and compared. The proportion of turning responses following rotations were expected to reduce incrementally with decreasing DoP as shown in other organisms[4,6,7].

4.2 Materials and methods

Adult *Drassodes* sp. were collected from dry stone walls and exposed rock faces at Shibden Valley, UK (Lat=53.758273, Long=-1.846054, mean zenith sky radiance between 2013-2018 from lightpollutionmap.info=4 nW/cm^{2}sr). Individuals were caught in the summer of 2020 and 2021 using pooters (30mm barrel, 7mm tube pooter, Natural History Book Service) when resting within their silk retreats during the day. Following capture, the spiders were transported to a laboratory in Bristol, England, and separated into cylindrical containers containing moss and orchid bark as refuge and sealed with foam lids. The containers were kept under laboratory conditions, exposed to stable temperatures and indirect broad-spectrum artificial light (Radion XR15, EcoTech Marine Inc.) matched to the natural light/dark cycle at the time of capture (Fig.4.1). The same light source was used to illuminate the trackball during the experiments which began shortly after dusk when the spiders naturally became active (see chapter 5). During the experiments, the light source was reduced to near-full-moon radiance (0.4 lux, full moonlight at optimal conditions modelled at 0.3 lux)[8]. The spiders were fed live fruit flies every seven days and given 3-4 drops of water from a pipette every three days.

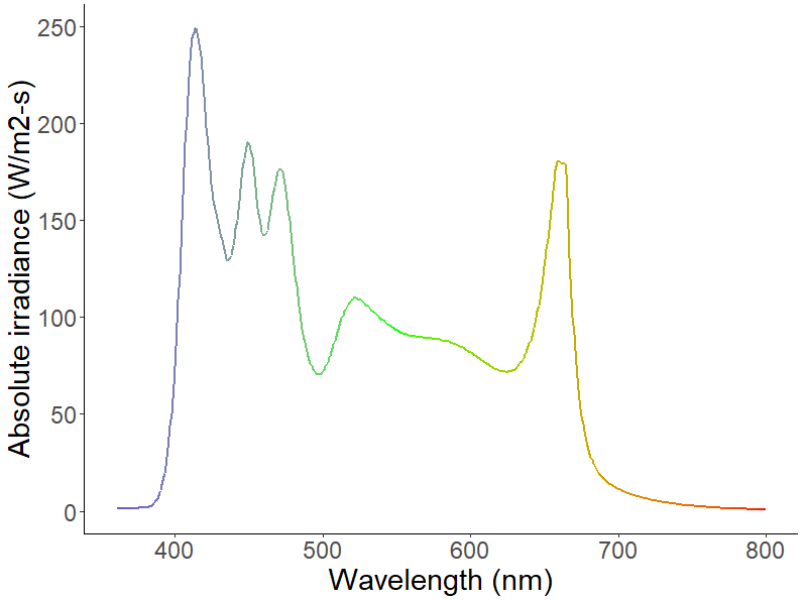

Figure 4.1. Emission spectrum of the broad-spectrum light source used to illuminate *Drassodes* sp. housed in the laboratory in Bristol, UK, taken using a QE65000 spectrometer and a P200-UV-VIS optical fibre (Ocean Insight Inc.) calibrated to a lamp of known spectral output (DH-2000, Ocean Insight Inc.).

4.2.1 Preparation of *Drassodes* sp.

To prepare them for the trackball, the spiders were first immobilised between a large piece of foam and Parafilm. A small hole in the Parafilm was cut above the dorsal cephalothorax and a drop of UV-activated glue (Bondic®) was applied to the exposed exoskeleton. A small square of adhesive metal tape was placed on top of the glue and the glue was cured with a UV LED. With the metallic square adhered to the dorsal cephalothorax, the spiders could then be magnetically tethered to the trackball (Fig.4.2). Following preparation, the spiders were returned to their individual containers and allowed to habituate to the tethers for >12 hours.

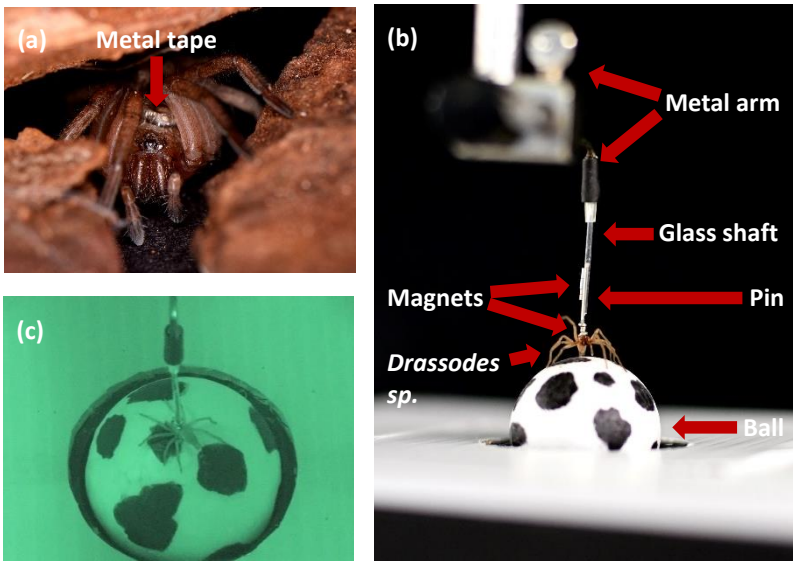

Figure 4.2. (a) Photograph of *Drassodes sp.* prepared for the trackball with a square of metal tape glued to the dorsal cephalothorax. Photograph used with permission from Sam England. (b) Photograph of a tethered *Drassodes* sp. on the trackball apparatus. The spiders were magneto-tethered within a screened experimental arena and positioned on a polystyrene ball, which rotated on an air cushion as the spider walked. Polarized filters (not shown) were above the animal while a video camera recorded behavioural responses in infrared. (c) Example image from an infrared video recording of *Drassodes sp.* on the trackball.

4.2.2 The trackball

The trackball apparatus consisted of a 16x16 cm square platform supported 26 cm in the air. In the centre of the platform was a polystyrene ball (2.7 cm diameter) in a conical support connected to an air supply (Fig.4.3a). When turned on, the air supply created an air cushion beneath the ball such that the ball could freely rotate within its support. Above the polystyrene ball was a small glass shaft connected to a metal arm (Fig.4.2b). A dressmaker pin with a disc magnet glued to the pinhead was suspended inside the glass shaft using external magnets. The metal tape glued to the cephalothorax of the spiders magnetically connected to this dressmaker pin thereby tethering the spiders on top of the trackball and allowing them to rotate the ball on the air cushion as they walked (Fig.4.2b). The arena was illuminated by two infra-red LED security lights invisible to the spiders[1,9] and individuals were recorded using an infrared video camera (HDR-CX405 Camcorder, Sony). The polystyrene ball was painted with irregular shapes in infrared-absorbing, black ink for video tracking (Fig.4.2c). The entire arena was screened from visual disturbance using blackout cloth and the spiders on the

trackball were screened from visual landmarks in the arena by diffuse, non-polarizing baking parchment (Fig.4.3a).

(a)

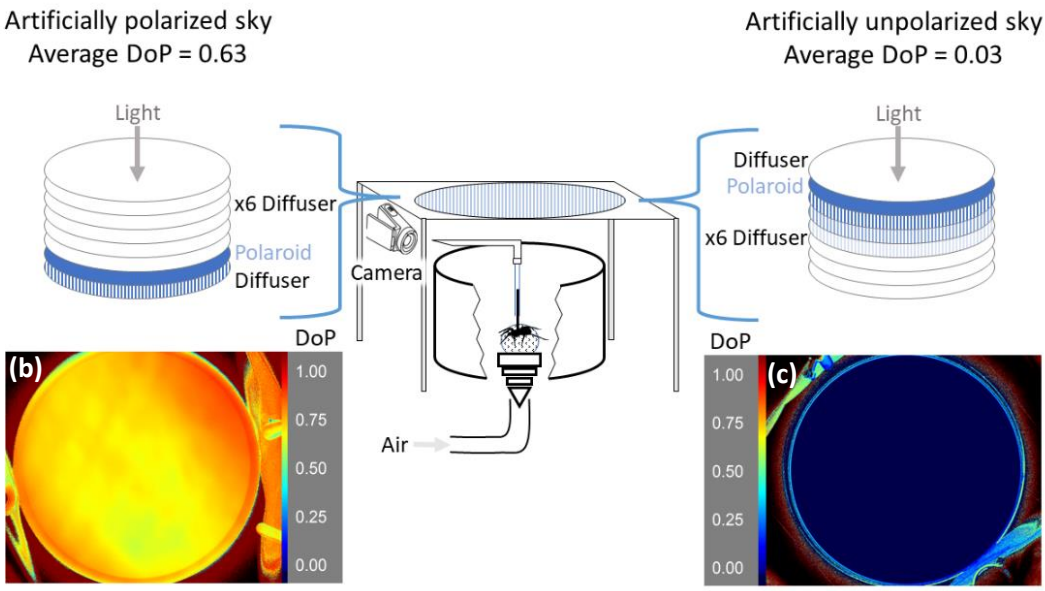

Figure 4.3. (a) The trackball apparatus for testing orientation under different simulations of skylight polarization. In a screened experimental arena, spiders were magneto-tethered on top of a polystyrene ball that rotated when they walked. The spiders were shown rotations of two, overhead artificially polarized light treatments while a video camera recorded behavioural responses in infrared. (b) and (c) are described in Figure 3.1 of chapter 3.

4.2.3 Experimental protocol

4.2.3.1 Experiment 1: Orientation performance and the presence of skylight polarization in *Drassodes* sp.

In the first trackball experiment, 31 spiders were exposed to the same four rotations of the polarized treatments used in the flight simulator experiment (see chapter 3) to test orientation performance under optimal skylight polarization (0.63 average DoP) and, under skylight polarization diminished by extreme light pollution (0.03 average DoP) (Fig.4.3b,c). Experiments started with a two-minute burn-in period under the artificially polarized or unpolarized sky at 0°. The behavioural responses of the spiders were recorded for 10 seconds before and after each rotation, and a minimum of 30 seconds separated all rotations. During the experiment, the spiders were monitored on a screen so that rotation of the filter stack did not occur when the spiders were stationary.

4.2.3.2 Experiment 2: Behavioural threshold of polarization sensitivity in *Drassodes* sp.

In the second trackball experiment, 31 spiders were exposed to four new polarized treatments of differing DoP (Fig.4.4). In a pseudo-random order, the spiders experienced a clockwise and anticlockwise, 90° manual rotation of artificially polarized skylight at 0.99 (positive control), 0.74, 0.63, and 0.37 DoP. The treatments were created using two circular filter stacks (45 cm diameter) of seven layers of ¼ diffuser (251 Quarter white diffusion, LEE Filters) and one layer of UV-transmissive polarizing filter (Rosco Polarising Filter, Rosco). The diffuser layers and polarizing filter were arranged such that one of the filter stacks transmitted polarized light of 0.99 DoP (no diffuser below the polarizing filter and x7 layers of diffuser above) and when inverted, transmitted polarized light at 0.37 DoP (x7 layers of diffuser below the polarizing filter). The second filter stack transmitted light of 0.74 DoP (x1 layer of thin batch diffuser below the polarizing filter and x6 layers of ¼ diffuser above) and when inverted, 0.63 DoP (x1 layer of thick batch diffuser below the polarizing filter and x6 layers of ¼ diffuser above). All DoP values were an average of three manual polarimetry measurements as described in chapter 3, section 3.2.3. As above, the spiders experienced a two-minute burn-in period prior to the first rotation of all treatments and were recorded for at least 20 seconds before the next rotation.

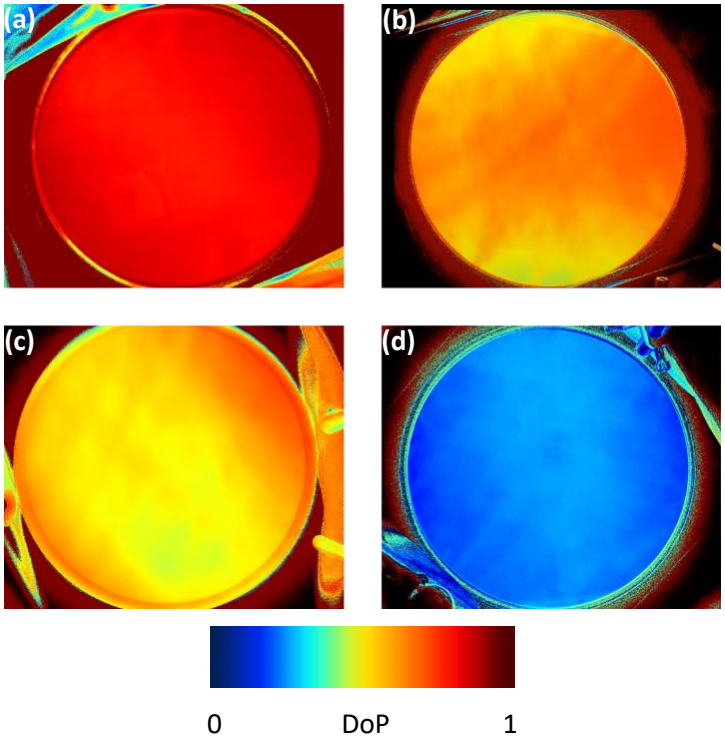

Figure 4.4. Photographic polarimetry image of the faces of the filter stacks with (a) 0.99, (b) 0.74, (c) 0.63, and (d) 0.37 DoP. Photographic polarimetry images taken using a polarization camera (Triton 5.0 MP Polarization Model, Lucid Vision Labs Inc.).

4.2.4 Statistical analysis

The following analyses were chosen to explore two central questions to this investigation: 1) does *Drassodes* sp. use the polarization of light for orientation (turning responses) and, 2) does the polarization of light affect *Drassodes* sp. ability to maintain a selected heading (directedness)?

To calculate turning response and directedness the fictive paths of the spiders were tracked using the open-source tracking software FicTrac[10]. FicTrac takes the absolute orientation of the ball rotation per frame relative to the fixed principal axes of the spider to give the spiders movements on a fictive 2D surface[10].

Turning responses

To establish whether individuals were more likely to turn following the rotation of the filters, the paths of the spiders five seconds before and after the rotation of the polarized treatments were plotted for both experiments (Fig.4.5) and presented to 22 (experiment 1) and 50 (experiment 2) human volunteers for blind scoring using the online platform Zooniverse (www.zooniverse.org). This generated a total of 124 plotted paths from experiment 1 (two rotations of two treatments across 31 spiders) and a total of 248 plotted paths from experiment 2 (two rotations of four treatments across

31 spiders). Volunteers were asked to decide whether the path showed a change in direction following the treatment rotation (marked with a '+' on the plotted path) (Fig.4.5). For a paired comparison, volunteers were required to score a balanced number of polarized and unpolarized paths, 4 volunteers in experiment 1 (n=18) and 19 volunteers in experiment 2 (n=31) did not achieve this and were consequently removed from the analysis.

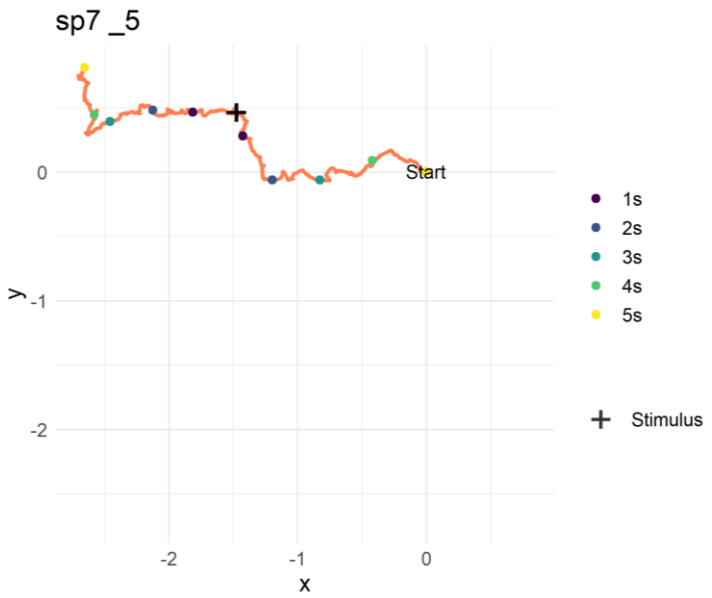

Figure 4.5. An example of a tracked path of a spider (orange) from the second trackball experiment, as presented to human volunteers for blind scoring. The time of the filter rotation is shown by the black cross and the number of seconds before and after the filter rotation is given by the coloured points.

Their binary responses were compared between treatments using a binomial generalised linear mixed model (GLMM) with volunteer score as the response variable; treatment, order of presentation, direction of treatment rotation, and the interaction between treatment and order of presentation as fixed factors; and spider ID and volunteer ID as random terms. All GLMMs had no link function. Model structure and link functions with the best model fit was selected using the Akaike information criterion (AIC) values and model diagnostic information[11]. Variance components were estimated using restricted maximum likelihood (REML) method. Models were selected using manual backwards-stepwise model refinement and the significance of fixed terms was determined using analysis of variance tests (ANOVA) and associated p-values[11]. Residual diagnostics of all models were done using the 'DHARMa'[12] package in R. All statistical analysis was conducted in R (R Studio v. 4.1.2, R Development Core Team 2021).

Directedness

The sinuosity of individual paths was calculated using the R package 'trajr'[13]. Sinuosity is the mean cosine of turning angles and step length and gives an estimate of the tortuosity (analogous to the directedness metric in chapter 3) of an animal's 2D path. Sinuosity values range from 0 (straight) to 1 (highly tortuous). The corrected sinuosity index (CSI), the mean cosine of turning angles and step length given as variation coefficient rather than a constant[13,14], was used to estimate tortuosity as it is suitable for a wider range of turning angle distributions and does not require a standardised step length. The CSI was calculated for the 5 seconds before and after treatment rotation.

To test for the effect of treatment on directedness overall, the CSI of the 5 seconds before treatment rotation were analysed using a beta GLMM with CSI as the response variable; treatment, order of presentation, and the interaction between treatment and order of presentation as fixed factors; and spider ID as a random term. To test for the effect of treatment rotation on directedness, the CSI was compared between treatments using a beta GLMM with CSI as the response variable; order of presentation, 5 second time bin (before or after rotation), treatment rotation direction, and the interaction between treatment and 5 second time bin as fixed factors, and spider ID as a random term. The GLMMs had a complementary log-log link function. Model structure and link functions were selected using the method described above and variance components were estimated using the REML method. Models were selected using manual backwards-stepwise model refinement as above, and residual diagnostics were done using the 'DHARMa' package in R. All statistical analysis was conducted in R.

4.3 Results

4.3.1 Orientation and the presence of skylight polarization

Turning responses

Controlling for the significant effects of order of presentation (binomial GLMM, d.f.=3, χ^2=9.67, p=0.02) and direction of treatment rotation (binomial GLMM, d.f.=1, χ^2=7.96, p=0.004), the spiders were 7% more likely to respond to the polarization treatment (binomial GLMM, d.f.=1, χ^2=7.92, p=0.004) (Fig.4.6). Paths depicting spiders exposed to a rotation of the unpolarized treatment (n=62) were scored a total of 698 times. Of these, 352 were reported to have turned in response to the treatment rotation (50%). Paths depicting spiders exposed to a rotation of the polarized treatment (n=62) were scored a total of 713 times. Of these, 412 were reported to have turned (57%).

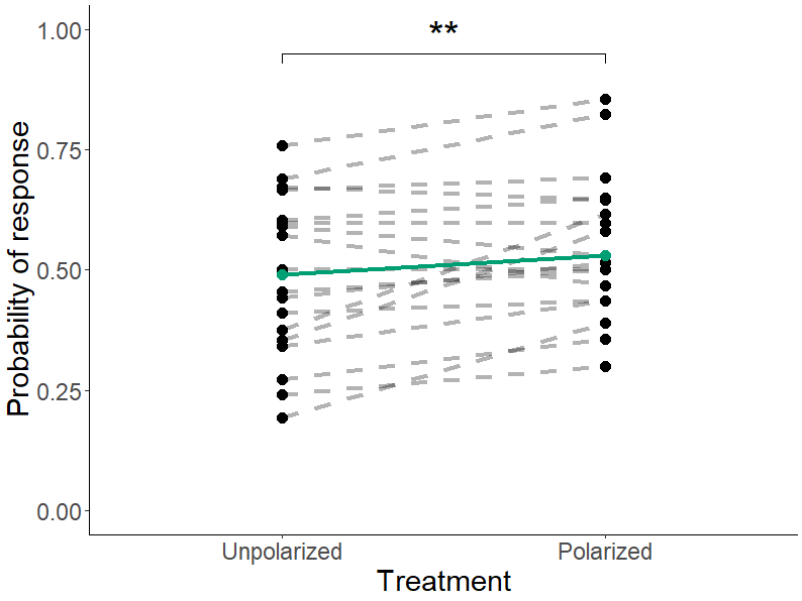

Figure 4.6. The probability of a turning response in *Drassodes* sp. following a 90° rotation of an overhead artificially unpolarized ('Unpolarized') and polarized treatment ('Polarized') according to 18 human volunteers blind to treatment when observing the 2D paths of the spiders. The mean probability of a positive (1, turn) and negative (0, no turn) choice of the volunteers are shown by the dashed lines and the model prediction of the binomial GLMM is shown by the green solid line. Annotations indicate the levels of significance of the GLMM as '***' p>0.001, '**' p>0.01, '*' p>0.05.

Directedness

Prior to any rotations, directedness was similar between the polarized (mean CSI=45) and unpolarized (mean CSI=0.43) treatments (beta GLMM, χ^2=0.93, d.f.=1, p=0.33), and was not affected by order of presentation (beta GLMM, χ^2=5.39, d.f.=3, p=0.14) (Fig.4.7a). Directedness reduced following rotations of the filter stack (beta GLMM, χ^2=42.27, d.f.=1, p<0.0001) independent of treatment (beta GLMM, χ^2=3.66, d.f.=2, p=0.15). The mean CSI increased following the rotation of both the polarized and unpolarized treatment by 14% and 10%, respectively (Fig.4.7b). Change in directedness before and after treatment rotation was not affected by order (beta GLMM, χ^2=6.02, d.f.=3, p=0.11) or rotation direction (beta GLMM, χ^2=1.88, d.f.=1, p=0.17).

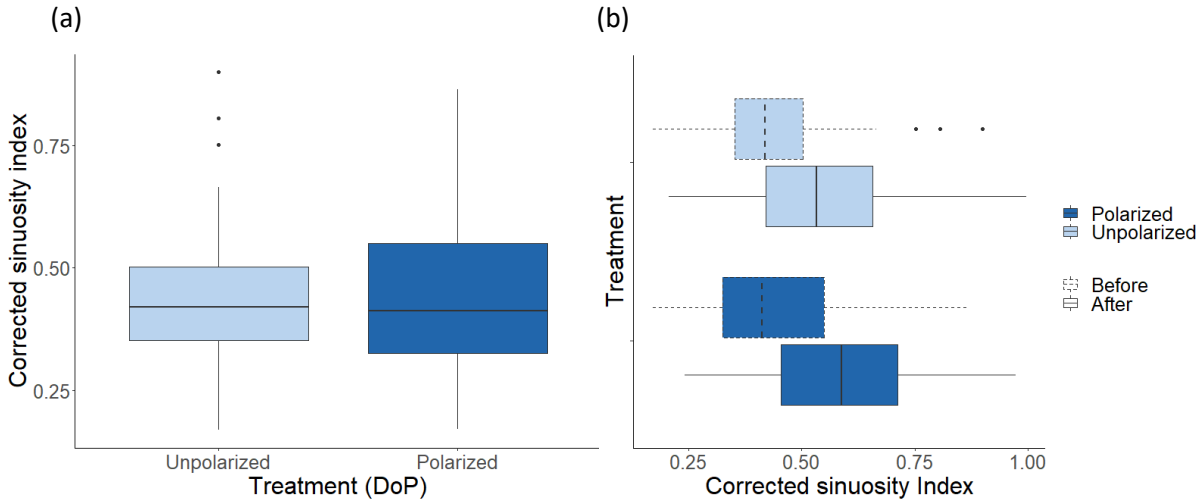

Figure 4.7. (a) The corrected sinuosity index of spiders' paths during 5 seconds of exposure to an overhead, artificially polarized treatment ('Polarized') and unpolarized treatment ('Unpolarized'). (b) Corrected sinuosity index in the 5 seconds before (dashed boxes) and 5 seconds after (solid boxes) rotations of the artificially polarized ('Polarized') and unpolarized ('Unpolarized') filters.

4.3.2 Behavioural threshold of polarization sensitivity

Turning responses

Controlling for the significant effects of direction of treatment rotation (binomial GLMM, d.f.=1, χ^2=14.89, p=0.0001), the spiders responded differently to the four polarization treatments as a function of order of presentation (binomial GLMM, d.f.=21, χ^2=73.90, p<0.0001) (Fig.4.8). Individuals did not respond more frequently to the positive control compared to any other treatment (Table 4.1).

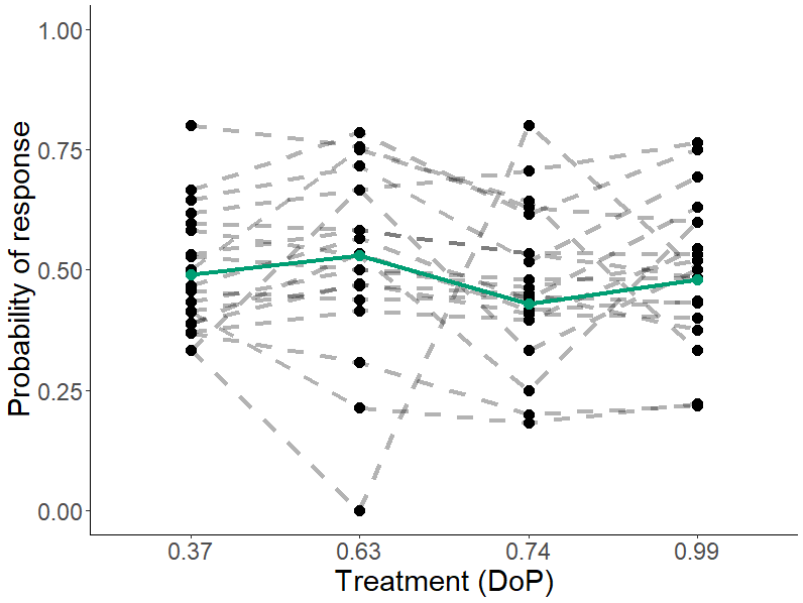

Figure 4.8. The probability of a turning response in *Drassodes* sp. following a 90° rotation of artificially polarized skylight of four DoP values according to the choices of 31 human volunteers blind to treatment when observing the 2D paths of the spiders. The mean probability of a positive (1, turn) and negative (0, no turn) choice of the volunteers are shown by the dashed lines and the model prediction of the binomial GLMM is shown by the green solid line.

Similarly, there was no difference in response rates between the 0.37 DoP treatment and the 0.63 and 0.74 DoP treatments (Table 4.1). The probability of a response to the treatment of the lowest DoP in this experiment (0.37 DoP, 49% probability) was similar to the negative control in experiment 1 (0.03 DoP, 50% probability).

Table 4.1. The choices of 31 human volunteers when asked to score whether the 2D paths of spiders showed a change in direction following a rotation of four polarized treatments of different DoPs.

Treatment (DoP)	N of scores	Scored as positive	Scored as positive (%)	n
0.99	763	369	48	31
0.74	747	341	45	31
0.63	761	406	53	31
0.37	772	385	49	31

Directedness

Prior to rotation, the directedness of individuals differed between treatments (beta GLMM, χ^2=11.40, d.f.=3, p=0.009) particularly between the 0.37 (mean CSI=0.52) and 0.74 (mean CSI=0.46) treatments (Fig.4.9a). This was not affected by order of presentation (beta GLMM, χ^2=12.559, d.f.=7, p=0.08). The overall directedness of the spiders increased following treatment rotation, and this changed as a function of treatment (beta GLMM, χ^2=16.76, d.f.=6, p=0.01). Directedness was significantly higher both before and after the rotations of the 0.74 DoP treatment compared to the 0.37 DoP treatment (Fig.4.9b). Change in directedness before and after treatment rotation was not impacted by order effects (beta GLMM, χ^2=8.14, d.f.=7, p=0.32) or the direction of treatment rotation (beta GLMM, χ^2=0.19, d.f.=1, p=0.66).

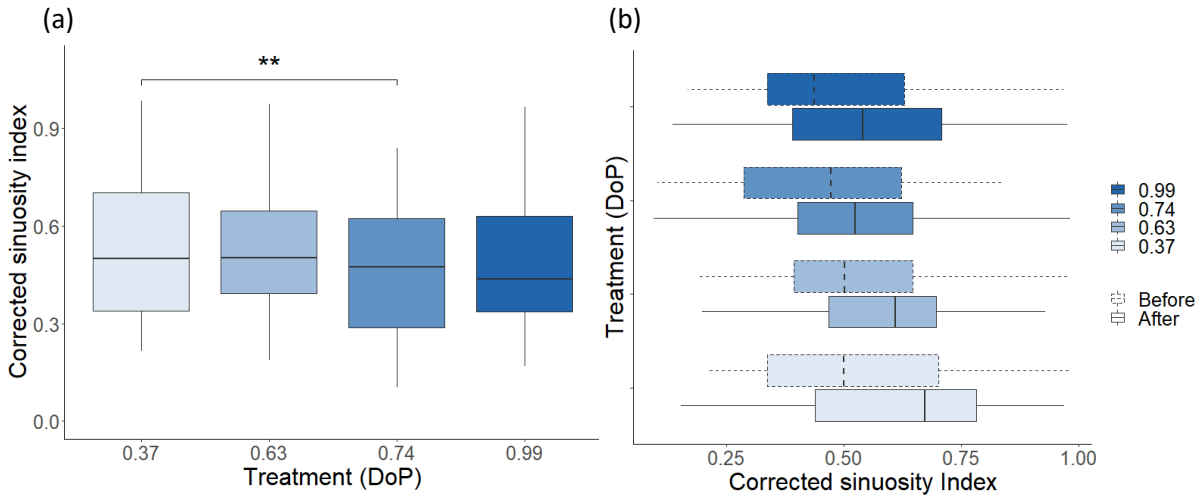

Figure 4.9. (a) The corrected sinuosity index of spiders' paths during 5 seconds of exposure to an overhead, artificially polarized treatment of four DoP values: 0.34, 0.67, 0.74, and 0.99. (b) The corrected sinuosity index of the paths of the spiders in the 5 seconds before (dashed boxes) and 5 seconds after (solid boxes) rotations of the four artificially polarized treatments. Annotations indicate the levels of significance of beta GLMMs as '***' p>0.001, '**' p>0.01, '*' p>0.05.

4.4 Discussion

4.4.1 Orientation and skylight polarization

Turning responses

Drassodes sp. were more likely to change direction following a manual rotation of an artificial 'sky' when the light was polarized. However, the effect size was small, the probability of a turning response being 7% higher than a response to an unpolarized 'sky', and there was evidence of order and directional biases in response rates. Individuals were equally likely to change direction or maintain the same direction following a rotation of the unpolarized treatment. It is possible that unintentional external stimuli (vibrations, shadow, etc.) were created by the manual rotation of the filter stack and disturbed the spiders, coupled with poor movement control caused by the magnetic tethering system. This may also account for the differences in response to the clockwise and anticlockwise rotations of the treatments, perhaps one direction created more disturbance than the other. Nonetheless, these factors are assumed to have caused the small effect size and high turning response to the unpolarized treatment rather than a lack of polarization-guided orientation in *Drassodes* sp. for three reasons: 1) Dacke (1999)[1] confirmed polarization-guided navigation in a more naturalistic experiment with untethered *Drassodes cupreus* walking on a flat surface, 2) the PMEs of *Drassodes* spiders are highly specialised skylight polarization detectors[1] and, 3) feedback from the human volunteers who observed the 2D paths of the spiders pronounced difficulty in scoring due to highly tortuous paths. Perhaps allowing the spiders to move more naturally within the arena, as in Dacke (1999)[1], would have yielded more reliable results. However, a robust turning response to a rotating overhead polarizer has been demonstrated in wolf spiders (*Pardosa tristis*) walking on an air-cushioned trackball by Dacke (2001)[5]. That being said, the sample sizes of this study were small and the distribution of turning responses across the tested individuals is not given, leading to questionable conclusions. Still, it is unclear why such results could not be repeated here. Filtering the paths of the spiders shown to the human volunteers using clearly defined ante-hoc criterion to select the best performing individuals could have benefitted the blind scoring[15].

Directedness

Prior to rotations of the polarized treatments, overall path directedness was neither straight or highly tortuous (mean CSI=0.44) whether exposed to polarization or not, but path directedness did decrease following treatment rotation (mean CSI=0.56). However, this effect was observed across both treatments which supports the suggestion that individuals were disturbed by accidental external

stimuli caused by the manual rotation of the filters. Overall, the general directedness of the paths was low enough to create difficulties for the human volunteers when blind scoring. Perhaps the mechanics of walking on the trackball caused many of the spiders to take a naturally oscillating path which masked any effects of polarization on both directedness and turning response. Path directedness was not investigated during Dacke's (2001) trackball experiment with *P. tristis*. As such it has yet to be studied in a ground spider in the context of polarization-guided navigation, but it has been shown to benefit directedness in a nocturnal dung beetle[6]. Again, perhaps the manipulation of more natural movements in *Drassodes* sp. would yield stronger conclusions on the mechanisms linking skylight polarization with path directedness.

Overall, the results of the first trackball experiment suggests that, at least in laboratory conditions, artificial skylight polarization can be used to inform orientation in *Drassodes sp.* but perhaps not as reliably as the real sky polarization pattern in the wild. There are several possible reasons for the limited success of this experiment in addition to those given above. Firstly, the real sky polarization pattern has a characteristic gradient in DoP and AoP across the sky that was absent from this experiment as the filters used to create the artificial pattern were spatially uniform in DoP and AoP. It would be interesting to further investigate how the absence of the DoP and AoP gradient of the polarization pattern impacts navigation both in *Drassodes* sp. and *Helicoverpa armigera* and how this relates to the effects of light pollution on the spatial characteristics of the pattern (see chapter 2). Secondly, and in addition to disturbance and poor movement control mentioned above, the lack of robustness in the results may be attributed to low motivation of individuals. Dacke (1999)[1] observed polarization-guided navigation in free walking spiders that were returning to their silk retreats following a foraging excursion. Such individuals would have been highly motivated to return to their retreats, enabling observations of navigational behaviour. Similarly, Dacke (2001) stimulated wolf spiders to run on a trackball by touching the abdomen or rear legs with a probe[5]. In contrast, individuals tethered to the trackball in this investigation were unstimulated and had limited motivation to navigate. Thus, experiments that exploit the natural motivations of spiders, particularly within an ecologically realistic context, are anticipated to achieve more reliable results.

4.4.2 Behavioural threshold of polarization sensitivity

Turning responses

A behavioural threshold of polarization sensitivity in *Drassodes* sp. could not be established. The probability of a turning response and path directedness was not reliably affected by increasing DoP and was subject to directional biases dependent on the direction of treatment rotation. The

probability of a turning response to the rotation of the 0.37 DoP treatment was similar to the negative control used in the previous experiment (DoP=0.03). This could suggest a sensitivity threshold of >0.37 DoP but given that the response probability did not consistently change with DoP, there were directional biases in responses to clockwise and anticlockwise rotations of the filters, and that any observable effect of this experiment is likely to be small, no conclusions can be reliably confirmed. Therefore, a behavioural threshold of polarization sensitivity in spiders remains elusive.

Directedness

The directedness of the spiders' paths prior to treatment rotation was like those observed in the first trackball experiment (overall mean=0.49), being neither straight nor tortuous. However, directedness did improve in the 0.74 DoP treatment (mean CSI=0.46) compared to the 0.37 DoP treatment (mean CSI=52), suggesting that the ability to maintain a heading may be enhanced with skylight polarization, but this result was not repeatable in both experiments. A DoP of 0.74 is unusually high for the natural polarization pattern[6]. Thus, if skylight polarization does indeed improve directedness, we would also expect to see an improvement in the more realistic 0.63 DoP treatment. Overall directedness reduced following treatment rotation, but unlike experiment 1, this changed as a function of treatment. The spiders of the 0.74 DoP treatment being more direct than those in the 0.37 DoP treatment, both before and after rotation. Again, directedness would be expected to change following treatment rotation of the 0.63 DoP treatment if the polarization of light was used as an orientational cue, so it is unclear what might be driving this difference. As mentioned above, a more naturalistic experiment that exploits a robust behaviour would help establish the threshold of polarization sensitivity in *Drassodes* sp..

4.5 Conclusions

Although *Drassodes* sp. responded differently to polarized and unpolarized treatments in the first trackball experiment, the effect size was small and the result was not repeatable in the proceeding experiment, bringing its validity into question. Given that polarization-guided navigation has already been established behaviourally in *Drassodes cupreus* and *Pardosa tristis*, along with the anatomical mechanisms underlying this behaviour, it is reasonable to assume that the trackball experiment was not successful at eliciting a robust behavioural response to the polarization of light in this instance. Therefore, unlike *Helicoverpa armigera*, strong conclusions on the threat of light pollution on nocturnal navigation in *Drassodes* sp. cannot be made in light of the results of the experiments

described here. The existing literature on polarization-guided navigation in spiders exploited the motivation to perform natural behaviours such as returning to a retreat[1] and evading danger[5] which was not present in this study. Future research is recommended to take a similar approach and investigate navigation using more naturalistic methods to attain reliable and robust results.

The next chapter will explore the impacts of skylight polarization cues and light pollution on the timing and initiation of navigational excursions in *H. armigera* and *Drassodes* sp., with particular emphasis on light pollution radiance and spectral composition. The timing of critical behaviours like migration and foraging are synchronised with ambient light levels creating cyclical patterns of behaviour known as circadian rhythms. As light pollution increases in radiance and changes in spectral content with the global transition to modern lighting technologies, it raises questions about the impacts of light pollution on the more fundamental aspects of ecology and the threat this poses to the survival of nocturnal arthropods.

References

1. Dacke M, Nilsson DE, Warrant EJ, Blest AD, Land MF, O'Carroll DC. 1999. Built-in polarizers form part of a compass organ in spiders. *Nature*, **401**(6752): 470-473. (DOI: 10.1038/46773)
2. Snyder AW. 1973. Polarization sensitivity of individual retinular cells. *Journal of Comparative Physiology*, **83**(4): 331-360. (DOI: 10.1007/bf00696351)
3. Henze MJ, Labhart T. 2007. Haze, clouds and limited sky visibility: Polarotactic orientation of crickets under difficult stimulus conditions. *Journal of Experimental Biology*, **210**(18): 3266-76. (DOI: 10.1242/jeb.007831)
4. Labhart T. 1996. How polarization-sensitive interneurones of crickets perform at low degrees of polarization. *Journal of Experimental Biology*, **199**(7): 1467-1475. (DOI: 10.1242/jeb.199.7.1467)
5. Dacke M, Doan TA, O'Carroll DC. 2001. Polarized light detection in spiders. *Journal of Experimental Biology*, **204**(14): 2481-90. (DOI: 10.1242/jeb.204.14.2481)
6. Foster JJ, Kirwan JD, el Jundi B, Smolka J, Khaldy L, Baird E. Byrne MJ, Nilsson DE, Johnsen S, Dacke M. 2019. Orienting to polarized light at night - matching lunar skylight to performance in a nocturnal beetle. *Journal of Experimental Biology*, **222**(2): jeb188532. (DOI: 10.1242/jeb.188532)
7. Khaldy L, Foster JJ, Yilmaz A, Belušič G, Gagnon Y, Tocco C, Byrne MJ, Dacke M. 2022. The interplay of directional information provided by unpolarised and polarised light in the heading direction network of the diurnal dung beetle *Kheper lamarcki*. *Journal of Experimental Biology*, **225**(3): jeb243734. (DOI: 10.1242/jeb.243734)
8. Kyba CCM, Mohar A, Posch T. 2017. How bright is moonlight? *Astronomy & Geophysics*, **58**(1): 1.31-1.32. (DOI: 10.1093/astrogeo/atx025)
9. Morehouse NI, Buschbeck EK, Zurek DB, Steck M, Porter ML. 2017. Molecular evolution of spider vision: New opportunities, familiar players. *Biological Bulletin*, **233**(1): 21-38. (DOI: 10.1086/693977)
10. Moore RJD, Taylor GJ, Paulk AC, Pearson T, van Swinderen B, Srinivasan MV. 2014. FicTrac: A visual method for tracking spherical motion and generating fictive animal paths. *Journal of Neuroscience Methods*, **225**: 106-119. (DOI: 10.1016/j.jneumeth.2014.01.010)
11. Thomas R, Lello J, Medeiros R, Pollard A, Robinson P, Seward A, Smith J, Vafidis J, Vaughan I. 2017. Statistical models: Model selection. In: Thomas R. (eds) 2nd Ed., Data analysis with R statistical software – A guidebook for scientists. Eco-explore, Cardiff, UK, pp. 69-71.
12. Hartig F. 2022. DHARMa: Residual diagnostics for hierarchical (multi-level / mixed) regression models. R package version 0.4.5. (https://CRAN.R-project.org/package=DHARMa)
13. McLean DJ, Volponi MAS. 2018. trajr: An R package for characterisation of animal trajectories. *Ethology*, **124**(6): 440-448. (DOI: 10.1111/eth.12739)
14. Benhamou S. 2004. How to reliably estimate the tortuosity of an animal's path: Straightness, sinuosity, or fractal dimension? *Journal of Theoretical Biology*, **229**(2): 209-220. (DOI: 10.1016/j.jtbi.2004.03.016)
15. Dreyer D, Frost B, Mouritsen H, Gunther A, Green K, Whitehouse M, Johnsen S, Heinze S, Warrant E. 2018. The Earth's magnetic field and visual landmarks steer migratory flight behaviour in the nocturnal Australian bogong moth. *Current Biology*, **28**: 2160-2166. (DOI: 10.1016/j.cub.2018.05.030)

5

Light pollution and nocturnal activity in Helicoverpa armigera *and* Drassodes *sp.*

The evidence given in the previous two chapters focused on the effects of light pollution during nocturnal journeys; this chapter aimed to investigate the impacts of light pollution prior to the initiation of those journeys to provide a holistic understanding of how light pollution effects several aspects of nocturnal navigation. By observing patterns of activity from sunset to sunrise, the experiments in this chapter were designed to explore the effect of light pollution radiance and spectral composition, as well as the diminishing effect of light pollution to skylight polarization, on the timing and initiation of nocturnal journeys. Initially, only *Helicoverpa armigera* was tested, but due to the success of the experiment and the discovery of *Drassodes* sp. within the Pyrenean field site, *Drassodes* sp. was tested in the final field season. As a result, there was limited time to complete the full series of experiments on *Drassodes* sp., which was used to test only for the effect of spectral composition on nocturnal activity. *H. armigera* was used in three experiments to test for the effects of spectral composition, radiance, and the presence of skylight polarization on nocturnal activity. For simplicity, the methods and results of the experiments are divided by species then discussed in parallel.

Contributions: Myself, my supervisors Nicholas Roberts (University of Bristol) and Lauren Sumner-Rooney (Leibniz Institute for Biodiversity and Evolution Research), and my collaborators Karl Wotton (University of Exeter), Toby Doyle (University of Exeter), Will Hawkes (University of Exeter), Richard Massy (University of Exeter), Seb Lloyd, Christian Drerup (University of Cambridge), and Siân Vincent Venables collected the animals. Myself, Lauren Sumner-Rooney, Seb Lloyd, Christian Drerup, and Siân Vincent Venables set up and managed the experimental apparatus when in the field. Ilse Daly wrote the Raspberry Pi program for video monitoring. I undertook data collection, data analysis, and authored the chapter in discussion with my supervisors.

5.1 Background

Circadian rhythms are endogenous cyclical changes in an organism's physiology or behaviour that are primarily regulated by daily changes in ambient light between day and night. Light pollution caused by artificial light at night alters the natural light regime by introducing light of unnatural spectral character, and at levels several times brighter than natural night skies, well beyond the normal diurnal period[1,2]. This can disrupt the regulation of activity patterns with the natural light cycle, causing a loss of rhythmicity and mistiming of rhythms (see chapter 1, section 1.2.2). Additionally, light pollution may also obscure or remove visual cues that drive specific nocturnal behaviours, such as celestial cues for orientation[3], which may subsequently reduce activity levels and further disrupt patterns of activity[2]. As a result, light pollution has been identified as one of the drivers of the large-scale insect declines seen in recent years[2,4].

The impacts of light pollution on the nocturnal activity of arthropods may differ relative to its spectral composition[5] which is changing globally due the widespread replacement of long wavelength shifted high-pressure sodium streetlights (HPS) with broad-spectrum light-emitting diodes (LEDs)[6,7] (see chapter 1, section 1.1.2.2). The spectral sensitivities of arthropod visual systems are generally most sensitive to shorter wavelengths in the part of the spectrum humans perceive as UV/blue[8-11]. Broad-spectrum LED light is therefore more likely to overlap with the spectral sensitivities of a variety of species than narrow-spectrum, longer wavelength dominated light from HPS lamps[5]. This means that, because nocturnal species are more sensitive to shorter wavelengths, the relative brightness of broad-spectrum LED streetlights in comparison to HPS streetlights will be greater[12-17]. Indeed, among nocturnal arthropods, light rich in short wavelengths is more likely to disrupt flight[18,19], and alter foraging[20,21] and reproductive behaviour[22-25]. As such, the impacts of light pollution on the nocturnal arthropods can vary substantially depending on the streetlighting technology.

Direct exposure to artificial light at sunset is likely to prevent ambient light intensity from decreasing to the levels normally required to trigger the onset of nocturnal arthropod activity (typically 0-10 lux[26-29]). The initiation of foraging activity in crepuscular bees is known to be constrained by light intensity and exposing individuals to abnormally high intensities forces nest-departure at erroneous times of day[27]. Both, *H. armigera* and *Drassodes* spp. synchronise activity with the onset of night[30,31,32] but the approximate reduction in intensity of ambient light required to initiate activity is known only in *H. armigera* (0-10 lux[29]). If similar lux values trigger nocturnal activity in both species, direct exposure to streetlights (typically restricted to 1-15 lux on minor roads in the UK[33]) is likely to affect the timing of nocturnal activity in *H. armigera* and *Drassodes* sp., with subsequent detrimental effects to their respective nocturnal journeys. However, intensity thresholds and patterns of activity in relation to

light pollution is not well understood in arthropods. Identifying species-specific thresholds for nocturnal activity and establishing common thresholds between species is key for assessing the implications for individual fitness, biodiversity loss, and determining target-specific mitigation.

In chapter 2, light pollution was shown to mask the skylight polarization pattern by reducing its spatial and temporal extent, and its degree of polarization (DoP). The polarization pattern is an important visual cue for nocturnal navigation, which can become impaired when the pattern is lost or reduced (see chapters 3 and 4). Given that the reductive effects of light pollution on the polarization pattern begin around 60 minutes after sunset (see chapter 2), around the time nocturnal journeys begin[30,34,35], it is possible that the loss or impairment of such important navigational cues also inhibits the initiation of these journeys. For example, the nocturnal migratory moth *Autographa gamma* initiates mass migratory events on nights of favourable winds only, which facilitate accurate orientation and energy efficient flight[36]. If the polarization pattern is an important source of orientation information for an individual, its absence may result in an erroneous trajectory or disorientation[37,38], which may deter an individual from starting a journey. However, such a hypothesis is speculative as the effect of the presence or absence of visual cues on the occurrence of navigational behaviour in nocturnal arthropods is unknown.

5.1.1 Aims and hypotheses

The following work aimed to establish the differential effects of different properties of artificial light pollution on the nocturnal activity of *H. armigera* and *Drassodes* sp.. By observing individuals from sunset to sunrise using infrared cameras, we compared the effect of broad-spectrum LED streetlights and narrow-, long-wavelength shifted HPS streetlights on nocturnal activity in *H. armigera* and *Drassodes* sp.. The activity of both species was expected to be lower under an LED streetlight. Then, we compared the effect of intensity using an LED streetlight at five different values between 0 and 10 lux on the nocturnal activity in *H. armigera* only. Activity was expected to decrease incrementally with increasing lux values. Finally, using both HPS and LED streetlights, we compared the effect of the polarization of light on nocturnal activity in *H. armigera*. Individuals were expected to be less active in the absence of a polarized cue if this cue is involved in journey initiation.

5.2 Materials and methods

Animals were collected and maintained as described in chapters 3 and 4 in September 2019 and 2021. All experiments and capture of animals in the Hautes-Pyrénées were conducted under the

authorisation of the Parc national des Pyrénées (2019 permit 2019-220, 2021 permit 2021-253). The experiments with *H. armigera* investigating the effects of spectral composition and artificial polarization on activity took place in Gèdre, France (Lat= 42.783519, Long= 0.034668) in September 2019, around 14 km north of the trapping location. The spectral composition experiment with *Drassodes* sp. and the intensity experiment with *H. armigera* took place in Gavarnie, France (Lat=42.759073, Long=0.002342) in September 2021, around 8km from the trapping location.

All the experiments described within this chapter shared the same principal method with minor variations for specific research questions. The principal method will be described first, followed by descriptions of the adaptations made to the experimental design for each iteration.

5.2.1 Principal methods

Moths and spiders were placed in individual transparent circular containers (DIA 14.22 x H6.86 cm and DIA 10 x D 1.5 cm, respectively) and suspended 0.7-1 metres above the ground between two large sheets of UV-transmissive Perspex to allow ambient light transmission and for protection from rain (Fig.5.1). Those that housed *Drassodes* sp. also contained a plastic lid (15 ml conical centrifuge tube lid, Falcon) with a notch cut out of the side on top of a small piece of black felt (DIA ~3 cm) for use as retreats. Individuals were shielded from lateral visual disturbance by opaque material lining the vertical edge of the containers and the overall set-up was sheltered from wind by walls of black fabric 2 metres high. Two infrared video cameras (Raspberry Pi Camera Board Night Vision & Adjustable Focus Lens, Raspberry Pi Foundation) were placed beneath the set-up for video monitoring and the apparatus was illuminated from above using commercial infrared security lights (JC Infrared Illuminator 6-Led Security Light, JCHENG Security). To create the light treatments for each experiment, an LED or HPS streetlight was placed 0.7-2.1 metres above the animals (Fig.5.1). The light intensity to which the animals were exposed was restricted to values within the range of UK urban streetlighting by placing layers of filters between the containers and the topmost Perspex layer (Fig.5.1). All lux measurements were taken inside a circular container at the centre of the Perspex using a light meter (CA 1110 Lightmeter, Chauvin Arnoux - Metrix). The type of filter and filter arrangement varied between experiments and are described separately below.

Animals were placed inside the experimental apparatus 60-30 minutes before sunset to give them time to recover from the disruption. Their activity was recorded for 10 seconds every 2.5 minutes from sunset to sunrise (total hours of recording per evening=11-12.5, total number of videos per evening=264-300). The video recordings were scored manually: for *H. armigera*, individuals walking, or flying were scored as ‘active’ and sedentary individuals with folded wings were scored as ‘inactive’;

for *Drassodes* sp., walking individuals were scored as 'active' and sedentary individuals with folded legs or individuals inside the retreats were scored as 'inactive'.

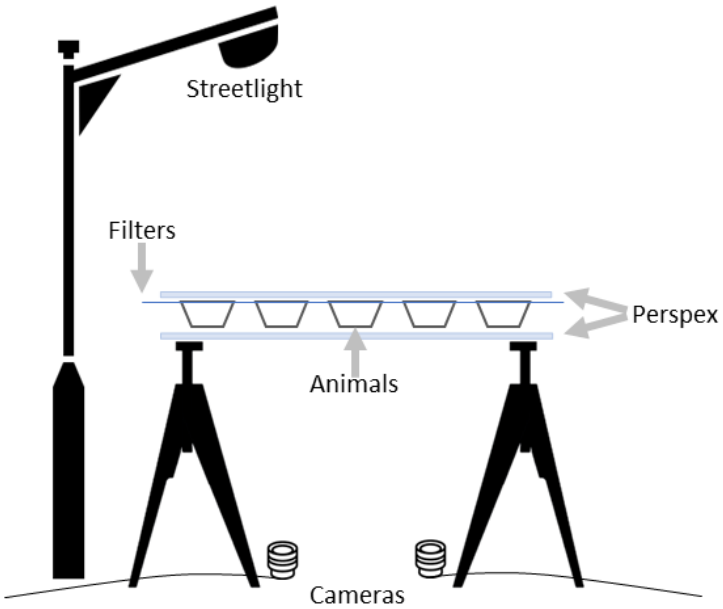

Figure 5.1. The principal design of the experimental apparatus used for activity experiments. Individuals were placed inside circular containers sandwiched between two layers of Perspex and filters. In experimental treatments, artificial light was provided from directly overhead. Individuals were filmed from beneath using infrared video cameras.

5.2.2 Experiments using *Helicoverpa armigera*

5.2.2.1 The effect of LED and HPS streetlights on activity

Helicoverpa armigera were exposed to one of three light treatments: no streetlight (control, 0-0.03 lux, n=44), an LED streetlight (12 lux, n=40), or a HPS streetlight (11 lux, n=48). A filter stack comprising six layers of ¼ diffuser (251 quarter white diffusion, Lee filters) and a layer of UV-transmissive polaroid (Rosco polarizing filter, Rosco) were placed above each moth to reduce the intensity of the light to values typically found in pedestrian areas of the UK (Fig.5.2). The activity of up to 12 naïve moths were recorded under one of the three light treatments each night and all light treatments were repeated four times across consecutive nights.

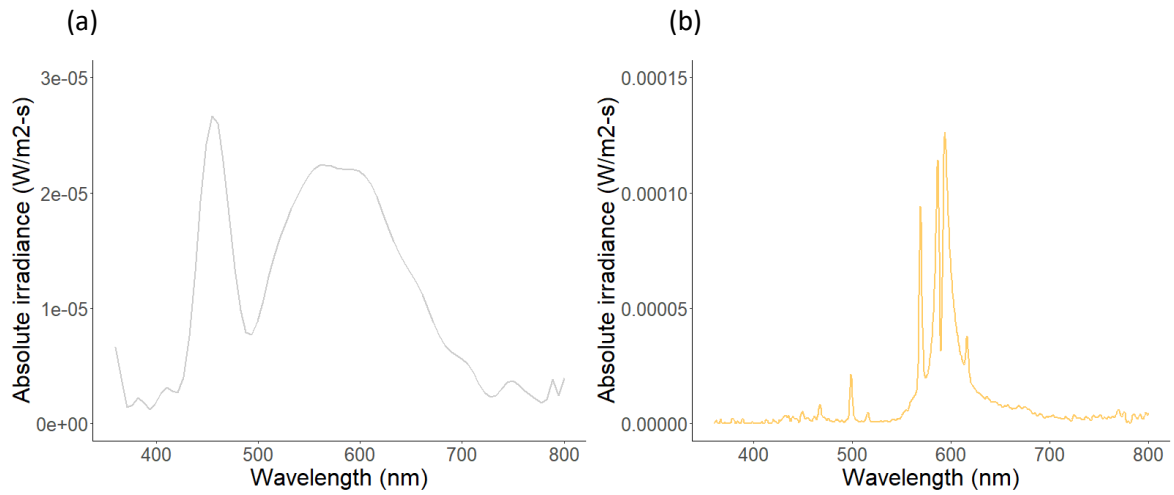

Figure 5.2. Emission spectra of the light treatments to which *Helicoverpa armigera* were exposed. (a) The LED streetlight and, (b) HPS streetlight transmitted through six layers of ¼ diffuser and one layer of UV-transmissive polaroid. All measurements were taken in laboratory conditions in February 2022 using a NIST calibrated StellarRAD spectrometer fitted with a cosine corrector (StellarNET Inc.).

5.2.2.2 The effect of streetlight intensity on activity

The nocturnal activity of *Helicoverpa armigera* was recorded under an LED streetlight of five intensities: 0-0.03 lux (control), 0.2 lux, 1 lux, 4 lux, and 10 lux across 12 evenings. The light intensities were created by placing layers of neutral-density (ND) filter (0.9 neutral-density filter and 2.1 neutral-density filter, Lee Filters) above the circular containers holding the moths (Table 5.1, Fig.5.3).

Table 5.1. Filter treatments applied to *Helicoverpa armigera* in the experiment used to test the effect of streetlight intensity on nocturnal activity.

Treatment	Layers 0.9	Layers 2.1	Lux	n
1	1	-	10	39
2	-	1	4	42
3	2	-	1	39
4	1	1	0.2	39
5	-	3	0-0.03	36

The position of the different filter layers was randomised each night to control for differences in horizontal illuminance caused by distance from the streetlight. Furthermore, the outside edge of the trestles supporting the containers housing the animals was lined with opaque plastic material to

screen horizontal and ground-reflected illuminance. The activity of up to 18 naïve moths were recorded each evening.

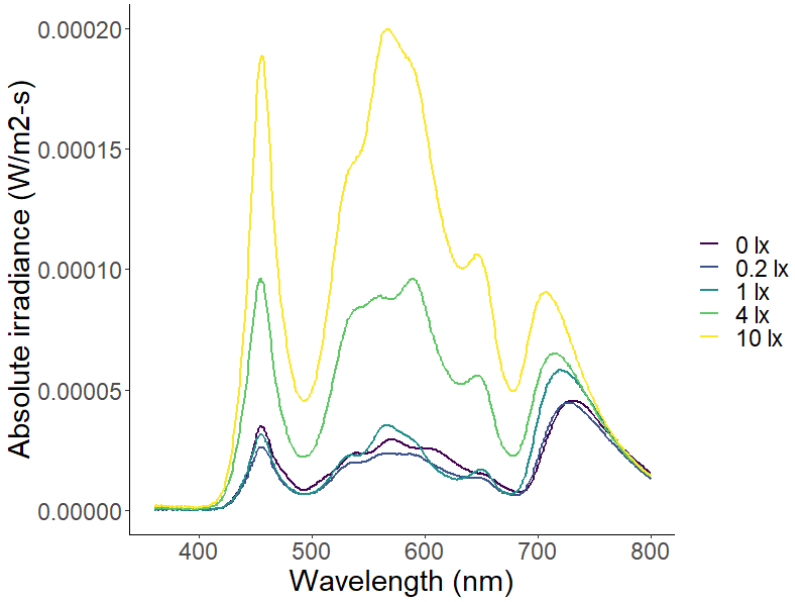

Figure 5.3. Emission spectra of the five intensity treatments to which *Helicoverpa armigera* was exposed. All measurements were taken in laboratory conditions in February 2022 using a QE65000 spectrometer and a P200-UV-VIS optical fibre (Ocean Insight Inc.) calibrated to a lamp of known spectral output (DH-2000, Ocean Insight Inc.).

5.2.2.3 The effect of the polarization of light on activity

This experiment was performed simultaneously with the experiment testing the differential effects of LED and HPS streetlights on activity. Within each of the three light treatments described in section 5.2.2.1, half (6/12) of the moths were exposed to one of two additional filter treatments: an artificially polarized 'sky' (n=65), or an artificially unpolarized 'sky' (n=67). The polarized treatments matched that used in chapter 3 wherein one face of the filter stack transmitted polarized light (x1 layer of ¼ diffuser below the polaroid and x6 layers of ¼ diffuser above, DoP=0.73) and, when inverted, the opposite face of the filter stack transmitted uniform, unpolarized light (x6 layers of ¼ diffuser below the polaroid and x1 layer of ¼ diffuser above, DoP=0.08) (Fig.5.4). The angle of polarization of the transmitted polarized light was defined by the transmission angle of the polaroid, which was manually aligned to be perpendicular to the position of the moon at sunset (thereby roughly aligned to the natural polarization pattern), and uniform across the diameter of the filter stack. The position of the two treatments were randomised each evening of recording.

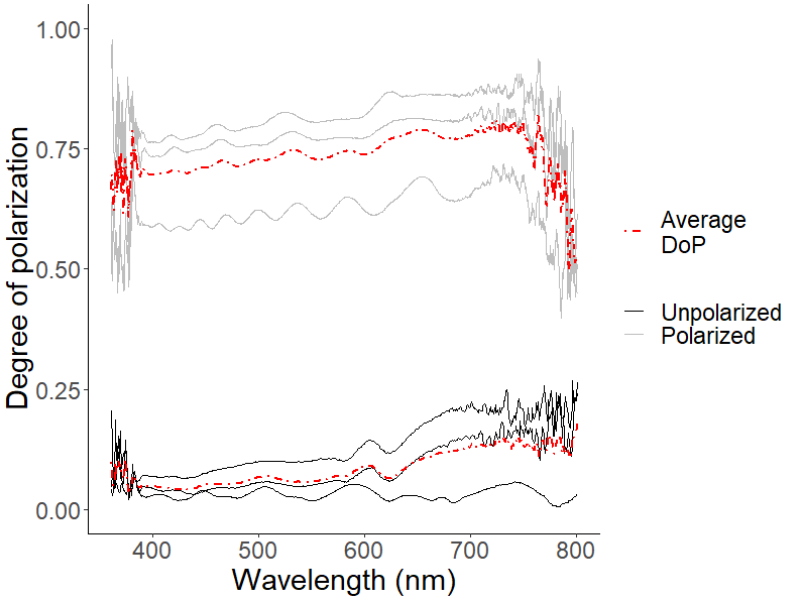

Figure 5.4. Degree of polarization of the polarized face of the filter stack (grey lines, average DoP of three measurements shown by the dashed line, wavelength range=360-800 nm) and the unpolarized face of the filter stack (black lines, average DoP of three measurements shown by the dashed line, wavelength range=360-800 nm) used to create the polarized light treatments. The DoP was calculated using irradiance measurements taken with a Glann-Thompson polarizing prism at 0°, 45°, 90°, and 135° rotations, a QE65000 spectrometer and a P200-UV-VIS optical fibre (Ocean Insight Inc.) (see chapter 3, section 3.2.3).

5.2.3 Experiments using *Drassodes* sp.

5.2.3.1 The effect of LED and HPS streetlights on activity

Two groups of 12 spiders experienced four consecutive evenings of natural darkness (control, 0-0.03 lux, n=12) followed by four evenings exposed to either an LED streetlight (LED group, 11 lux, n=12) or a HPS streetlight (HPS group, 11 lux, n=12) in a repeated measures design. A layer of ND filter (0.9 neutral-density filter, Lee Filters) was placed above the spiders to reduce the intensity of the light to reflect realistic streetlight values (Fig.5.5). The position of the circular containers housing the spiders was randomised each night within the apparatus. The outside edge of the trestles used to suspend the animals above ground was lined with opaque plastic material to screen horizontal and ground-reflected illuminance. Animals within their individual containers were removed from the experimental arena during the day and placed indoors to prevent overheating.

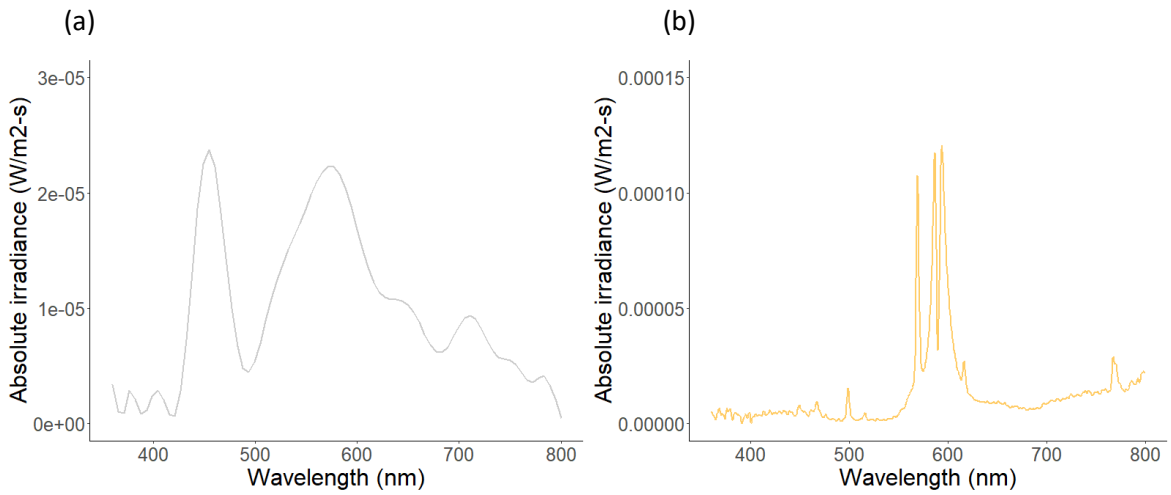

Figure 5.5. Emission spectra of the light treatments to which *Drassodes* sp. were exposed. (a) The LED streetlight and, (b) HPS streetlight transmitted through a layer of ND filter. All measurements were taken in laboratory conditions in February 2022 using a NIST calibrated StellarRAD spectrometer fitted with a cosine corrector (StellarNET Inc.).

5.2.4 Statistical analysis

The following analyses were chosen to explore three central questions to this investigation: 1) is the overall level of nocturnal activity affected by streetlights (general additive models), 2) are there peaks in the distribution of activity throughout the night and is this affected by streetlights (entrainment index) and, 3) is the total level of activity within these peaks affected by streetlights (activity index)?

Overall nocturnal activity

General additive models (GAMs) were used to analyse nocturnal activity in all three experiments. GAMs allow for the inclusion of random and fixed terms as well as auto-regressive structures that account for both repeated measures and temporally autocorrelated data, common to time-series experiments. The counts of active individuals per 2.5 minute time interval were included in all models as the response variable. Light treatment was included as the explanatory variable, day as a random effect, and the time interval was fitted with a smoother using a Gaussian process to account for temporal autocorrelation[39]. For the experiment testing for the polarization of light on activity, the polarization treatment was used as the explanatory variable. The models used to analyse *H. armigera* activity had a Poisson structure with a log link function or a zero-inflated Poisson structure with no link function. The model structure with the best model fit was selected using the Akaike information criterion (AIC) values and model diagnostic information[40]. To account for the repeated measures

design of the *Drassodes* sp. experiment, spider ID was included as a random term and the response variable was the binary 'active' or 'inactive' score of each spider per 2.5 minute time bin. These models therefore had a binomial structure with probit link function. Variance components were estimated using the Restricted Maximum Likelihood method (REML). Models were selected using manual backwards-stepwise model refinement and the significance of fixed terms was determined using analysis of variance tests (ANOVA) and associated p-values[40]. All GAMs were produced using the 'mgcv'[41] package in R (R Studio v. 4.1.2, R Development Core Team 2021). Residual diagnostics of all models were completed using the 'gam.check' function in the 'mgcv' package.

Entrainment and activity indices

An entrainment index (EI) and activity index (AI) were also used to compare nocturnal activity. The entrainment index is the ratio of peak activity to overall activity across the sampling period[42,43]. An entrainment index approaching 1 indicates that the individual was mostly active within a defined time window, and an entrainment index close to 0 indicates that the individual was mostly active outside of this focal window; intermediate values indicate distributed activity across the whole sampling period. Based on visual inspection of the control (natural darkness) data[42,43], the first two hours of the sampling period (0-120 minutes after sunset) were defined as the focal activity window. Therefore, the ratio of the total counts of activity within this window to the overall sampling period (11-12.5 hours) served as the entrainment index of each animal. We also developed an activity index metric which gives the average activity count in the focal window. In all experiments, activity was recorded every 2.5 minutes for 11-12.5 hours, therefore, the activity index can be defined as the cumulative number of active counts in the first 48 videos (0-120 minutes after sunset) of all individuals within a treatment group divided by the group sample size. The entrainment and activity indices of the spectral composition and polarization experiments were statistically compared between treatments using Wilcoxon signed-rank tests. To account for multiple comparisons of the five light treatments of the intensity experiment, Kruskal-Wallis tests were used to compare EI and AI between treatments and post-hoc Dunn tests with Bonferroni correction were used to calculate the significance of each comparison. All analyses were completed using base functions in R.

5.3 Results

5.3.1 *Helicoverpa armigera*

5.3.1.1 The effect of LED and HPS streetlights on nocturnal activity

The number of moths active across the whole night was greater in the control treatment than the LED or HPS treatments (Poisson GAM: deviance=-639.24, d.f.=-1.62, p<0.0001) (Fig.5.6). The greatest proportion of moths were active 0-120 minutes after sunset (focal window) in the control treatment (peak proportion of moths active=80%) which slowly reduced throughout the night before reaching 0% before sunrise (Fig.5.6). In LED and HPS treatments, the proportion of moths active was near-zero throughout the night except for a small rise in activity in the final hours of the evening, particularly evident in the LED treatment (peak proportion of moths active in the focal window=0 and 2%, respectively; and, in the final 6 hours=13 and 6%, respectively) (Fig.5.6).

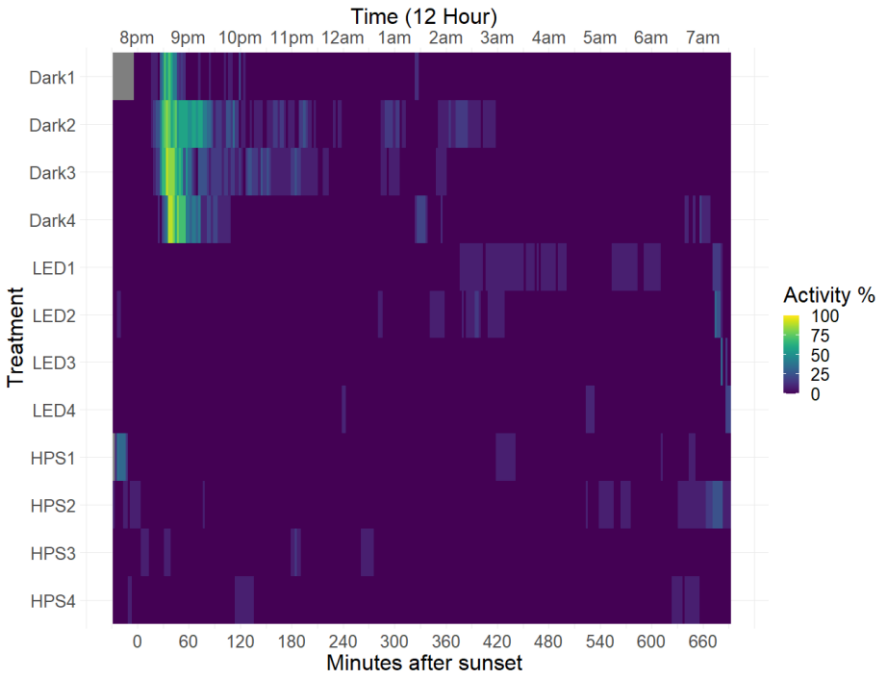

Figure 5.6. Proportion of *Helicoverpa armigera* showing activity in 2.5 minute bins, in four repeats of control ('Dark'), LED streetlight ('LED'), and high-pressure sodium streetlight ('HPS') treatments from sunrise to sunset in the Hautes-Pyrénées.

In agreement with the observed patterns in nightly activity across treatments, entrainment indices for moths exposed to both streetlight treatments were significantly lower than the controls (mean EI: control=0.81, LED=0, HPS=0.09; Wilcoxon signed-rank test: control vs. LED, n=40, W=1760, p<0.0001 and control vs. HPS, n=44, W=1977, p<0.0001) (Fig.5.7a). Additionally, entrainment indices were different between the two streetlight treatments (Wilcoxon signed-rank test: HPS vs. LED, n=40,

W=860, p=0.03). Activity indices were also significantly lower than the control, with average activity in both light treatments remaining close to zero within the focal window (mean AI: control=0.27, LED=0, HPS=0.01; Wilcoxon signed-rank test: control vs. LED, n=40, W=1760, p<0.0001 and control vs. HPS, n=44, W=2101, p<0.0001) (Fig.5.7b). Activity indices were also different between the two light treatments (Wilcoxon signed-rank test: n=48, W=860, p=0.03) (Fig.5.7b).

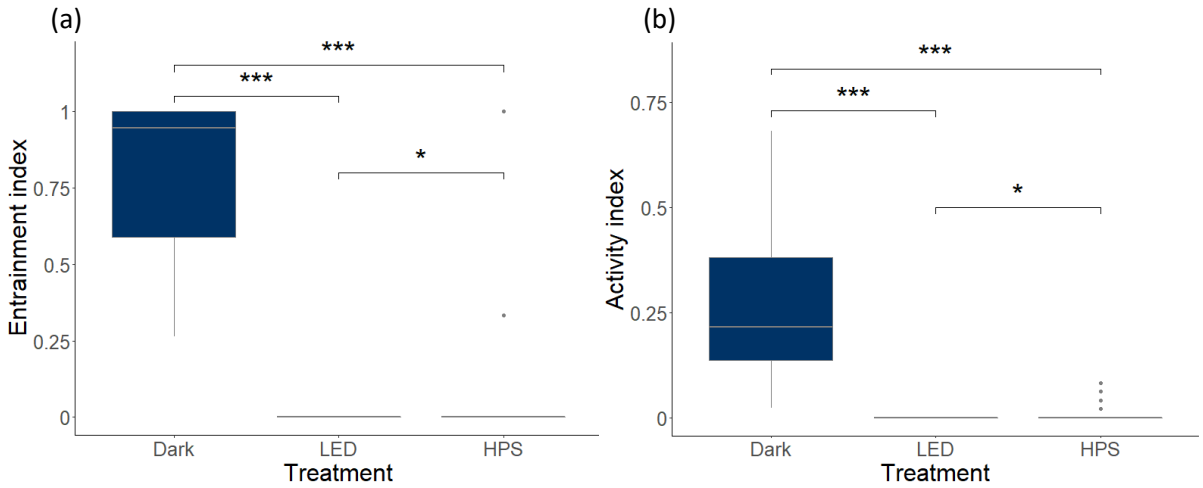

Figure 5.7. (a) Entrainment and (b) activity indices of individual *Helicoverpa armigera* in the control ('Dark'), LED streetlight ('LED'), and the high-pressure sodium streetlight ('HPS') treatments. The mean EI of the LED and HPS treatments were 0 and 0.09, respectively and the mean AI of the LED and HPS treatments were also 0 and 0.01, respectively. Annotations indicate the levels of significance of Wilcoxon signed-rank tests as '***' p>0.001, '**' p>0.01, '*' p>0.05.

5.3.1.2 The effect of streetlight intensity on activity

The proportion of moths active changed depending on streetlight intensity (Poisson GAM: deviance=-142.46, d.f.=-3.99, p<0.0001). Moths were most active 0-120 minutes after sunset in the control treatment (peak proportion of moths active=33%) which gradually reduced until sunrise (peak proportion of moths active outside focal window=5-10%) (Fig.5.8).

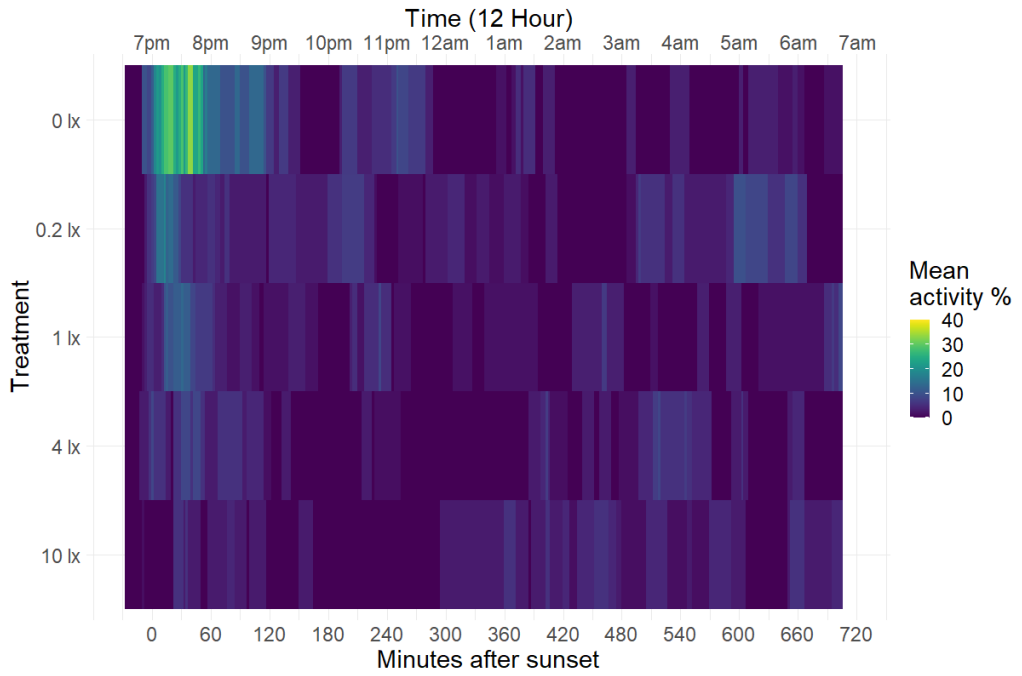

Figure 5.8. Proportion of *Helicoverpa armigera* showing activity in 2.5 minute bins when exposed to an LED streetlight at five intensities (0 lx, 0.2 lx, 1 lx, 4 lx, and 10 lx) from sunset to sunrise in the Hautes-Pyrénées.

Conversely, the proportion of moths active in the 10 lux treatment 0-120 minutes after sunset was minimal (peak proportion of moths active=6%) and remained low throughout the night (peak proportion of moths active outside focal window=3-8%). In the 0.2 and 1 lux treatments, the proportion of active moths also peaked within 0-120 minutes after sunset (peak proportion of moths active=18 and 13%, respectively), but the peak was less distinct than the control treatment and activity remained low for the rest of the night (peak proportion of moths active outside the focal window=6-10%) (Fig.5.8.). The activity level within the 4 lux treatment was similar to the 10 lux treatment, with no clear peak in activity 0-120 minutes after sunset (peak proportion of moths active in the focal window=8% and outside the focal window=3-8%) (Fig.5.8).

Table 5.2. Pairwise comparisons using Dunn tests with Bonferroni corrections of the entrainment indices ('EI') and activity indices ('AI') of *Helicoverpa armigera* exposed to five light treatments to test the effect of streetlight intensity on nocturnal activity. Annotations indicate the levels of significance as '***' p>0.001, '**' p>0.01, '*' p>0.05.

Treatment	**Comparison**	**EI**		**AI**	
		Z	**p**	**Z**	**p**
0 lx	0.2 lx	2.80	0.05	3.20	0.01*
0 lx	1 lx	2.65	0.07	2.71	0.06
0 lx	4 lx	3.98	0.0006***	4.04	0.0003***
0 lx	10 lx	4.55	0.00005***	4.17	0.00001***
0.2 lx	1 lx	-0.13	1	-0.47	1
0.2 lx	4 lx	1.14	1	0.92	1
0.2 lx	10 lx	1.77	0.75	1.69	0.90
1 lx	4 lx	1.27	1	1.340	1
1 lx	10 lx	1.89	0.58	2.15	0.31
4 lx	10 lx	-0.65	1	-0.79	1

Both the entrainment and activity indices were affected by light treatment (EI: Kruskal-Wallis, χ^2=24.04, d.f.=4, p<0.0001; AI: Kruskal-Wallis, χ^2=27.61, d.f.=4, p<0.0001) (Table 5.2). The EI and AI of the moths were significantly lower in the 10 and 4 lux treatment compared to the control (mean EI: 10 lux=0.12, 4 lux=0.15, control=0.53; mean AI: 10 lux=0.02, 4 lux=0.05, control=0.21) (Fig.5.9). Additionally, the average activity within the focal window of the 0.2 lux treatment (mean AI=0.07) was lower than the control (mean AI=0.21) (Fig.5.9b).

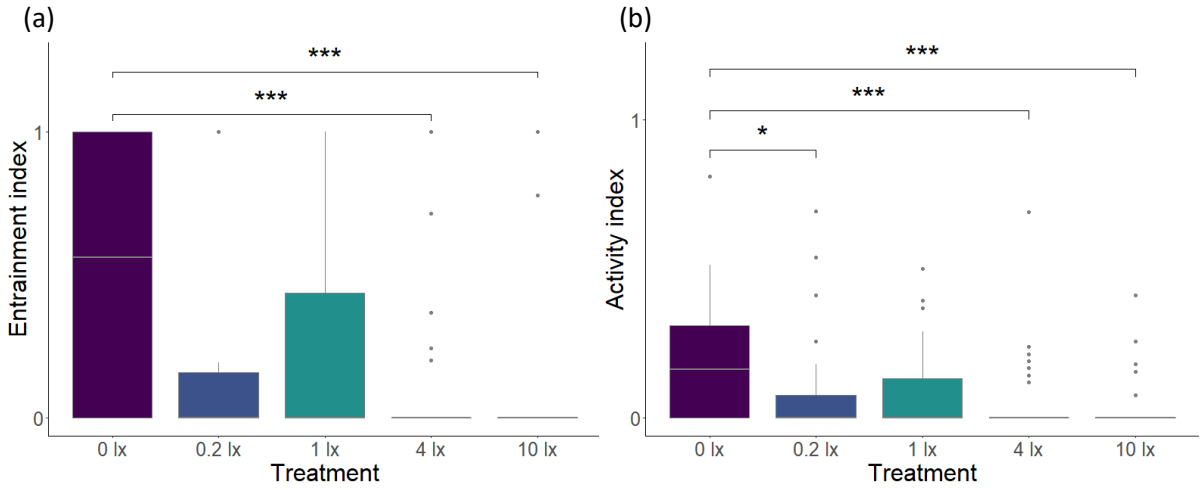

Figure 5.9. (a) The entrainment and (b) activity indices of *Helicoverpa armigera* exposed to the five intensity treatments (0lx, 0.2lx, 1lx, 4lx, and 10lx). Annotations indicate levels of significance of Kruskal-Wallis tests with Bonferroni corrections as '***' p>0.001, '**' p>0.01, '*' p>0.05.

5.3.1.3 The effect of the polarization of light on activity

The average proportion of active *H. armigera* was 33% higher in the absence of an artificially polarized 'sky' (Poisson GAM: deviance=-14.13, d.f.=-0.98, p=0.0002) (Fig.5.10). However, the overall proportion of active moths was small in both filter treatments (mean proportion of moths active throughout the night: polarized treatment=2.14, unpolarized treatment=2.76). As above, the greatest proportion of moths were active in the first 120 minutes after sunset in both treatments (peak proportion of moths active: polarized=27%, unpolarized=28%) and activity dropped following this period (peak proportion of moths active=4-8%).

(a) Polarized

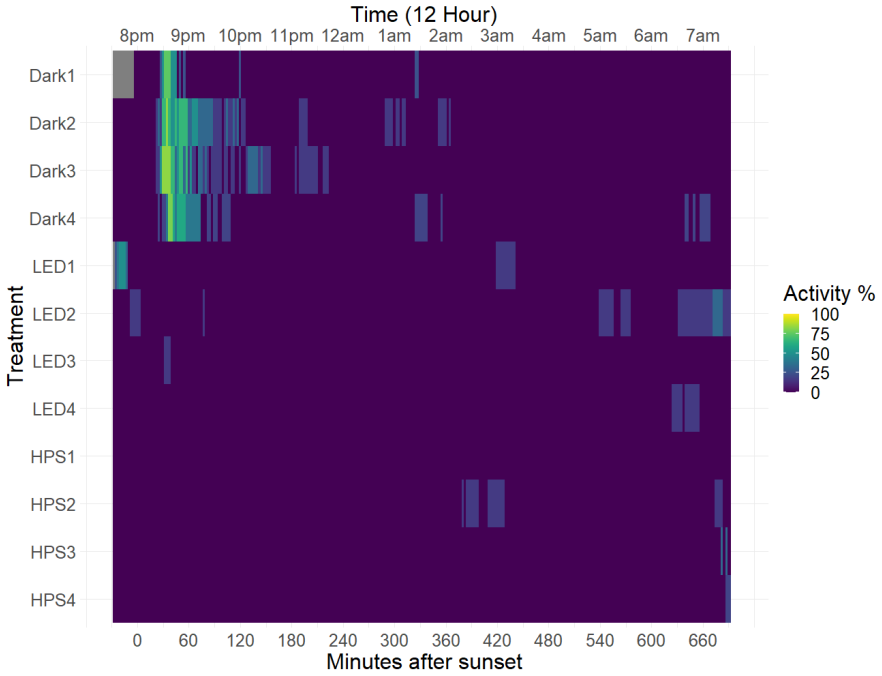

(b) Unpolarized

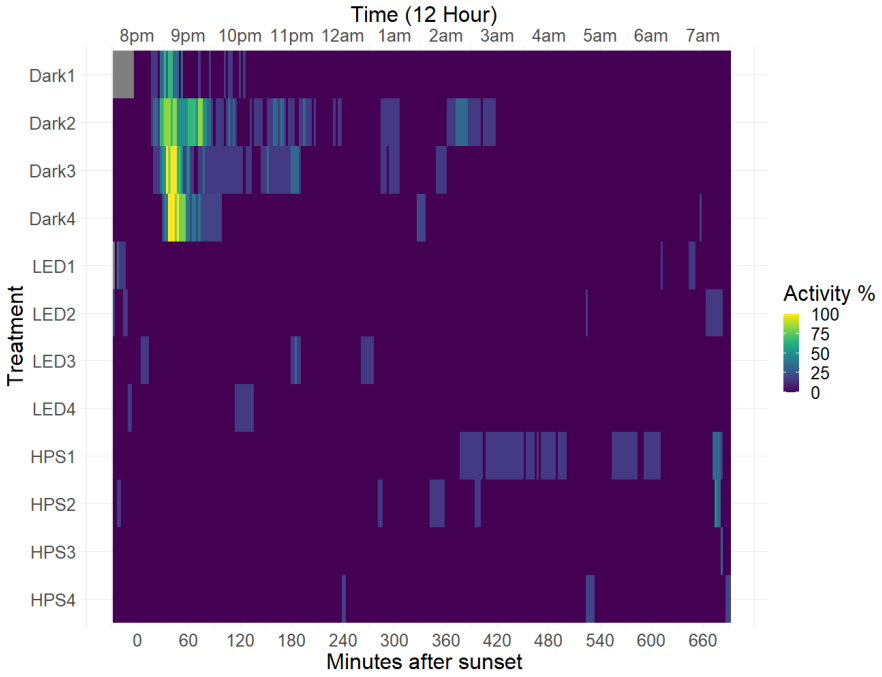

Figure 5.10. Proportion of *Helicoverpa armigera* active in 2.5-minute bins, exposed to (a) an artificially polarized 'sky' and, (b) an artificially unpolarized 'sky' under the three light treatments used to test the effect of streetlight spectral composition on nocturnal activity in the Hautes-Pyrénées.

No differences in EI were observed in the presence or absence of polarization (mean EI: polarized treatment=0.30, unpolarized treatment=0.29; Wilcoxon signed-rank test: n=65, W=2201, p=0.90)

(Fig.5.11a). There was also no difference in AI between the two treatments, the average activity of the moths being low within the focal window of both treatments (mean AI: polarized treatment=0.05, unpolarized treatment=0.06; Wilcoxon signed-rank test: n=65, W=2154, p=0.90) (Fig.5.11b).

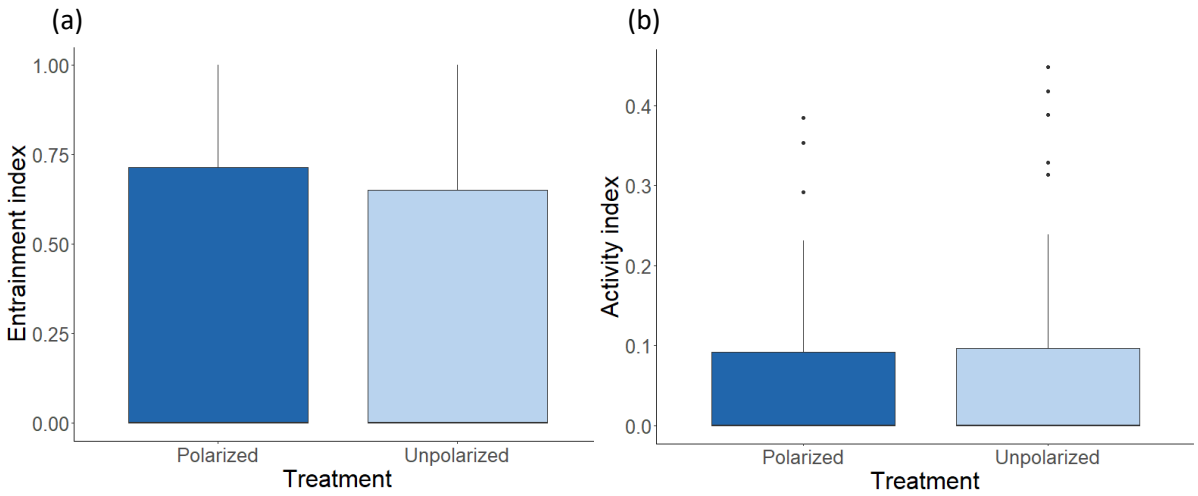

Figure 5.11. (a) Entrainment and (b) activity indices of individual *Helicoverpa armigera* exposed to an artificially polarized 'sky' ('Polarized') and an artificially unpolarized 'sky' ('Unpolarized').

5.3.2 *Drassodes* sp.

5.3.2.1 The effect of LED and HPS streetlights on nocturnal activity

The nocturnal activity of *Drassodes* sp. changed with exposure to both streetlights (LED group binomial GAM: deviance=-0.06, d.f.=-0.004, p=0.007; HPS group binomial GAM: deviance=0.002, d.f.=0.00007, p=0.0002). For clarity, the results of both groups will be described separately.

LED

During the control treatment, the proportion of spiders active was greatest 0-120 minutes after sunset (peak proportion of spiders active=40%) (Fig.5.12). This gradually dropped throughout the night from 40% in the first 2 hours after sunset, to 23% 2-4 hours after sunset, to 13% in the final 6 hours of the night. When the LED streetlight was turned on, no peak activity was observed 0-120 minutes after sunset, the proportion of active spiders instead remaining ~17% throughout the night (peak proportion of spiders active: 0-2 hours after sunset=14%, 2-4 hours after sunset=17%, final 6 hours of the night=21%).

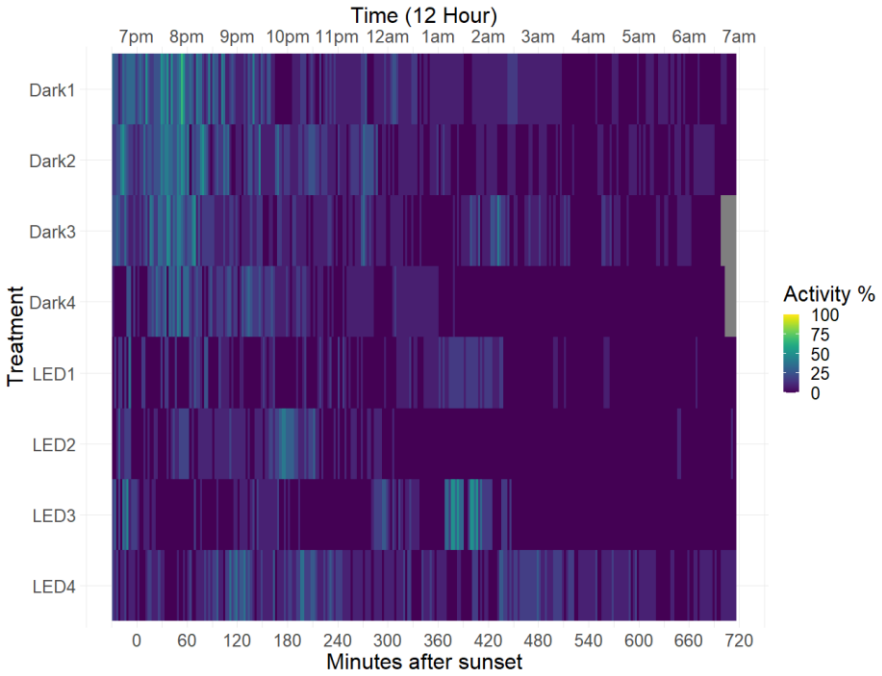

Figure 5.12. Proportion of *Drassodes* sp. showing activity in 2.5 minute bins in four consecutive nights of a control ('Dark') treatment followed by four nights of a LED streetlight ('LED') treatment from sunrise to sunset in the Hautes-Pyrénées.

No significant differences were observed in EI between the LED light treatment (mean EI=0.54) and the control (mean EI=0.37; paired Wilcoxon signed-rank test: n=12, V=52, p=0.33) (Fig.5.13a). However, the spiders were 75% less active within the focal window under the LED treatment (mean AI=0.9) than the control (mean AI=3.7; paired Wilcoxon signed-rank test: n=12, V=78, p=0.002) (Fig.5.13b).

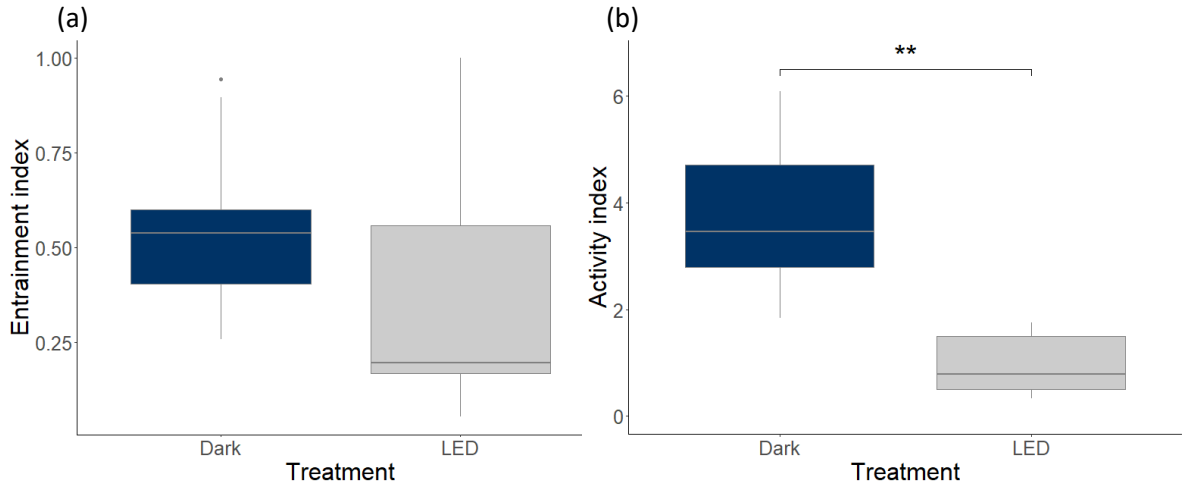

Figure 5.13. Average (a) entrainment and (b) activity indices of *Drassodes* spiders exposed to four consecutive nights of a control treatment ('Dark') followed by four nights of a LED treatment ('LED'). Annotations indicate the levels of significance of paired Wilcoxon signed-rank tests as '***' p>0.001, '**' p>0.01, '*' p>0.05.

HPS

During the control treatment, the proportion of spiders active was greatest 0-120 minutes after sunset (peak proportion of spiders active=69%) (Fig.5.14). The maximum proportion of active spiders reduced following the focal window but was maintained at ~30% throughout the night (peak proportion of spiders active: focal window=69%, 2-4 hours after sunset=38%, final 6 hours=31%). When the HPS streetlight was turned on, activity reduced and the proportion of active spiders remained ~25% throughout the night (peak proportion of spiders active: 0-2 hours after sunset=27%, 2-4 hours after sunset=25%, final 6 hours of the night=21%).

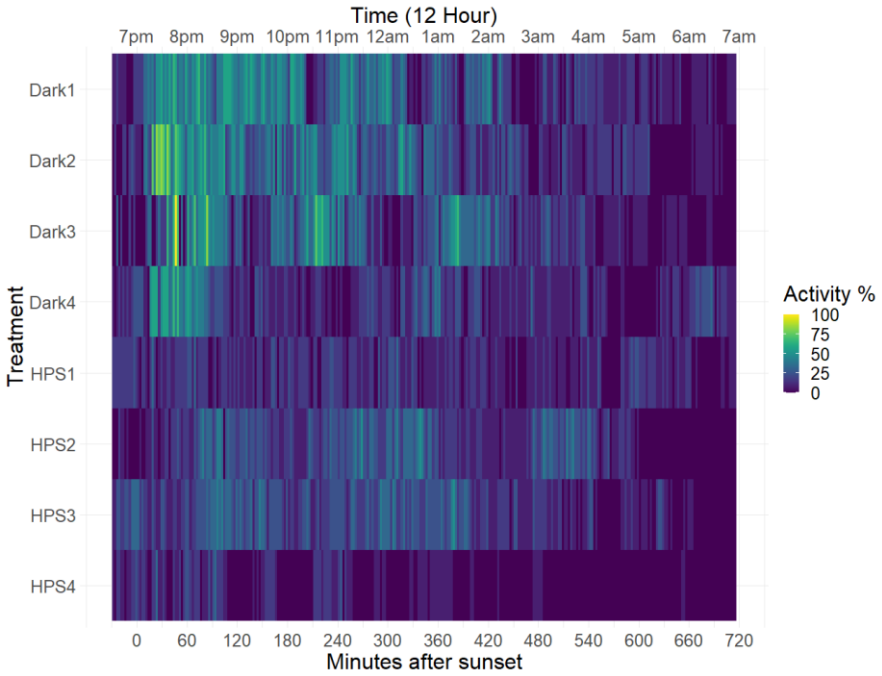

Figure 5.14. Proportion of *Drassodes* sp. showing activity in 2.5 minute bins in four consecutive nights of a control ('Dark') treatment followed by four nights of a HPS streetlight ('HPS') treatment from sunrise to sunset in the Hautes-Pyrénées.

No changes in the average EI of the spiders were observed between the control treatment (mean EI=0.32) and the light treatment (mean EI=0.23; paired Wilcoxon signed-rank test, n=12, V=64, p=0.05) (Fig.5.15a). However, total activity with the focal window reduced by 55% between the control (mean AI=5.90) and the light treatment (mean AI=2.65; paired Wilcoxon signed-rank test, n=12, V=70, p=0.01) (Fig.5.15b).

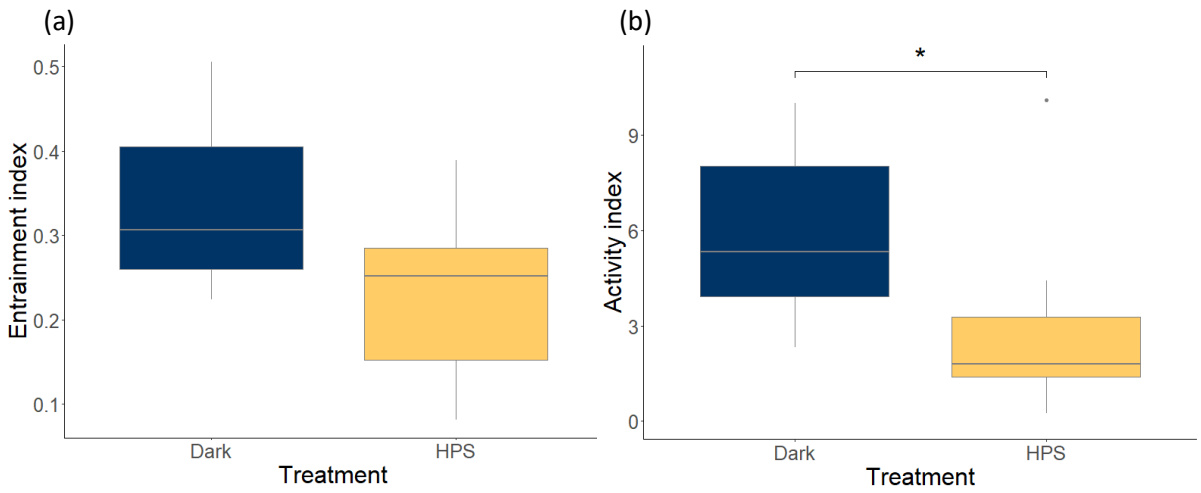

Figure 5.15. Average (a) entrainment and (b) activity indices of *Drassodes* spiders exposed to four consecutive nights of a control treatment ('Dark') followed four nights of a HPS treatment ('HPS'). Annotations indicate the levels of significance of paired Wilcoxon signed-rank tests as '***' p>0.001, '**' p>0.01, '*' p>0.05.

5.4 Discussion

5.4.1 The effect of LED and HPS streetlights on nocturnal activity

Direct exposure to both HPS and LED streetlights significantly reduced the nocturnal activity of *H. armigera* and *Drassodes* sp., with almost complete inhibition throughout the night in the former. This effect was particularly strong in the first two hours (focal window) after sunset when *H. armigera* and *Drassodes* sp. typically initiate nocturnal excursions[30,31]. The activity profiles of individuals not exposed to any streetlight showed a single peak within the focal window which was followed by a moderate level of activity through the remainder of the first half of the night, before dropping within the final 6 hours. In *H. armigera*, exposure to either HPS or LED streetlights eliminated the activity peak within the focal window and reduced the number of active moths to near-zero for most of the night. In *Drassodes* sp., the effect of both streetlights on overall nightly activity was similar albeit less dramatic, reducing the total activity in the focal window by ~50% and reducing overall nightly activity to less than a third. However, although the total activity reduced within the focal window, the activity peak was not eliminated. Light at night reduced the number of spiders active, particularly in the first two hours of the night, but did not affect the timing of that activity. Thus, direct exposure to streetlighting of both broad-spectrum and long-wavelength narrow spectrum reduces the overall level of nocturnal activity and reduces the maximum level of activity in both *H. armigera* and *Drassodes* sp., but only affected the distribution of maximum activity in *H. armigera*.

In both species, the reduction of activity within the focal window was more pronounced under the LED than the HPS streetlight, suggesting that the perceived brightness of the LED light was higher than that of the HPS, and substantially above the intensity threshold required to initiate natural nocturnal activity. The greater effect of the LED streetlight was expected given that its spectral composition is more likely to overlap with the spectral sensitivities of the animals. Such differential effects have been observed in the capture rates of nocturnal insects by light traps with total number of captured insects[13,14], abundance of nocturnal predators like spiders[15], and species diversity[16] all increasing under broad-spectrum LED light compared to HPS or long-wavelength shifted narrow-spectrum lights. Specifically in nocturnal lepidopterans and spiders, traps that are illuminated by broad-spectrum lighting increased the diversity, abundance, and species richness of the animals captured, particularly when the light contained UV[15,22,24,25]. Thus, broad-spectrum light is more likely to attract a greater abundance and diversity of moths and spiders and, once lured by the light, we have shown that broad-spectrum light is more likely to inhibit important behaviours like migration and foraging.

Despite the differential effects of the two light spectra, both significantly affected the activity of moths and spiders. Individuals that shelter during the day within direct exposure to either type of streetlight will exhibit suppressed and disrupted activity during the night. For migrating *H. armigera*, this will likely prevent initiation of migratory flight and potentially trap individuals in unintended locations or delay migratory movements (see chapter 3). *H. armigera* is a facultative migrator, moving to new feeding and breeding grounds when conditions become unfavourable, such as with the changing of seasons. Thus, altered migratory behaviour resulting in inefficient migratory movements will have implications for species fitness and dispersal, as well as economic implications due to its status as an economically important crop pest[44]. Furthermore, this negative impact may not be exclusive to migratory behaviour: the activity profiles of non-migrating *H. armigera* show a second peak in the latter half of the night, when mate-finding typically occurs[31,45]. Reproduction is known to be affected by light exposure in other nocturnal lepidopterans[23]. Therefore, it is likely that the negative effects of light pollution in *H. armigera* could include delayed or inhibited reproduction in addition to the impacts to migration. Further research on the effects of light pollution during different life history stages will help identify the various pathways by which it affects species fitness in nocturnal lepidopterans and crop pest dynamics in agroecosystems.

For foraging *Drassodes* spiders, the suppression of nocturnal activity may reduce prey capture through reducing the number of foraging bouts attempted by individuals. Prey capture rates are known to increase within the vicinity of streetlights in web-weaving spiders[46,47], as is spider abundance, due to the aggregation of high densities of prey species around light at night[15,48]. Thus, whilst prey capture rates might initially increase following recruitment into the lit area of streetlights, the suppressive

effect of light on nocturnal activity is likely to reduce prey capture over time in free-hunting spiders and potentially trap individuals in these areas. Indeed, research on the effects of prolonged exposure to light at night on an orb-web spider showed that initial fitness increases caused by increased prey capture are offset by significant developmental costs such as increased juvenile mortality and reduced egg-laying[50]. Furthermore, a general reduction in nocturnal activity and thus, feeding rates of a predator like *Drassodes* sp. will have implications for predator-prey population dynamics[47,48,49] as well as individual fitness and dispersal. Like *H. armigera*, the negative impacts of light pollution may not be exclusive to foraging behaviour as a general reduction in nocturnal activity is also likely to reduce mate finding and reproduction[50]. However, light pollution did not affect the timing of activity or the distribution of activity peaks in *Drassodes* sp., meaning the important nocturnal behaviours like foraging may not become asynchronized with nocturnal *Zeitgebers*, sensory cues, or the emergence of nocturnal prey. Again, further research on the effects of light pollution during different life history stages will help identify the various pathways by which they affect species fitness and predator-prey interactions.

5.4.2 The effect of streetlight intensity on activity

Exposure to LED streetlights at intensities of 4 lux or greater dramatically reduced nocturnal activity in *H. armigera*. In the 0 lux treatment and, to a lesser degree, the 0.2 and 1 lux treatments, activity followed a similar pattern to moths under naturally dark conditions: activity was highest 0-120 minutes after sunset, followed by a moderate level of activity before dropping to almost no activity during the final 6 hours of the night. Similar activity profiles in both experiments strongly suggest that light intensity is an important trigger of nocturnal activity and celestial cues such as starlight and the skylight polarization pattern (which would not have been visible under the experimental filters) are less important. However, they do demonstrate that they are active in the window of the night most affected by the masking effects of light pollution on the polarization pattern (>1 hour post-sunset, see chapter 2). Peak activity at the start of the night was eliminated by exposure to the LED streetlight at 10 lux. Yet, there was a subtle peak in activity between 0-120 minutes after sunset in the 4 lux treatment. This suggests that the intensity required to trigger nocturnal flight is between 0 and 4 lux, which agrees with the existing literature[28,29], and that ambient light intensity must be as low as 0-0.2 lux for the uninhibited initiation of migratory flight.

Therefore, direct exposure to streetlights of moderate-low intensities has the potential to dramatically affect the seasonal onset of migratory flight in *H. armigera*. The typical intensity of moonlight at full moon at mid-latitudes under normal atmospheric conditions is between 0.05-0.2 lux[51]. Thus, our results suggest that exposure to light even slightly brighter than the full moon may reduce the number

of flying individuals. Indeed, there is anecdotal evidence to suggest that moonlight itself can supress flight initiation[29]. As most streetlights in the UK are between 2-50 lux at ground-level, current streetlight intensities have the potential to significantly reduce lepidopteran activity within urbanised areas[33]. Furthermore, direct streetlight exposure alone may not only interfere with nocturnal activity patterns; indirect exposure through urban skyglow may also reach intensities brighter than the moon and impact activity[52,53]. However, the activity profiles of *H. armigera* under light intensities of 0.2-4 lux were similar in shape to individuals under natural light conditions, albeit with a much-reduced peak in activity. As such, lowering streetlight intensity to <5 lux may allow some moths to migrate through urbanised areas relatively uninhibited, or allow some moths trapped within urbanised areas to disperse. Given that ambient light intensity thresholds of 0-4 lux are important for the initiation of flight in many species of lepidopterans[28,29], it is assumed that this conclusion can be extrapolated to other nocturnal migratory species. Similarly, many of these species are, like *H. armigera*, important agricultural pests and as such the effects of streetlight exposure on lepidopteran activity is likely to have significant economic consequences to the productivity of agroecosystems[44,54].

5.4.3 The effect of the polarization of light on activity

Counter to expectations, the proportion of active *H. armigera* was higher in the absence of an artificially polarized 'sky' between sunset and sunrise. However, general activity within the focal window was not affected by the presence or absence of the polarization of light. It is unclear why *H. armigera* might be more active in the absence of overhead skylight polarization. As mentioned in previous chapters, the artificially polarized 'sky' used in this investigation did not have a pattern in DoP and AoP like the characteristic 'band' of the real sky polarization pattern. The unnatural uniformity of the polarized 'sky' to which the moths were exposed may therefore have been insufficient to guide orientation and deterred some individuals from initiating flight. However, this did not prevent *H. armigera* from orientating to the polarized treatment during the flight simulator experiments described in chapter 3; it is unclear whether orientation might have improved if a more naturalistic polarization pattern was used. Further research is required to explicitly investigate the effect of the pattern of lunar polarization on nocturnal activity.

5.5 Conclusions

Light pollution has the potential to inhibit or alter time-sensitive behaviours essential for survival, with broader implications for dispersal, species fitness, community composition, and agroecosystems. By

investigating two species, this study has identified common impacts of light pollution on nocturnal activity in arthropods of different ecologies and life histories that include: a reduction in overall nightly activity, changes to the distribution of activity over time, and a reduction in the maximum level of activity during times of naturally elevated activity. These results demonstrate the importance of both the spectral composition and intensity of streetlighting, which must be considered when predicting and assessing the impacts of direct exposure to streetlighting on nocturnal arthropods. Tuning both characteristics of streetlights to longer wavelengths and lower intensities could help to mitigate the impacts of light pollution on the nocturnal world without compromising the functionality and social benefits of streetlighting.

References

1. Davies TW, Bennie J, Inger R, Gaston KJ. 2013. Artificial light alters natural regimes of night-time sky brightness. *Scientific Reports*, **3**: 2045-2322. (DOI: 10.1038/srep01722)
2. Gaston KJ, Davies TW, Nedelec SL, Holt LA. 2017. Impacts of artificial light at night on biological timings. *Annual Review of Ecology, Evolution, and Systematics*, **48**(1): 49-68. (DOI: 10.1146/annurev-ecolsys-110316-022745)
3. Foster JJ, Tocco C, Smolka J, Khaldy L, Baird E, Byrne MJ, Nilsson DE, Dacke M. Light pollution forces a change in dung beetle orientation behavior. *Current Biology*, **31**(17): 3935-3942. (DOI: 10.1016/j.cub.2021.06.038)
4. Owens ACS, Cochard P, Durrant J, Farnworth B, Perkin EK, Seymoure B. 2020. Light pollution is a driver of insect declines. *Biological Conservation*, **241**: 108259. (DOI: 10.1016/j.biocon.2019.108259)
5. Gaston KJ, Davies TW, Bennie J, Hopkins J. 2012. Review: Reducing the ecological consequences of night-time light pollution: options and developments. *Journal of Applied Ecology*, **49**(6): 1256-1266. (DOI: 10.1111/j.1365-2664.2012.02212.x)
6. Kyba CCM, Kuester T, de Miguel AS, Baugh K, Jechow A, Hölker F, Bennie J, Elvidge CD, Gaston KJ, Guanter L. 2017. Artificially lit surface of Earth at night increasing in radiance and extent. *Science Advances*, **3**(11): e1701528. (DOI: 10.1126/sciadv.1701528)
7. Pagden M, Ngahane K, Amin SR. 2020. Changing the colour of night on urban streets - LED vs. part-night lighting system. *Socio-Economic Planning Sciences*, **69**: 100692. (DOI: 10.1016/j.seps.2019.02.007)
8. Belušič G, Sporar K, Meglic A. 2017. Extreme polarisation sensitivity in the retina of the corn borer moth *Ostrinia*. *Journal of Experimental Biology*, **220**(11): 2047-2056. (DOI: 10.1242/jeb.153718)
9. Morehouse NI, Buschbeck EK, Zurek DB, Steck M, Porter ML. 2017. Molecular evolution of spider vision: New opportunities, familiar players. *Biological Bulletin*, **233**(1): 21-38. (DOI: 10.1086/693977)
10. Yan S, Zhu JL, Zhu WL, Zhang XF, Li Z, Liu XX, Zhang QW. 2014. The expression of three opsin genes from the compound eye of *Helicoverpa armigera* (Lepidoptera: Noctuidae) is regulated by a circadian clock, light conditions and nutritional status. *PLOS One*, **9**(10): e111683. (DOI: 10.1371/journal.pone.0111683)
11. Stalleicken J, Labhart T, Mouritsen H. 2006. Physiological characterization of the compound eye in monarch butterflies with focus on the dorsal rim area. *Journal of Comparative Physiology A*, **192**(3): 321-331. (DOI: 10.1007/s00359-005-0073-6)
12. Macgregor CJ, Pocock MJO, Fox R, Evans DM. 2019. Effects of street lighting technologies on the success and quality of pollination in a nocturnally pollinated plant. *Ecosphere*, **20**(1): e02550. (DOI: 10.1002/ecs2.2550)
13. Pawson SM, Bader MKF. 2014. LED lighting increases the ecological impact of light pollution irrespective of color temperature. *Ecological Applications*, **24**(7): 1561-1568. (DOI: 10.1890/14-0468.1)
14. Longcore T, Aldern HL, Eggers JF, Flores S, Franco L, Hirshfield-Yamanishi E, Petrinec LN, Yan WA, Barroso AM. 2015. Tuning the white light spectrum of light emitting diode lamps to reduce attraction of nocturnal arthropods. *Philosophical Transactions of the Royal Society B.* **370**: 20140125. (DOI: 10.1098/rstb.2014.0125)

15. Davies TW, Bennie J, Cruse D, Blumgart D, Inger R, Gaston KJ. 2017. Multiple night-time light-emitting diode lighting strategies impact grassland invertebrate assemblages. *Global Change Biology*, **23**(7): 2641-2648. (DOI: 10.1111/gcb.13615)
16. Wakefield A, Broyles M, Stone EL, Harris S, Jones G. 2017. Quantifying the attractiveness of broad-spectrum streetlights to aerial nocturnal insects. *Journal of Applied Ecology*, **55**(2): 714-722. (DOI: 10.1111/1365-2664.13004)
17. Davies TW, Bennie J, Inger R, De Ibarra NH, Gaston KJ. 2013. Artificial light pollution: are shifting spectral signatures changing the balance of species interactions? *Global Change Biology*, **19**(5): 1417-1423. (DOI: 10.1111/gcb.12166)
18. Brehm G, Niermann J, Nino LMJ, Enseling D, Justel T, Axmacher JC, Warrant E, Fiedler K. 2021. Moths are strongly attracted to ultraviolet and blue radiation. *Insect Conservation and Diversity*, **14**(2): 188-198. (DOI: 10.1111/icad.12476)
19. Sun YX, Tian A, Zhang XB, Zhao ZG, Zhang ZW, Ma RY. 2014. Phototaxis of *Grapholitha molesta* (Lepidoptera: Olethreutidae) to different light sources. *Journal of Economic Entomology*, **107**(5): 1792-1799. (DOI: 10.1603/ec14155)
20. van Langevelde F, van Grunsven RHA, Veenendaal EM, Fijen TPM. 2017. Artificial night lighting inhibits feeding in moths. *Biology Letters*, **13**(3): 20160874. (DOI: 10.1098/rsbl.2016.0874)
21. Heiling AM. 1999. Why do nocturnal orb-web spiders (Araneidae) search for light? *Behavioral Ecology and Sociobiology*, **46**(1): 43-49. (DOI: 10.1007/s002650050590)
22. Plummer KE, Hale JD, O'Callaghan MJ, Sadler JP, Siriwardena GM. 2016. Investigating the impact of street lighting changes on garden moth communities. *Journal of Urban Ecology*, **2**(1): juw004. (DOI: 10.1093/jue/juw004)
23. van Geffen KG, van Eck E, de Boer RA, van Grunsven RHA, Salis L, Berendse F, Veenendaal EM. 2015. Artificial light at night inhibits mating in a geometrid moth. *Insect Conservation and Diversity*, **8**(3): 282-287. (DOI: 10.1111/icad.12116)
24. van Langevelde, F, Ettema JA, Donners M, WallisDeVries MF, Groenendijk D. 2011. Effect of spectral composition of artificial light on the attraction of moths. *Biological Conservation*, **144**(9): 2274-2281. (DOI: 10.1016/j.biocon.2011.06.004)
25. Somers-Yeates R, Hodgson D, McGregor PK, Spalding A, Ffrench-Constant RH. 2013. Shedding light on moths: shorter wavelengths attract noctuids more than geometrids. *Biology Letters*, **9**(4): 20130376. (DOI: 10.1098/rsbl.2013.0376)
26. Chen F, Shi J, Keena M. 2016. Evaluation of the effects of light intensity and time interval after the start of scotophase on the female flight propensity of Asian gypsy moth (*Lepidoptera*: *Erebidae*). *Environmental Entomology*, **45**(2): 404-409. (DOI: 10.1093/ee/nvv222)
27. Kelber A, Warrant EJ, Pfaff M, Wallen R, Theobald JC, Wcislo WT, Raguso RA. 2006. Light intensity limits foraging activity in nocturnal and crepuscular bees. *Behavioral Ecology*, **17**(1): 63-72. (DOI: 10.1093/beheco/arj001)
28. Dreisig H. 1980. The importance of illumination level in the daily onset of flight activity in nocturnal moths. *Physiological Entomology*, **5**: 327–342. (DOI: 10.1111/j.1365-3032.1980.tb00243.x)
29. Persson B. 1971. Influence of light on flight activity of Noctuids (Lepidoptera) in South Sweden. *Insect Systematics & Evolution*, **2**: 215–232. (DOI: 10.1163/187631271X00220)
30. Dacke M, Nilsson DE, Warrant EJ, Blest AD, Land MF, O'Carroll DC. 1999. Built-in polarizers form part of a compass organ in spiders. *Nature*, **401**(6752): 470-473. (DOI: 10.1038/46773)
31. Riley JR, Armes NJ, Reynolds DR, Smith AD. 1992. Nocturnal observations on the emergence and flight behavior of *Helicoverpa armigera* (Lepidoptera, Noctuidae) in the post-rainy season in

central India. *Bulletin of Entomological Research*, **82**(2): 243-256. (DOI: 10.1017/s0007485300051798)

32. Dent DR, Pawar CS. 1988. The influence of moonlight and weather on catches of *Helicoverpa armigera* (Hubner) (Noctuidae: Lepidoptera) in light and pheromone traps. *Bulletin of Entomological Research*, **78**(3): 365-377. (DOI: 10.1017/s0007485300013146)
33. British Standards Institution (BSI). 2015. Road lighting - Part 2: Performance requirements. BS EN 13201-2:2015, London, BSI
34. Feng HQ, Wu XF, Wu B, Wu KM. 2009. Seasonal Migration of *Helicoverpa armigera* (Lepidoptera: Noctuidae) over the Bohai Sea. *Journal of Economic Entomology*, **102**(1): 95-104. (DOI: 10.1603/029.102.0114)
35. Feng HQ, Wu KM, Cheng DF, Guo YY. 2004. Northward migration of *Helicoverpa armigera* (Lepidoptera: Noctuidae) and other moths in early summer observed with radar in northern China. *Journal of Economic Entomology*, **97**(6): 1874-1883. (DOI: 10.1093/jee/97.6.1874)
36. Chapman JW, Reynolds DR, Mouritsen H, Hill JK, Riley JR, Sivell D, Smith AD, Woiwod IP. 2008. Wind selection and drift compensation optimize migratory pathways in a high-flying moth. *Current Biology*, **18**(7): 514-518. (DOI: 10.1016/j.cub.2008.02.080)
37. Foster JJ, Kirwan JD, el Jundi B, Smolka J, Khaldy L, Baird E. Byrne MJ, Nilsson DE, Johnsen S, Dacke M. 2019. Orienting to polarized light at night - matching lunar skylight to performance in a nocturnal beetle. *Journal of Experimental Biology*, **222**(2): jeb188532. (DOI: 10.1242/jeb.188532)
38. Dreyer D, Frost B, Mouritsen H, Gunther A, Green K, Whitehouse M, Johnsen S, Heinze S, Warrant E. 2018. The Earth's magnetic field and visual landmarks steer migratory flight behaviour in the nocturnal Australian bogong moth. *Current Biology*, **28**: 2160-2166. (DOI: 10.1016/j.cub.2018.05.030)
39. Simpson GL. 2018. Modelling palaeoecological time series using generalised additive models. *Frontiers in Ecology and Evolution*, **6**. (DOI: 10.3389/fevo.2018.00149)
40. Thomas R, Lello J, Medeiros R, Pollard A, Robinson P, Seward A, Smith J, Vafidis J, Vaughan I. 2017. Statistical models: Model selection. In: Thomas R. (eds), 2nd Ed., Data analysis with R statistical software – A guidebook for scientists. Eco-explore, Cardiff, UK, pp. 69-71.
41. Wood SN. 2004. Stable and efficient multiple smoothing parameter estimation for generalized additive models. *Journal of the American Statistical Association*, **99**(467): 673-686. (DOI: 10.1198/016214504000000980)
42. Cho E, Oh JH, Lee E, Do YR, Kim EY. 2016. Cycles of circadian illuminance are sufficient to entrain and maintain circadian locomotor rhythms in *Drosophila*. *Scientific Reports*, **6**: 2045-2322. (DOI: 10.1038/srep37784)
43. Gentile C, Sehadova H, Simoni A, Chen C, Stanewsky R. 2013. Cryptochrome antagonizes synchronization of *Drosophila's* circadian clock to temperature cycles. *Current Biology*, **23**(3): 185-195. (DOI: 10.1016/j.cub.2012.12.023)
44. Fitt GP. 1989. The ecology of Heliothis species in relation to agroecosystems. *Annual Review of Entomology*, **34**: 17-52. (DOI: 10.1146/annurev.en.34.010189.000313)
45. Saito O. 2000. Flight activity changes of the cotton bollworm, *Helicoverpa armigera* (Hubner) (Lepidoptera: Noctuidae), by aging and copulation as measured by flight actograph. *Applied Entomology and Zoology*, **35**(1): 53-61. (DOI: 10.1303/aez.2000.53)
46. Willmott NJ, Henneken J, Elgar MA, Jones TM. 2019. Guiding lights: Foraging responses of juvenile nocturnal orb-web spiders to the presence of artificial light at night. *Ethology*, **125**(5): 289-297. (DOI: 10.1111/eth.12852)

47. Yuen SW, Bonebrake TC. 2017. Artificial night light alters nocturnal prey interception outcomes for morphologically variable spiders. *Peerj*, **5**: e4070. (DOI: 10.7717/peerj.4070)
48. Adams MR, 2000. Choosing hunting sites: Web site preferences of the orb weaver spider, *Neoscona crucifera*, relative to light cues. *Journal of Insect Behavior*, **13**(3): 299-305. (DOI: 10.1023/a:1007771332721)
49. Michalko R, Pekar S, Dul'a M, Entling MH. 2019. Global patterns in the biocontrol efficacy of spiders: A meta-analysis. *Global Ecology and Biogeography*, **28**(9): 1366-1378. (DOI: 10.1111/geb.12927)
50. Willmott NJ, Henneken J, Selleck CJ, Jones TM. 2018. Artificial light at night alters life history in a nocturnal orb-web spider. *Peerj*, **6**: e5599. (DOI: 10.7717/peerj.5599)
51. Kyba CCM, Mohar A, Posch T. 2017. How bright is moonlight? *Astronomy & Geophysics*, **58**(1): 1.31–1.32. (DOI: 10.1093/astrogeo/atx025)
52. Jechow A, Kyba CCM, Hölker F. 2020. Mapping the brightness and color of urban to rural skyglow with all-sky photometry. *Journal of Quantitative Spectroscopy & Radiative Transfer*, **250**: 106988. (DOI: 10.1016/j.jqsrt.2020.106988)
53. Torres D, Tidau S, Jenkins S, Davies T. 2020. Artificial skyglow disrupts celestial migration at night. *Current Biology*, **30**(12): E696-E697. (DOI: 10.1016/j.cub.2020.05.002)
54. Jones CM, Parry H, Tay WT, Reynolds DR, Chapman JW. 2019. Movement ecology of pest *Helicoverpa*: Implications for ongoing spread. *Annual Review of Entomology*, **64**: 277-295. (DOI: 10.1146/annurev-ento-011118-111959)

6

Conclusions and future research

This project has addressed important questions regarding how light pollution affects the navigation and periodic activity of two ecologically different nocturnal arthropods.

Helicoverpa armigera and *Drassodes* spp. have been presumed and are known, respectively, to use the skylight polarization pattern as a visual cue to guide navigation. They therefore offer the opportunity to: i) generate new knowledge of their sensory and behavioural ecology and ii) provide an interesting comparative system for studying the different, but related, behaviours of long-distance migration versus central-place foraging. These groups represent evolutionarily distant and ecologically divergent lineages but with common navigational strategies and patterns of nocturnal movement. As such, we can try to determine which effects of light pollution on nocturnal navigation might be shared across species, and which are more likely to be species or context specific. Only by understanding the impacts of light pollution in their meaningful biological context – including their extent and their variation across arthropod groups – can we hope to inform targeted and efficient mitigation measures.

This chapter summarises the key findings of this work, considers their wider impacts on this growing field of research, and discusses some developing ideas for future research to better understand the mechanisms and ecological consequences of the multiple impacts of light pollution on nocturnal arthropods.

6.1 Key findings

- Light pollution affected the maximum degree of polarization, persistence, and spatial extent of the skylight polarization pattern.
- The impact of light pollution on the spatial and temporal extent and strength of the lunar polarization pattern varied with moon phase. Only the polarization pattern of a full moon retained its 'band' shape at a maximum DoP of ~0.25 for more than two hours after sunset.
- Light pollution of low to moderate radiance (6-20 nW/cm^2sr) dramatically reduced the spatial distribution and maximum DoP of the lunar polarization pattern of a full moon, the magnitude

of the effect increasing with increasing radiance; light pollution of high radiance (>20 nW/cm^2sr) reduced the pattern to near-extinction.

- Photoreceptor contrast of the lunar polarization pattern in the visual systems of *H. armigera* and, to a lesser extent, *Drassodes* sp. decreased with increasing light pollution radiance.
- *H. armigera* flew in a south-southwest direction independent of polarization but were more likely to cluster around a mean direction when flying beneath artificially polarized skylight. This is the first time that orientation using the skylight polarization pattern has been demonstrated in a nocturnal lepidopteran.
- Individual moths did not change orientation by >45° or change directedness following a 90° rotation of the artificially polarized skylight or unpolarized skylight but grouped direction and mean directedness did change following rotation of the artificially polarized cue.
- When walking on a trackball, *Drassodes sp.* were significantly more likely to change orientation direction following the rotation of artificially polarized skylight compared to artificially unpolarized skylight, but the effect size was small and path directedness did not change.
- Unfortunately, the trackball assay was not successful in finding a behavioural threshold of polarization sensitivity in *Drassodes* sp., which has yet to be discovered in any species of spider.
- The nocturnal activity of *H. armigera* from sunset to sunrise was significantly reduced under both LED and HPS sodium streetlights compared to a natural night sky control, most noticeably in the LED. This effect was seen at intensities of 0.2 lux but was mostly prominent at intensities >4 lux and in the first two hours after sunset when the moths would naturally be taking flight. No evidence of an effect of the presence or absence of artificially polarized skylight on activity was found.
- Similarly, the nocturnal activity of *Drassodes* sp. from sunset to sunrise was significantly reduced under both LED and HPS streetlight of a similar intensity. The effect was particularly pronounced under the LED streetlight during the first half of the night, when the spiders would naturally begin their foraging excursions.

6.2 Discussion

6.2.1 Moon phase, light pollution, and the skylight polarization pattern

Moon phase and light pollution

For the first time, this research has characterised the temporal and spatial behaviour of the skylight polarization pattern of the whole sky at night across four moon phases and in areas of low (0.48 nW/cm^{2}sr) and high (42.77 nW/cm^{2}sr) light pollution. Previously, comparisons of the lunar polarization pattern across moon phase[1] and between areas of low and high light pollution[2] had only occurred at single times and locations and had not sampled the whole sky in the latter case, giving limited insight into the temporal and spatial impacts of light pollution or moon phase. Whole sky time series measurements of the solar and lunar polarization patterns, including the transition between both, has been previously described but never within the context of light pollution and across limited moon phases and a low temporal resolutions[3,4].

Light pollution reduced the maximum DoP of the skylight polarization pattern by ~25%, the spatial distribution of the pattern by >20% and reduced the persistence of the pattern by ~1.5 hours. All these impacts varied with moon phase. Only the polarization pattern of a full moon maintained its characteristic 'band' shape at DoPs ~0.25 for several hours of the night in light-polluted areas, with the patterns of the quarter moons losing all these characteristics 30-90 minutes early under light pollution. The DoP of the lunar polarization pattern has been shown to change as a function of moon phase[1]. Here I have shown that high light pollution increases the magnitude of this effect, reducing not only the DoP but the spatial and temporal extent of the lunar polarization pattern, which is likely to have an exacerbating effect on the nocturnal behaviour of arthropods (see sections 6.2.2 and 6.2.3).

Light pollution radiance

Additionally, the relationship between the characteristics of the lunar polarization pattern of the full moon and light pollution radiance was characterised for the first time. I found that the DoP and spatial distribution of the lunar polarization pattern of the full moon (>80% illumination) changed as a function of radiance. Light pollution of low to moderate radiance (6-20 nW/cm^{2}sr) dramatically reduced these characteristics of the lunar polarization pattern and light pollution of high radiance (>20 nW/cm^{2}sr) reduced the pattern to near-extinction in some cases. Thus, the density and intensity of lighting within an urban area could have significant consequences for the detection of the polarization pattern by nocturnal arthropods. This investigation took measurements at singular time points, at different locations across Europe, and during different lunar elevations. In comparison with the time

series measurements of the moon phase investigation (at radiance levels of 42.77 nW/cm^{2}sr), which did not see the polarization pattern of the full moon reduced to extinction as in some of the singular measurements. Clearly, the behaviour of the lunar polarization pattern is highly dynamic and dependent on a wide range of factors including light pollution and moon phase, but also weather, season, and latitude. With such inherent variability in the behaviour of the polarization pattern, light pollution as an anthropogenic stressor represents an additional and highly persistent threat to its reliability as a navigational cue.

It is important to consider the detrimental effects of air pollution to the skylight polarization pattern. Whilst the concentration of pollutant aerosols is highly spatially and temporally variable, their effects on skylight polarization can be significant[5,6]. Given that there is likely to be a positive correlation between air pollution concentration and light pollution radiance related to urban infrastructure and population density, I cannot reliably disentangle the effects of air pollution from light pollution in my results[7]. However, the effects of both on skylight polarization are the same and as such, I do not anticipate that the overall results of this investigation would change with the removal of air pollution as a factor. Rather, it is considered an additional anthropogenic stressor that further degrades the reliability of skylight polarization for navigation arthropods.

6.2.2 Comparing the effects of light pollution on moth and spider navigation

Navigation using the skylight polarization pattern

The results of the tethered experiments investigating the use of the polarization of light for navigation in *H. armigera* and *Drassodes* sp. suggest that skylight polarization contributes to adaptive trajectory selection and orientation, although, the results obtained from the trackball experiments with *Drassodes* sp. are less convincing. I have also demonstrated that light pollution can obscure the skylight polarization pattern and that this effect is directly related to light pollution radiance. Therefore, by extrapolating both results, it is assumed that light pollution has the potential to impair at least some aspects of polarization-guided navigation. In *H. armigera*, when inside a flight simulator, these aspects include group heading selection, directedness, and orientation, something that has remained ambiguous in the lepidopteran despite the widespread assumption of its occurrence[8,9,10]. When *Drassodes* sp. is tethered on a trackball, polarized light was observed to inform orientation alone, but the effect size was small compared to other studies[11,12] and not repeatable. This is partly due to differences in the motivational context of *Drassodes* sp. compared to *H. armigera*, the latter being caught and tested during highly directional, seasonal migrations and the former being caught with no immediate motivation to navigate. Thus, we could not expect *Drassodes* sp. to select and converge on a particular trajectory as they were given no motivation to do so. A lack of motivation

may also be responsible for the small effect size and low repeatability of the trackball experiments. The use of a trackball to test navigation in arthropods is a well-established method that has been used for many decades[13]. Aranae[12], Blattodae[14], Diptera[15,16], Hymenoptera[17], and Orthoptera[18] are some of the many arthropods that have been successfully tested on trackballs. Only a few of these examples[16,18] describe spontaneous responses to changes in polarization, with most using additional stimuli such as a natural horizon[15], displacement[17], or physical touch[12] to encourage movement. Moreover, the reduction in directedness of *Drassodes* sp. following filter rotation of all experimental treatments, and the significant effects of the direction of treatment rotation and order of presentation, indicates that the spiders were unintentionally disturbed and fatigued during the experiments. As such, and unfortunately, strong conclusions on polarization-guided navigation in Drassodes sp. cannot be made here. That being said, it is curious that the individual responses of *H. armigera* did not match the grouped observations, an occurrence I have attributed to small effect sizes within individuals contributing to a cumulatively larger effect size at group level. The Mouritsen-Frost flight simulator, like the trackball, is a well-established method for testing flight characteristics in insects[9,10,19-22]. However, only some of the studies testing individual responses to the relocation of a directional cue[9,10,20,22] were able to stimulate individuals to change their heading direction[10,20]. Perhaps small effect sizes are a common caveat affecting many of the studies that test the tethered movement of animals within artificial arenas.

Nevertheless, I have provided evidence to suggest that light pollution can impair navigation in nocturnal arthropods by masking the skylight polarization pattern important for orientation. For *H. armigera*, the risk of disorientation from the loss of the polarization pattern will vary spatially depending on how close and how often its migratory route connects to lit areas of urbanisation >6 nW/cm^{2}sr. Even temporary loss of polarization of ~3 minutes can cause some detrimental impact to the flight performance of *H. armigera*. If polarization is not regained within this time, or alternative cues cannot replace the weighted importance of polarization to the animal's directional compass, even brief lapses in orientation could prove highly problematic. A change in direction or loss of directedness could position the animals towards lit areas, inducing a 'flight-to-light' response[23,24] that lures them into the lit zones of urbanisation. Given that direct exposure to lights of <5 lux can inhibit activity, any animal lured into this lit zone is very likely to become trapped within it, thus ending or significantly delaying its migration and simultaneously increasing the risk of predation[25-28], exhaustion, and starvation. If *H. armigera* escapes the lure of light, the consequences of disorientation may still be significant, causing erroneous trajectories and longer journey lengths that increase energy expenditure and delay, and possibly prevent, the location of suitable feeding and breeding grounds.

The latter effect being particularly important to the productivity and profitability of agroecosystems[29].

For *Drassodes* sp., if light pollution does disrupt polarization-guided navigation, the impacts are also likely to be spatially variable, but at a smaller scale. Spiders that build their retreats within the lit zone of urban areas, or close to urban areas where skyglow is >20 nW/cm^{2}sr, may not be able to use the skylight polarization pattern for orientation unless they travel beyond this zone to areas <6 nW/cm^{2}sr. This is assuming that a photoreceptor contrast of ~0.1-0.2 is not a perceivable contrast. In which case, the spiders would not be able to use skylight polarization at the start of their journeys (perhaps when they are calibrating their celestial compass with learning walks as seen in ants and other ground spiders[30,31]) and at the end of their journeys, instead using it only when it becomes available. Consequently, skylight polarization may not be useful for homeward trajectory selection in this instance but may be useful as a widefield visual landmark for orientation when walking. On the other hand, spiders that build their retreats in areas of radiance lower than 6 nW/cm^{2}sr will be able to use skylight polarization during the outward and returning legs of their excursions but will lose this ability when wandering into areas of higher radiance. This is likely to have more substantial consequences as the likelihood of successfully returning to a retreat is significantly reduced without skylight polarization throughout the journey[11], probably resulting in increased energy expenditure through longer journey lengths and, at the extreme, the forced building of new retreats. Longer journey lengths will also increases the risk of intra- and interspecific physical conflicts. However, there is still much to be learnt about *Drassodes* sp. movement ecology. For example, it is unknown whether they do perform learning walks, or how far a typical nightly excursion can be and how often they occur, nor do we know their retreat site fidelity and how often they disperse. Such fundamental information must be gained before we can extrapolate any ecological and physiological meaning to reduced orientation ability caused by light pollution.

The timing of nocturnal activity

Both *H. armigera* and *Drassodes* sp. synchronise the initiation of their nocturnal journeys with the onset of night, and exposure to streetlights (even of EU-recommended lux intensities) decreased the average number of nocturnal journeys initiated by both species. However, the relative magnitude of the effect to both species was variable. In *H. armigera*, exposure to light pollution of >10 lux reduced the average number of active individuals from 80% in the first two hours post-sunset to 0-2%, whereas in *Drassodes* sp., the average activity of the spiders fell from 40-69% to 14-27%. Under natural dark conditions, this peak in activity two hours post-sunset exponentially decreased to near-zero in the final 6 hours of the night in H. *armigera*. Whilst *Drassodes* sp. shared the same peak in activity two

hours post-sunset, up to a third of individuals remained active until just before sunrise. Such differential effects between the two species are likely to be a result of natural differences in the nocturnal activity profiles of the two species. *Drassodes* spp. have been observed to maintain activity beyond sunrise[11] whereas *H. armigera* restricts it nocturnal migrations to the night[32,33]. Also, taking flight is a behaviour that occurs at a very specific period of the night. If already in flight after this take-off period, we could expect the moths to continue their activity, possibly even after the lunar polarization pattern disappears. However, if individuals are still grounded after this period, their motivation to take off might be lost, an effect observed in sandhoppers when migrating seaward to forage[34]. Thus, there may be more flexibility in the circadian behaviour of spiders that could alleviate the effects of light pollution on activity that is not present in the moths. Differential effects may also be partly explained by the experimental apparatus restricting flight take-off in the moths but being less restrictive on the natural movements of the spiders. The nightly migratory flight of *H. armigera* lasts between 6 and 8 hours[32] but the general activity observed here declined 2 hours post-sunset, possibly due to exhaustion or lack of motivation after several failed attempts at take-off. The spiders, however, were able to move relatively unrestricted. Further research on the entrainment of activity patterns to light across the full 24-hour day/night cycle will help determine the biological mechanisms behind such differences in responses to light pollution.

The activity of both *H. armigera* and *Drassodes* sp. was impacted by light pollution, but the relative magnitude of these impacts was species-specific, possibly reflecting a difference in the ecological demands of the behaviours (foraging and migration) under observation. Therefore, we might expect the consequences of light pollution to species fitness and survival to also be species-specific. For *H. armigera*, the impacts of light pollution to nocturnal activity could be potentially catastrophic. Many species of lepidopteran are drawn to light at night due to a well conserved 'flight-to-light' behaviour[24,35]. This inherent attraction to lit areas and cities increases the likelihood that *H. armigera* will be lured towards streetlights and subsequently trapped beneath them due to light-induced take-off suppression. If individuals are trapped for long enough, they will perish before completing their migration. Particularly as the risk of predation increases significantly beneath streetlights as predators such as bats[26] and spiders[25,27,28] are known to take advantage of the high concentrations of prey species lured to streetlights. If individuals are able to escape the lit area of streetlights, their migration will be stalled, delayed or misguided, an effect observed in several migratory birds[36,37,38] and transiting bats[26], potentially preventing them from finding suitable feeding and breeding grounds. Furthermore, delayed take-off could mean that migratory flight begins when cues such as the lunar polarization pattern or the moon are waning or not visible, potentially impairing orientation and increasing the likelihood of 'flight-to-light' behaviour towards high-intensity artificial light sources as

seen in migratory birds[38] and ball-rolling dung beetles[23]. Therefore, the suppression of nocturnal activity caused by light pollution has direct effects on both the survival and fitness of *H. armigera*.

In *Drassodes* sp., exposure to streetlights of >10 lux did not completely inhibit nocturnal activity, so the risk of becoming trapped by light is lower. This is the first time the impacts of light pollution on the nocturnal activity of a spider have been characterised. Rather than being lured in by bright light at night, spiders are known to actively seek out lit areas to exploit the high abundance of prey species, providing increased prey capture rates and an initial increase in fitness[25,27,28]. However, although activity was not completely inhibited in this investigation, it was still reduced, meaning the benefits of higher prey capture rates around streetlights may be offset by a reduction in the total number of foraging excursions taken by *Drassodes* sp.. Indeed, light at night affected the development and activity of freshwater shredders, whilst simultaneously increasing foraging rate, with implications for leaf litter breakdown and nutrient cycling in freshwater ecosystems[39]. As spiders are important insect predators, changes in prey capture and foraging rate could have serious implications for predator-prey dynamics and insect assemblages[40]. Furthermore, chronic exposure to light at night is known to be detrimental to development, juvenile mortality, and egg-laying in spiders[41]. This effect will be compounded by lower activity rates beneath streetlights ultimately prolonging nightly exposure to light through stalled dispersal and inhibited nightly excursions.

The timing of activity was not affected by exposure to streetlights. The ~30% of spiders that were active beneath streetlights were still synchronised with natural *Zeitgebers* and would have begun nocturnal excursions when celestial cues like the lunar polarization pattern and moon were still visible in the sky. Therefore, the impacts caused by the mistiming of nocturnal excursions observed in H. armigera will be less significant in *Drassodes* sp., although still present in ~70% of individuals. Therefore, the suppression of nocturnal activity caused by light pollution has direct effects on the fitness of *Drassodes* sp., but unlike *H. armigera*, may have a less significant impact on adult survival. Similarly, as mentioned above, the observed flexibility in the circadian behaviour of the spiders could alleviate some of the impacts of light pollution on spider activity that would not be possible in migrating moths.

6.2.3 Natural and anthropogenic factors compounding the effects of light pollution on nocturnal navigation

Radiance

The modelled perception of the skylight polarization pattern in the visual systems of *H. armigera* and *Drassodes* sp. was negatively correlated with radiance increasing from 0 and 50 nW/cm^{2}sr. However,

how this might translate to impacts on the navigation of moths and spiders remains unclear. As I could not identify behavioural thresholds of polarization detection in *H. armigera* or *Drassodes* sp., the relationship between radiance and orientation performance is still unknown. Further experiments that isolate a robust orientation response to a change in skylight polarization are necessary before reliable estimates of a detection threshold can be established in either moths or spiders.

Conversely, the experiments testing the effects of an LED streetlight of variable intensity on the nocturnal activity of *H. armigera* was more successful. The results show a clear effect of light intensities of >4 lux which significantly reduced the number of moths active within the first two hours post-sunset and across the whole night. Even light intensities of 0.2 lux (similar illuminance to the light of a full moon) reduced the average activity of the moths two hours post-sunset by 15%. Given that the EU standards for residential streetlighting restricts horizontal lux to 1-50 lux[42], direct light pollution from all streetlights are a considerable threat to nocturnal lepidopteran activity for the reasons discussed in the previous section. Similar results have been observed in the Asian Gypsy moth (*Lymantria dispar*) which was less likely to perform wing fanning and walking behaviours (typically associated with pre-flight) with increasing light intensity (between 0.05 and 0.4 lux) and were more likely to perform these behaviours at different times relative to a control treatment[42]. However, take-off was not affected by light intensity in *L. dispar*, suggesting that the effect of radiance may be behaviour specific. I did not include observations of walking and wing fanning behaviour in *H. armigera*, but as these are known precursors for take-off, perhaps they would be important to observe in future experiments. Changing ambient light intensities of ranges between 0 and 5 lux is also known to affect the occurrence of bat activity[26] and drift in aquatic invertebrates[44], increasing intensities either negatively or positively affecting activity relative to the light-sensitivity of different species[26]. It seems that lux values of ~5 or less may be of critical importance to the activity of a wide range of species and the negative impacts of radiance observed here may not be exclusive to nocturnal arthropods. This reinforces the importance of tuning light pollution radiance as an effective mitigation strategy to alleviate the impacts of light pollution on the nocturnal world.

Spectral composition

The global trend towards retrofitting narrow-spectrum yellow lighting with broad-spectrum white lighting is expected to exacerbate the impacts of light pollution to diurnal and nocturnal arthropods because of their increased sensitivity to wavelengths in the range of ~350 to 550 nm[11,45,46]. Such differential effects have been observed in insect and spider abundance[40,47,48] and species diversity[49] captured by light traps using LED and HPS lamps. Furthermore, the shorter wavelengths in broad-spectrum light are more likely to be absorbed by the protein cryptochrome in the photoreceptors of

the eyes, consequently delaying or advancing the clock phase[50], and ultimately impacting the timing of nocturnal navigation. Indeed, a narrow-spectrum HPS streetlight affected the intensity and duration of nocturnal activity of *H. armigera* and *Drassodes* sp. significantly less than a broad-spectrum LED streetlight. Therefore, this investigation supports the results of similar studies and agrees that HPS and narrow-spectrum, long-wavelength shifted lights have less of an impact on nocturnal arthropods than broad-spectrum white lights. However, overall activity in both species was still lower when exposed to a HPS streetlight compared to a control. Therefore, it would be foolish to assume that tuning the spectral composition of light pollution to longer wavelengths would act as a silver bullet for alleviating the impacts of light pollution. Instead, the results of this project indicate that lighting of long-wavelengths at low radiance, in combination, will better mitigate the effects of light pollution on the nocturnal world.

It would be interesting to investigate the relative impacts of HPS and LED streetlights on orientation in *H. armigera* and *Drassodes* sp.. Broad-spectrum LED light increases the radiance of skyglow due to the stronger scattering of shorter wavelengths in the atmosphere[51,52]. LED light is therefore expected to have a stronger masking effect on the skylight polarization pattern, which will adversely affect nocturnal navigation. Increased absorption of short wavelengths may also cause physiologically and anatomically plastic changes to the visual systems of arthropods. For example, increased expression of certain opsins in *H. armigera*[46] and decreased rhabdom size in crabs[53] have both been reported in response to constant UV (365 nm), blue (450 nm) and green (505 nm) light, and LED light at night, respectively. These plastic effects are likely to occur at different magnitudes depending on life stage; epigenetic effects like opsin expression could be critical during development, whereas anatomical effects will be more important in adulthood. Changes in opsins expression and rhabdom size affects the spectral sensitivity and overall sensitivity of an eye. Thus, the detection of light of certain wavelengths and intensities, linked to specific behaviours like the detection of skylight polarization, could be compromised by exposure to light pollution. How this might affect navigation is unclear, observations of orientation accuracy following chronic or short-term exposure to lights of different spectrums may provide insights into their differential effects to navigation.

Moon phase

The results of the photographic polarimetry experiments showed that moon phase compounds the obscuring effect of light pollution on the polarization pattern. This is due to natural changes in moon luminance changing the spatial and temporal distribution of the pattern and its DoP. This project has demonstrated that skylight polarization is used for orientation in *Drassodes* sp. and *H. armigera* and that light pollution, coupled with low moon illuminance (quarter moon illuminance or less compared

to near-full illuminance), effectively eliminates the lunar polarization pattern at night. Thus, true nocturnal navigation using the polarization pattern may not be possible in light-polluted areas during nights when <25% of the moon is illuminated, around half of the lunar cycle.

Of course, there is no lunar polarization pattern during a new moon and the crescent moons, which tend to rise during the day[54], so the navigational system of nocturnal arthropods must be flexible. One potential mechanism that creates flexibility is the synchronisation of nocturnal movements with moonlight and the lunar cycle. It has been suggested that *Drassodes cupreus* is maximally active when the polarization pattern is at its strongest[11] and that the flight of nocturnal lepidopterans is influenced by moonlight[29,55]. On nights of low or no moon luminance, arthropods reliant on the light of the moon for navigation may not initiate nocturnal journeys, staying within their nests or delaying migration until suitable conditions occur. Delayed mass migrations have been observed in *Autographa gamma*, which wait for favourable winds before taking flight[56], a behaviour that is thought to be widespread amongst migrating lepidopteran[57,58]. Thus, if *H. armigera* also delays its migration until a favourable window in visual and meteorological cues occurs, exposure to light pollution during this critical window could have serious implications for immigration of whole populations. In *Drassodes* sp., this would affect foraging, prey capture rates and potentially mate-finding and reproduction with similarly serious implications for individual fitness.

The activity experiments described in this thesis did not include investigations into the influence of moonlight on nocturnal activity as they were performed between the 1st and 3rd quarter moon phases, when moonlight is mostly present at high illuminance for several hours at night. Relatively little is known about the behaviour and ecology of *Drassodes* sp. and most of what is known about *H. armigera* is centred on its control as an agricultural pest. It would be beneficial to improve our understanding of these animals' fundamental behaviour, such as patterns of nocturnal activity relative to moonlight as well as other factors like the length and duration of journeys relative to environmental factors, to better predict the impacts of light pollution on individual fitness and survival.

6.3 Final conclusions and future research directions

This body of work provides new evidence identifying light pollution as a shared threat to nocturnal activity and navigation in ground-dwelling and aerial arthropods moving at different spatial scales. The results reported here suggest that light pollution can:

1) Adversely affect individuals during their nocturnal journeys by masking the skylight polarization pattern used during orientation.
2) Affect individuals yet to begin their nocturnal journeys by disrupting the synchronisation of activity with the onset of night.

For the first time, this project gives high-resolution observations of the effects of light pollution on the temporal and spatial characteristics of the skylight polarization pattern along a radiance gradient. This provides an important resource for estimating the behaviour of the skylight polarization pattern under a range of conditions. A further novel discovery is the evidence for improved orientation and directedness with skylight polarization in a nocturnal lepidopteran, an effect long assumed but never demonstrated experimentally. Finally, through observing differences in activity between streetlights of different spectral content and radiance, this research has gained new insights into the differential effects of several characteristics of light pollution on nocturnal arthropod activity. The combined conclusions of this work could inform the tailoring of effective and realistic mitigation of ecological light pollution and help prevent the global decline in invertebrate abundance.

To improve our understanding of the impacts of light pollution on the movements of *H. armigera*, *Drassodes* sp., and any other species of focus, it is important to first establish the fundamentals of their movement ecology: when do they begin their journeys and is this influenced by certain sensory cues, what is the purpose of the journey, how often do they occur and how long do they persist, and what visual cues are important for their navigation? Only then can we begin to disentangle how light pollution as an anthropogenic stressor might impact the survival and fitness of a species through its effects on nocturnal journeys. Future research on navigation in *H. armigera* and *Drassodes* sp. should first determine the influence of the moon and the lunar polarization pattern on the timing of nocturnal journeys, as the synchronisation of nocturnal journeys with the lunar calendar could affect the susceptibility to the masking effects of light pollution depending on moon illumination. It would also be pertinent to establish the physiological effects of streetlight exposure (of different spectra and brightness) in the eyes of *H. armigera* and *Drassodes* sp., does the increased inhibition of activity under broad-spectrum light correlate with an up or down regulation of certain visual pigments in the eyes, and how does this effect the detection of visual cues like the skylight polarization pattern? Very little is known of the epigenetic and developmental effects of light pollution exposure, these could be key areas of research that help elucidate the mechanisms behind observed behavioural effects. As behavioural thresholds for polarization sensitivity could not be established during this project, this avenue of research remains relatively unexplored yet highly important for determining the link between disrupted nocturnal behaviour and light pollution radiance. Similarly, the activity experiments of chapter 5 are a simple and effective method for testing the effect of light pollution

radiance and spectral composition on nocturnal activity. This method can be adapted for the observation of many behaviours, across many species, under a range of lighting treatments and as such represents and exciting opportunity for the study of light pollution and behaviour.

Finally, it would be helpful to determine the relative effects of light and air pollution on the masking of the polarization pattern. Here, I have assumed that light pollution represents the biggest threat to the skylight polarization pattern, but there is limited evidence to support such an assumption. We could be grossly underestimating the ecological impacts of anthropogenic pollutants if we continue to narrow our focus by studying their effects in isolation. Much is still to be discovered in this important field of research that will increase our understanding of the effects of light pollution on the nocturnal world and encourage the protection of the night sky and the animals it supports.

References

1. Foster JJ, Kirwan JD, el Jundi B, Smolka J, Khaldy L, Baird E. Byrne MJ, Nilsson DE, Johnsen S, Dacke M. 2019. Orienting to polarized light at night - matching lunar skylight to performance in a nocturnal beetle. *Journal of Experimental Biology*, **222**(2): jeb188532. (DOI: 10.1242/jeb.188532)
2. Kyba CCM, Ruhtz T, Fischer J, Hölker F. 2011. Lunar skylight polarization signal polluted by urban lighting. *Journal of Geophysical Research - Atmospheres*, **116**: D24106. (DOI: 10.1029/2011JD016698)
3. Cronin TW, Warrant EJ, Greiner B. 2006. Celestial polarization patterns during twilight. *Applied Optics*, **45**(22): 5582-5589. (DOI: 10.1364/ao.45.005582)
4. Barta A, Farkas A, Szaz D, Egri A, Barta P, Kovacs J, Csak B, Jankovics I, Szabo G, Horvath G. 2014. Polarization transition between sunlit and moonlit skies with possible implications for animal orientation and Viking navigation: Anomalous celestial twilight polarization at partial moon. *Applied Optics*, **53**(23): 5193-5204. (DOI: 10.1364/ao.53.005193)
5. Cui Y, Zhang XG, Zhou XC, Liu YF, Chu JK. 2019. Effect of aerosol on polarization distribution of sky light. Acta Optica Sinica, **39**(6): 0601001. (DOI: 10.3788/aos201939.0601001)
6. Kreuter A, Emde C, Blumthaler M. 2010. Measuring the influence of aerosols and albedo on sky polarization. *Atmospheric Research*, **98**(2-4): 363-367. (DOI: 10.1016/j.atmosres.2010.07.010)
7. Cavazzani S, Ortolani S, Bertolo A, Binotto R, Fiorentin P, Carraro G, Zitelli V. 2020. Satellite measurements of artificial light at night: Aerosol effects. *Monthly Notices of the Royal Astronomical Society*, **499**(4): 5075-5089. (DOI: 10.1093/mnras/staa3157)
8. Belušič G, Sporar K, Meglic A. 2017. Extreme polarisation sensitivity in the retina of the corn borer moth *Ostrinia*. *Journal of Experimental Biology*, **220**(11): 2047-2056. (DOI: 10.1242/jeb.153718)
9. Stalleicken J, Mukhida M, Labhart T, Wehner R, Frost B, Mouritsen H. 2005. Do monarch butterflies use polarized skylight for migratory orientation? *Journal of Experimental Biology*, **208**(12): 2399-2408. (DOI: 10.1242/jeb.01613)
10. Reppert SM, Zhu HS, White RH. 2004. Polarized light helps monarch butterflies navigate. *Current Biology*, **14**(2): 155-8. (DOI: 10.1016/j.cub.2003.12.034)
11. Dacke M, Nilsson DE, Warrant EJ, Blest AD, Land MF, O'Carroll DC. 1999. Built-in polarizers form part of a compass organ in spiders. Nature, **401**(6752): 470-473. (DOI: 10.1038/46773)
12. Dacke M, Doan TA, O'Carroll DC. 2001. Polarized light detection in spiders. *Journal of Experimental Biology*, **204**(14): 2481-90. (DOI: 10.1242/jeb.204.14.2481)
13. Buchner E. 1976. Elementary motion detectors in an insect visual system. *Biological Cybernetics*, **24**(2): 85-101. (DOI: 10.1007/bf00360648)
14. Okada J, Toh Y. 2000. The role of antennal hair plates in object-guided tactile orientation of the cockroach (*Periplaneta americana*). *Journal of Comparative Physiology A*, **186**(9): 849-857. (DOI: 10.1007/s003590000137)
15. Vishniakou I, Ploger PG, Seelig JD. 2019. Virtual reality for animal navigation with camera-based optical flow tracking. *Journal of Neuroscience Methods*, **327**: 108403. (DOI: 10.1016/j.jneumeth.2019.108403)
16. Vonphilipsborn A, Labhart T. 1990. A behavioural study of polarization-vision in the fly, *Musca domestica*. *Journal of Comparative Physiology A*, **167**(6): 737-743. (DOI: 10.1007/bf00189764)

17. Dahmen H, Wahl VL, Pfeffer SE, Mallot HA, Wittlinger M. 2017. Naturalistic path integration of Cataglyphis desert ants on an air-cushioned lightweight spherical treadmill. *Journal of Experimental Biology*, **220**(4): 634-644. (DOI: 10.1242/jeb.148213)
18. Henze MJ, Labhart T. 2007. Haze, clouds and limited sky visibility: Polarotactic orientation of crickets under difficult stimulus conditions. *Journal of Experimental Biology*, **210**(18): 3266-76. (DOI: 10.1242/jeb.007831)
19. Dreyer D, Frost B, Mouritsen H, Gunther A, Green K, Whitehouse M, Johnsen S, Heinze S, Warrant E. 2018. The Earth's magnetic field and visual landmarks steer migratory flight behaviour in the nocturnal Australian bogong moth. *Current Biology*, **28**: 2160-2166. (DOI: 10.1016/j.cub.2018.05.030)
20. Franzke M, Kraus C, Dreyer D, Pfeiffer K, Beetz MJ, Stockl AL, Foster JJ, Warrant EJ, el Jundi B. 2020. Spatial orientation based on multiple visual cues in non-migratory monarch butterflies. *Journal of Experimental Biology*, **223**(12): jeb223800. (DOI: 10.1242/jeb.223800)
21. Giraldo YM, Leitch KJ, Ros IG, Warren TL, Weir PT, Dickinson MH. 2018. Sun navigation requires compass neurons in *Drosophila*. *Current Biology*, **28**(17): 2845-2852. (DOI: 10.1016/j.cub.2018.07.002)
22. Mouritsen H, Frost BJ. 2002. Virtual migration in tethered flying monarch butterflies reveals their orientation mechanisms. *Proceedings of the National Academy of Sciences*, **99**(15): 10162-10166. (DOI: 10.1073/pnas.152137299)
23. Foster JJ, Tocco C, Smolka J, Khaldy L, Baird E, Byrne MJ, Nilsson DE, Dacke M. 2021. Light pollution forces a change in dung beetle orientation behavior. *Current Biology*, **31**(17): 3935-3942. (DOI: 10.1016/j.cub.2021.06.038)
24. Donners M, van Grunsven RHA, Groenendijk D, van Langevelde F, Bikker JW, Longcore T, Veenendaal E. 2018. Colors of attraction: Modeling insect flight to light behavior. *Journal of Experimental Zoology Part A*, **329**(8-9): 434-440. (DOI: 10.1002/jez.2188)
25. Willmott NJ, Henneken J, Elgar MA, Jones TM. 2019. Guiding lights: Foraging responses of juvenile nocturnal orb-web spiders to the presence of artificial light at night. *Ethology*, **125**(5): 289-297. (DOI: 10.1111/eth.12852)
26. Azam C, Le Viol I, Bas Y, Zissis G, Vernet A, Julien JF, Kerbiriou C. 2018. Evidence for distance and illuminance thresholds in the effects of artificial lighting on bat activity. *Landscape and Urban Planning*, **175**: 123-135. (DOI: 10.1016/j.landurbplan.2018.02.011)
27. Yuen SW, Bonebrake TC. 2017. Artificial night light alters nocturnal prey interception outcomes for morphologically variable spiders. *Peerj*, **5**: e4070. (DOI: 10.7717/peerj.4070)
28. Adams MR, 2000. Choosing hunting sites: Web site preferences of the orb weaver spider, *Neoscona crucifera*, relative to light cues. *Journal of Insect Behavior*, **13**(3): 299-305. (DOI: 10.1023/a:1007771332721)
29. Nowinszky L, Puskas J, Barczikay G. 2015. The relationship between polarized moonlight and the number of pest microlepidoptera specimens caught in pheromone traps. *Polish Journal of Entomology*, **84**(3): 163-176. (DOI: 10.1515/pjen-2015-0014)
30. Grob R, Cunz OH, Grubel K, Pfeiffer K, Rossler W, Fleischmann PN. 2022. Rotation of skylight polarization during learning walks is necessary to trigger neuronal plasticity in Cataglyphis ants. *Proceedings of the Royal Society B*, **289**(1967): 20212499. (DOI: 10.1098/rspb.2021.2499)
31. Norgaard T, Gagnon YL, Warrant EJ. 2012. Nocturnal homing: Learning walks in a wandering spider? *PLOS One*, **7**(11): e49263. (DOI: 10.1371/journal.pone.0049263)

32. Feng HQ, Wu KM, Cheng DF, Guo YY. 2004. Northward migration of *Helicoverpa armigera* (Lepidoptera: Noctuidae) and other moths in early summer observed with radar in northern China. *Journal of Economic Entomology*, **97**(6): 1874-1883. (DOI: 10.1093/jee/97.6.1874)
33. Persson B. 1971. Influence of light on flight activity of Noctuids (Lepidoptera) in South Sweden. Insect Systematics & Evolution, **2**(3): 215–232. (DOI: 10.1163/187631271X00220)
34. Torres D, Tidau S, Jenkins S, Davies T. 2020. Artificial skyglow disrupts celestial migration at night. *Current Biology*, **30**(12): E696-E697. (DOI: 10.1016/j.cub.2020.05.002)
35. Altermatt F, Ebert D. 2016. Reduced flight-to-light behaviour of moth populations exposed to long-term urban light pollution. *Biology Letters*, **12**(4): 20160111. (DOI: 10.1098/rsbl.2016.0111)
36. La Sorte FA, Horton KG. 2021. Seasonal variation in the effects of artificial light at night on the occurrence of nocturnally migrating birds in urban areas. *Environmental Pollution*, **270**: 116085. (DOI: 10.1016/j.envpol.2020.116085)
37. Cabrera-Cruz SA, Smolinsky JA, McCarthy KP, Buler JJ. 2019. Urban areas affect flight altitudes of nocturnally migrating birds. *Journal of Animal Ecology*, **88**(12): 1873-1887. (DOI: 10.1111/1365-2656.13075)
38. Van Doren BM, Horton KG, Dokter AM, Klinck H, Elbin SB, Farnsworth A. 2017. High-intensity urban light installation dramatically alters nocturnal bird migration. *PNAS*, **114**(42): 11175-11180. (DOI: 10.1073/pnas.1708574114)
39. Czarnecka M, Kobak J, Grubisic M, Kakareko T. 2021. Disruptive effect of artificial light at night on leaf litter consumption, growth and activity of freshwater shredders. *Science of the Total Environment*, **786**: 147407. (DOI: 10.1016/j.scitotenv.2021.147407)
40. Davies TW, Bennie J, Cruse D, Blumgart D, Inger R, Gaston KJ. 2017. Multiple night-time light-emitting diode lighting strategies impact grassland invertebrate assemblages. *Global Change Biology*, **23**(7): 2641-2648. (DOI: 10.1111/gcb.13615)
41. Willmott NJ, Henneken J, Selleck CJ, Jones TM. 2018. Artificial light at night alters life history in a nocturnal orb-web spider. *Peerj*, **6**: e5599. (DOI: 10.7717/peerj.5599)
42. British Standards Institution (BSI). 2015. Road lighting - Part 2: Performance requirements. BS EN 13201-2:2015, London, BSI
43. Chen F, Shi J, Keena M. 2016. Evaluation of the effects of light intensity and time interval after the start of scotophase on the female flight propensity of Asian gypsy moth (Lepidoptera: Erebidae). *Environmental Entomology*, **45**(2): 404-409. (DOI: 10.1093/ee/nvv222)
44. Holt CS, Waters TF. 1967. Effect of light intensity on the drift of stream invertebrates. *Ecology*, **48**(2): 225-234. (DOI: 10.2307/1933104)
45. van der Kooi CJ, Stavenga DG, Arikawa K, Belušič G, Kelber A. 2021. Evolution of insect color vision: From spectral sensitivity to visual ecology. *Annual Review of Entomology*, **66**: 435-461. (DOI: 10.1146/annurev-ento-061720-071644)
46. Yan S, Zhu JL, Zhu WL, Zhang XF, Li Z, Liu XX, Zhang QW. 2014. The expression of three opsin genes from the compound eye of *Helicoverpa armigera* (Lepidoptera: Noctuidae) is regulated by a circadian clock, light conditions and nutritional status. *PLOS One*, **9**(10): e111683. (DOI: 10.1371/journal.pone.0111683)
47. Pawson SM, Bader MKF. 2014. LED lighting increases the ecological impact of light pollution irrespective of color temperature. *Ecological Applications*, **24**(7): 1561-1568. (DOI: 10.1890/14-0468.1)

48. Longcore T, Aldern HL, Eggers JF, Flores S, Franco L, Hirshfield-Yamanishi E, Petrinec LN, Yan WA, Barroso AM. 2015. Tuning the white light spectrum of light emitting diode lamps to reduce attraction of nocturnal arthropods. *Philosophical Transactions of the Royal Society B,* **370**: 20140125. (DOI: 10.1098/rstb.2014.0125)
49. Wakefield A, Broyles M, Stone EL, Harris S, Jones G. 2017. Quantifying the attractiveness of broad-spectrum streetlights to aerial nocturnal insects. *Journal of Applied Ecology*, **55**(2): 714-722. (DOI: 10.1111/1365-2664.13004)
50. Hardin PE. 2011. Molecular genetic analysis of circadian timekeeping in *Drosophila*. *Genetics of Circadian Rhythms*, **74**: 141-173. (DOI: 10.1016/b978-0-12-387690-4.00005-2)
51. Kyba CCM, Kuester T, de Miguel AS, Baugh K, Jechow A, Hölker F, Bennie J, Elvidge CD, Gaston KJ, Guanter L. 2017. Artificially lit surface of Earth at night increasing in radiance and extent. *Science Advances*, **3**(11): e1701528. (DOI: 10.1126/sciadv.1701528)
52. Aube M. 2015. Physical behaviour of anthropogenic light propagation into the nocturnal environment. *Philosophical Transactions of the Royal Society B*, **370**: 20140117. (DOI: 10.1098/rstb.2014.0117)
53. Brodrick EA, Roberts NW, Sumner-Rooney L, Schleputz CM, How MJ. 2012. Light adaptation mechanisms in the eye of the fiddler crab, *Afruca tangeri*. *Journal of Comparative Neurology*, **529**(3): 616-634. (DOI: 10.1002/cne.24973)
54. Cronin TW, Johnsen S, Marshall NJ, Warrant EJ. 2014. Light and the optical environment. In: Cronin TW, Johnsen S, Marshall NJ, Warrant EJ. (eds) Visual ecology. Princeton University Press, Woodstock, Oxfordshire, UK.
55. Dent DR, Pawar CS. 1988. The influence of moonlight and weather on catches of *Helicoverpa armigera* (Hübner) (Lepidoptera, Noctuidae) in light and pheromone traps. *Bulletin of Entomological Research*, **78**(3): 365-377. (DOI: 10.1017/s0007485300013146)
56. Chapman JW, Reynolds DR, Mouritsen H, Hill JK, Riley JR, Sivell D, Smith AD, Woiwod IP. 2008. Wind selection and drift compensation optimize migratory pathways in a high-flying moth. *Current Biology*, **18**(7): 514-518. (DOI: 10.1016/j.cub.2008.02.080)
57. Chapman JW, Nesbit RL, Burgin LE, Reynolds DR, Smith AD, Middleton DR, Hill JK. 2010. Flight orientation behaviors promote optimal migration trajectories in high-flying insects. *Science*, **327**(5966): 682-685. (DOI: 10.1126/science.1182990)
58. Chapman JW, Reynolds DR, Smith AD, Riley JR, Pedgley DE, Woiwod IP. 2002. High-altitude migration of the diamondback moth *Plutella xylostella* to the UK: A study using radar, aerial netting, and ground trapping. *Ecological Entomology*, **27**(6): 641-650. (DOI: 10.1046/j.1365-2311.2002.00472.x)